Reviews of Geophysics

REVIEW ARTICLE
10.1029/2023RG000825

Pan-European Landslide Risk Assessment: From Theory to Practice

Francesco Caleca[1], Luigi Lombardo[2], Stefan Steger[3], Hakan Tanyas[2], Federico Raspini[1], Ashok Dahal[2], Constantinos Nefros[4], Mihai Ciprian Mărgărint[5], Vincent Drouin[6], Mateja Jemec-Auflič[7], Alessandro Novellino[8], Marj Tonini[9], Marco Loche[10,11], Nicola Casagli[1,12], and Veronica Tofani[1]

[1]Department of Earth Sciences, University of Florence, Florence, Italy, [2]Faculty of Geo-Information Science and Earth Observation (ITC), University of Twente, Enschede, The Netherlands, [3]GeoSphere Austria, Vienna, Austria, [4]School of Mining and Metallurgical Engineering, National Technical University of Athens, Athens, Greece, [5]Faculty of Geography and Geology, Alexandru Ioan Cuza University of Iaşi, Iaşi, Romania, [6]Iceland Met Office, Reykjavík, Iceland, [7]Geological Survey of Slovenia, Ljubljana, Slovenia, [8]British Geological Survey, Keyworth, UK, [9]Faculty of Geosciences and Environment, Institute of Earth Surface Dynamics, University of Lausanne, Lausanne, Switzerland, [10]Czech Academy of Sciences, Prague, Czech Republic, [11]Institute of Hydrogeology, Engineering Geology and Applied Geophysics, Charles University, Prague, Czech Republic, [12]National Institute of Oceanography and Applied Geophysics - OGS, Trieste, Italy

Key Points:

- Landslide risk assessment is hardly implemented when the analysis scale involves large areas due to methodological and data limitations
- A Pan-European analysis is implemented to identify areas more susceptible to landslides and assess associated potential consequences
- Interactive Web Applications represent a modern solution for sharing risk results with users and raising public awareness

Correspondence to:
F. Caleca,
francesco.caleca@unifi.it

Citation:
Caleca, F., Lombardo, L., Steger, S., Tanyas, H., Raspini, F., Dahal, A., et al. (2025). Pan-European landslide risk assessment: From theory to practice. *Reviews of Geophysics*, *63*, e2023RG000825. https://doi.org/10.1029/2023RG000825

Received 16 JAN 2024
Accepted 1 FEB 2025

Author Contributions:
Conceptualization: Francesco Caleca, Luigi Lombardo, Federico Raspini, Veronica Tofani
Data curation: Francesco Caleca, Luigi Lombardo
Formal analysis: Francesco Caleca
Investigation: Francesco Caleca, Luigi Lombardo
Methodology: Francesco Caleca, Luigi Lombardo, Stefan Steger
Resources: Francesco Caleca, Luigi Lombardo, Federico Raspini, Constantinos Nefros, Mihai Ciprian Mărgărint, Vincent Drouin, Mateja Jemec-Auflič, Alessandro Novellino, Marj Tonini, Marco Loche, Veronica Tofani
Software: Francesco Caleca, Stefan Steger, Hakan Tanyas, Ashok Dahal
Supervision: Luigi Lombardo, Federico Raspini, Nicola Casagli, Veronica Tofani

Abstract Assessing landslide risk is a fundamental requirement to plan suitable prevention actions. To date, most risk studies focus on individual slopes or catchments. Whereas regional, national or continental scale assessments are hardly available because of methodological and/or data limitations. In this contribution, we present an overview of all requirements and limitations in landslide risk studies across all spatial scales, by means of a hybrid form that combines elements of original research with the comprehensive characteristics of a review study. The review critically analyses each component in the landslide risk analysis providing a detailed explanation of their state-of-the-art, with dedicated sections on susceptibility, hazard, exposure, and vulnerability. To put the theoretical framework to test, we also dive into a case study, expressed at the continental scale. Specifically, we take the main European mountain ranges and provide the reader with a textbook example of risk assessment for such a large territory. In doing so, we take into account issues associated with cross-national differences in landslide mapping. As a result, we identify landslide-prone European landscape and explore the associated possible economic consequences (human settlements and agricultural areas). We also analyze the population at risk during daytime and nighttime. Moreover, a modern view of the problem is explored in the form of how risk outcomes should be delivered to master planners and geoscientific personnel alike. Specifically, we convert our output into an interactive Web Application (https://pan-european-landslide-risk.github.io/) to include notions of scientific communication both to a large public as well as to a technical audience.

Plain Language Summary Landslide risk assessment is essential for planning preventive measures, and safeguarding human properties and health. However, existing studies often limit their analysis to individual slopes or catchments. Conversely, risk analysis is hardly implemented when the scale involves regions, nations, or continents. This limitation arises from challenges in data acquisition and methodology. This contribution presents a hybrid structure, merging review and original research contents. The review part analyzes landslide risk components, focusing on modeling landslide occurrence, response and exposure of elements at risk. The original research component conducts a continental-scale case study, specifically in the European landscape. A two-step protocol addresses cross-national differences in landslide mapping and data storage, identifying areas more inclined to trigger landslides and assessing potential economic losses for human settlements and agriculture. The population at risk is analyzed across daytime and nighttime by combining landslide likelihood with the corresponding population distribution. A key aspect is represented by a modern view of how to disseminate the findings of such studies. We implement a user-friendly Web Application to share our output. This initiative aims to improve accessibility to crucial information and raise awareness about landslide threats.

1. Introduction

Landslides represent a significant threat with potentially severe impacts on human lives and properties (Froude & Petley, 2018; Haque et al., 2016). This risk is further intensified by human activities, which can increase the likelihood and impact of landslides (Apon et al., 2024; Jaboyedoff et al., 2016). In the last decades, the increasing

Validation: Francesco Caleca, Luigi Lombardo
Visualization: Francesco Caleca, Luigi Lombardo, Ashok Dahal
Writing – original draft: Francesco Caleca, Luigi Lombardo, Hakan Tanyas, Ashok Dahal
Writing – review & editing: Francesco Caleca, Luigi Lombardo, Hakan Tanyas, Federico Raspini, Veronica Tofani

frequency and magnitude of extreme meteorological events (Huggel et al., 2012; Stoffel et al., 2014), as well as the expansion of human footprint in landslide-prone areas (Dille et al., 2022; Görüm & Fidan, 2021; Haque et al., 2019; Ozturk et al., 2022; Petley, 2012), has certainly highlighted the need to predict where and when landslides may occur, and possible losses in case of landsliding. This increased need to estimate landslide occurrence and consequences is also driven by multiple factors. Looking at the global level, population growth and weak governance have led to greater exposure to landslides, particularly in low and middle-income countries (Depicker et al., 2021). Another key factor is land use and cover changes (e.g., deforestation, road construction, intensive agriculture), which have significantly altered landslide controls (Cendrero et al., 2020; Lacroix, Dehecq, & Taipe, 2020). Additionally, climate change plays notable role, as its impacts are often more challenging to assess in many regions compared to those of land use changes (Masson-Delmotte et al., 2021). Therefore, understanding which places may be affected by landslides and what elements are exposed to them are crucial for effective land-use planning, and risk management (Corominas et al., 2014; Fell et al., 2005, 2008).

Landslide risk analysis or modeling aims to identify what economic and social losses an area could suffer if affected by landslides (M. Rossi et al., 2019). Therefore, it is an ideal instrument upon which to plan effective mitigation strategies (Dai et al., 2002). However, at a careful analysis of the literature on landslide risk, what stands out is that most of the available research is dedicated to site-specific case studies (Gatto et al., 2023; Remondo et al., 2008; Uzielli et al., 2015; Zêzere et al., 2008). The few existing exceptions hardly encompass basin or regional scale (Caleca et al., 2022; Catani et al., 2005; Crawford et al., 2022; Depicker et al., 2021; Lu et al., 2014; Peng et al., 2015), and even less is available for very wide regions (Caleca, Scaini, et al., 2024; Gaprindashvili & Van Westen, 2016; M. Rossi et al., 2019). The reason behind this trend has mostly to do with the limitations in accessing data related to: (a) systematic and reliable landslide inventories either manually (Colombo et al., 2005) or (semi-) automatically (Bhuyan et al., 2023) mapped, and each risk component. The latter consists of the susceptibility term (C. Van Westen et al., 2006) and the spatial thematic data it requires (e.g., topography, geology, soil properties, etc.) (Budimir et al., 2015), as well as the temporal (Guzzetti et al., 1999) and intensity (Lari et al., 2014) characteristics of the landslide process, vulnerability (B. Ahmed, 2021), and exposure information (Pellicani et al., 2014).

Each one of the main risk components and sub-components may be more available than others, but further differences also depend on the data context one may work on. For instance, if vulnerability data is most likely the least available component irrespective of the geographic area of interest, the accessibility to landslide inventories largely varies depending on the given country. And, because there is no standard on what information a landslide inventory should present, not only their availability but also the content dramatically changes.

To bring things into context through practical examples, Italy has an open national polygonal inventory, IFFI, and each landslide record is associated with failure mechanism and partially with the time of occurrence (Trigila et al., 2007). To make up for the fact that this inventory does not fully inform users about the landslide timing, a more recent effort led to a second open national inventory, FraneItalia (Calvello & Pecoraro, 2018). There, the occurrence date is associated with each record, although landslides do not report the failure mechanism and are expressed as points. These points may even indicate widespread landsliding rather than individual failures. Moreover, each point reports its confidence level. A further notable example is the ITALICA (ITAlian rainfall-induced LandslIdes CAtalogue) inventory presented by Peruccacci et al. (2023). This database provides temporal and spatial information on rainfall-induced landslides across Italy, covering events that occurred between January 1996 and December 2021. In this catalog, landslide occurrences are also represented as points, with both spatial and temporal accuracy levels indicated. This is already an indication of the variability one has to deal with, even in data-rich contexts. To further elaborate on such variability, below, we will further examine the situation in a few more data-rich cases (e.g., USA, Switzerland, and Colombia) before exploring data-scarce ones. Unlike the European community, the USA maintains a standardized database that covers its entire territory. The inventory is compiled by the U.S. Geological Survey (USGS) and is freely accessible. For a complete technical description, we refer the reader to Mirus et al. (2020). The USGS inventory includes both polygonal and point data on landslides, which are collected from a variety of sources, including federal, state, and local agencies as well as academic institutions. The inventory consistently reports information such as location, data sources, and oftentimes general characteristics (e.g., type and material involved). However, details like date of occurrence, fatalities, or damage are not always available. To account for challenges related to inconsistent reporting, data gaps, and varying levels of detail and coverage, the USGS classifies the collected landslides into five confidence levels using a semi-quantitative scale, ranging from 1 (lowest confidence) to 8 (highest confidence). Information on landslide damage is also part of the Swiss hazard inventory (Hilker et al., 2009). However, the problem here is that the inventory

is specifically made to report damage. Thus, each point (it is not a polygonal inventory) is located where the given phenomenon produced a financial loss rather than where the process started. This being said, the hazard inventory metadata also includes the date of occurrence and classifies each record by type, differentiating among "debris flows," "landslide," "rockfall" (and floods). Another example of a rich and open national landslide database is that of Colombia. Specifically, more than one exists, though they both fall within the Sistema de Información de Movimientos en Masa (Information System of Mass Movements) or SIMMA in short. The system allows access to what it refers to as a landslide catalogue or inventory. The first reports historical landslides obtained from secondary sources, civil protection or Red Cross, and because of this, it also contains a field indicating the potential uncertainty in the event location. As for other attributes, it reports the point coordinates, class and associated losses, either in the form of injured or victims and economic damage. Regarding the inventory, it essentially represents a better version of the former, mainly because landslides are recorded after mapping on the basis of satellite images (hence a better spatial identification of the event) and/or fieldwork activities. Even in this case, landslides are identified as points, and the attributes include time of occurrence, in addition to class and losses.

The diversity in all these systems limits the production of standard hazard and risk products, but the situation becomes even more dire when looking into a data-scarce context. For instance, African countries are mostly unequipped with a centralized landslide database and most of the available information is the outcome of individual efforts. In this sense, well known is the unifying effort made by Broeckx et al. (2018) and the data-sharing platform (link-here) maintained by the geomorphological team working at AfricaMuseum. There, national landslide inventories relative to Burundi, the Democratic Republic of Congo, and Rwanda can be openly accessed, and a number of associated studies can be found in Jacobs et al. (2017), Kubwimana et al. (2021), and Dille et al. (2019). Beyond the Central African sector, few additional studies cover regional (Monsieurs et al., 2018) and national (Niyokwiringirwa et al., 2024) scales in the neighboring areas. Moreover, even fewer of these consistently map landslides as polygons (Depicker et al., 2020), provide occurrence time (Deijns et al., 2024) and quantify elements at risk (Ferrer et al., 2024). To explore other data-scarce geographic contexts and some of the initiatives to close the gap with data-rich counterparts, we'll mention a few studies of relevance, which will also highlight variability in landslide reports even more. In this sense, the work of Chang et al. (2023) constitutes an example of exceptional richness focused on landslide mapping and risk assessment in Afghanistan. The authors themselves state that their national landslide inventory is the first of its kind, and with it, they produced the first robust national risk assessment. However, the time span for the landslide mapping only covers the period from 2015 to 2023, during which they only mapped 3,000 slope failures (left unclassified). In this sense, their work inevitably misrepresents failure mechanisms and temporal trends. Zooming out once again and looking across Asia, very few open databases exist. A further example is represented by the online Indonesian Disaster Data and Information Database (DIBI), which can be accessed online at DIBI-link. Notably, the landslide inventory provided by DIBI includes spatial and temporal information on recorded landslides as well as their consequences (Ngadisih et al., 2017). However, this data is limited to landslides causing fatalities. Moreover, this landslide inventory also lacks appropriate georeferences and information on landslides' sizes and volumes (Samodra et al., 2018).

It is with such observations in mind that we thought of exploring and documenting the limited literature on regional-to-national scale risk assessment. In fact, it is largely because of these inconsistencies, lack of data and international standards that the geoscientific community have not been able to provide methodological improvements. Given this background, this paper provides a comprehensive review of the relevant literature. Specifically, we analyze the literature on landslide risk, and thus, we also go through state-of-art approaches associated with several relevant concepts, including landslide susceptibility, hazard, exposure, and vulnerability. The literature review reveals that while there are studies modeling landslide occurrence on a regional/continental scale (Broeckx et al., 2018; Günther et al., 2014; Mirus et al., 2024; D. Wang et al., 2021), most risk assessments are either site-specific (Agliardi et al., 2009; Budetta, 2002; Corominas et al., 2019; Uzielli et al., 2015) or presented qualitatively (X. Liu & Miao, 2018) when applied to larger areas. To bridge this gap between theory and practice, we incorporate a case study at the continental level. By focusing on major European mountain ranges, we offer a textbook example of large-scale risk assessment. Specifically, the landslide risk analysis aims to estimate potential economic losses in terms of human properties (human settlements and agricultural areas). We do all the analyses based on geomorphologically meaningful hillslope partitions, Slope Units (SUs; Alvioli et al., 2016; Carrara, 1988; Giles & Franklin, 1998). Each one of these SUs constitutes the prediction target of a Binomial Generalized Additive Model (GAM) equipped with a bias capture/removal term (Steger, Brenning, Bell, & Glade, 2016). The bias we aim at removing is due to the inaccuracies of multiple landslide inventory sources (Loche et al., 2022), being originated by

different mapping groups and even national research organizations. This procedure allows for identifying the European landslide-prone areas in terms of spatial probability of landslide occurrence (i.e., susceptibility). Landslide risk is later computed, adjusting for the necessary approximations due to the size and complexity of the study area. Specifically, the landslide hazard is expressed via the occurrence probability due to the impossibility of quantifying landslide type, frequency and size across the whole European landscape. The spatial distribution of exposed elements and their associated economic values are computed using open data, such as the GHS-BUILT-S (Pesaresi & Politis, 2022) or CORINE Land Cover (Bossard et al., 2000) databases. The vulnerability of exposed elements is set to 1, that is, we hypothesize that in the occurrence of a landslide, any structure in its path would suffer irreparable damage. Similarly to the hazard case, such simplification is due to the lack of continent-wide vulnerability data: intensity of the phenomenon and structural resistance of the elements at risk (Glade, 2003b). The integration of these data allows for defining landslide risk throughout the European mountain ranges. Furthermore, the analysis explores the population at risk within the study area. Notably, we provide a cartographic representation that illustrates the population at risk during both daytime and nighttime. This representation is achieved by combining the spatial distribution of landslide susceptibility with population density data for each daily context. This overall protocol is to date, the most comprehensive in the literature, and we assume its findings to be useful even beyond the context of academic research. It is the product of a large-scale collaborative initiative that has involved several national geological agencies in Europe. The findings are meant to provide valuable insights into the varying degrees of potential economic losses faced by different regions. This knowledge can inform land-use planning, risk reduction strategies, and emergency preparedness and ultimately contribute to more resilient European societies and sustainable development in landslide-prone areas. By addressing these critical aspects, we aim to contribute to the ongoing efforts to mitigate the impacts of landslides and foster a more resilient Europe. For this reason, we opted to share our results in an interactive Web Application (WebApp), accessible at this link: https://pan-european-landslide-risk.github.io/.

2. Review of Landslide Risk Assessment

Analyzing landslide risk is a complex procedure that presents several challenges. These vary with the scale of the analyses and they arise from various factors, including data limitations, associated uncertainties and the dynamic nature of landslides (C. Van Westen et al., 2006). The first and most exhaustive definition of landslide risk has been provided by Varnes (1984), who denotes it as the expected number of lives lost, persons injured, damage to property and disruption of economic activity due to a particular damaging phenomenon for a given area and reference period. This definition has been translated into mathematical form and modified with time by numerous geoscientists, with seminal contributions on the topic such as Fell (1994), Leroi (1996), Lee and Jones (2004), and Corominas et al. (2014, 2023). In this overall context, if we consider the scenario of a single landslide, the risk can be analytically expressed as follows:

$$R = P(M_i)\,P(X_j|M_i)\,P(T|X_j)\,V_{ij}C, \tag{1}$$

where the risk (R) is related to a landslide of magnitude (M_i) affecting a specific element depends on the distance (X_j) between the element itself and the landslide source. Then, $P(M_i)$ denotes the probability of occurrence of a landslide with magnitude M_i, whereas $P(X_j|M_i)$ is the probability of a landslide reaching the element at risk located to a distance X from the landslide source and with an intensity j. $P(T|X_j)$ is the probability that an element will be present at place X at the time of occurrence of landslide (T), V_{ij} is the vulnerability of the element to a landslide with magnitude i and intensity j and C is the value of the element.

If we extend the scenario to multiple landslide occurrences, the risk Equation 1 can be re-written as follows (C. Van Westen et al., 2006):

$$R = \sum\left(H\sum(EV)\right) \tag{2}$$

where the landslide risk (R) is given by Hazard (H), Exposure (E) and Vulnerability (V) of elements at risk.

As seen in the equations presented above, the susceptibility is just one element of the landslide hazard definition (Caleca et al., 2022; Lombardo et al., 2021) and similarly, the hazard itself is an element of the risk definition (Corominas et al., 2014; Fell & Hartford, 2018). Exposure and vulnerability, on the other hand, could be expressed in multiple ways, associated with interactions between hazards and elements under consideration.

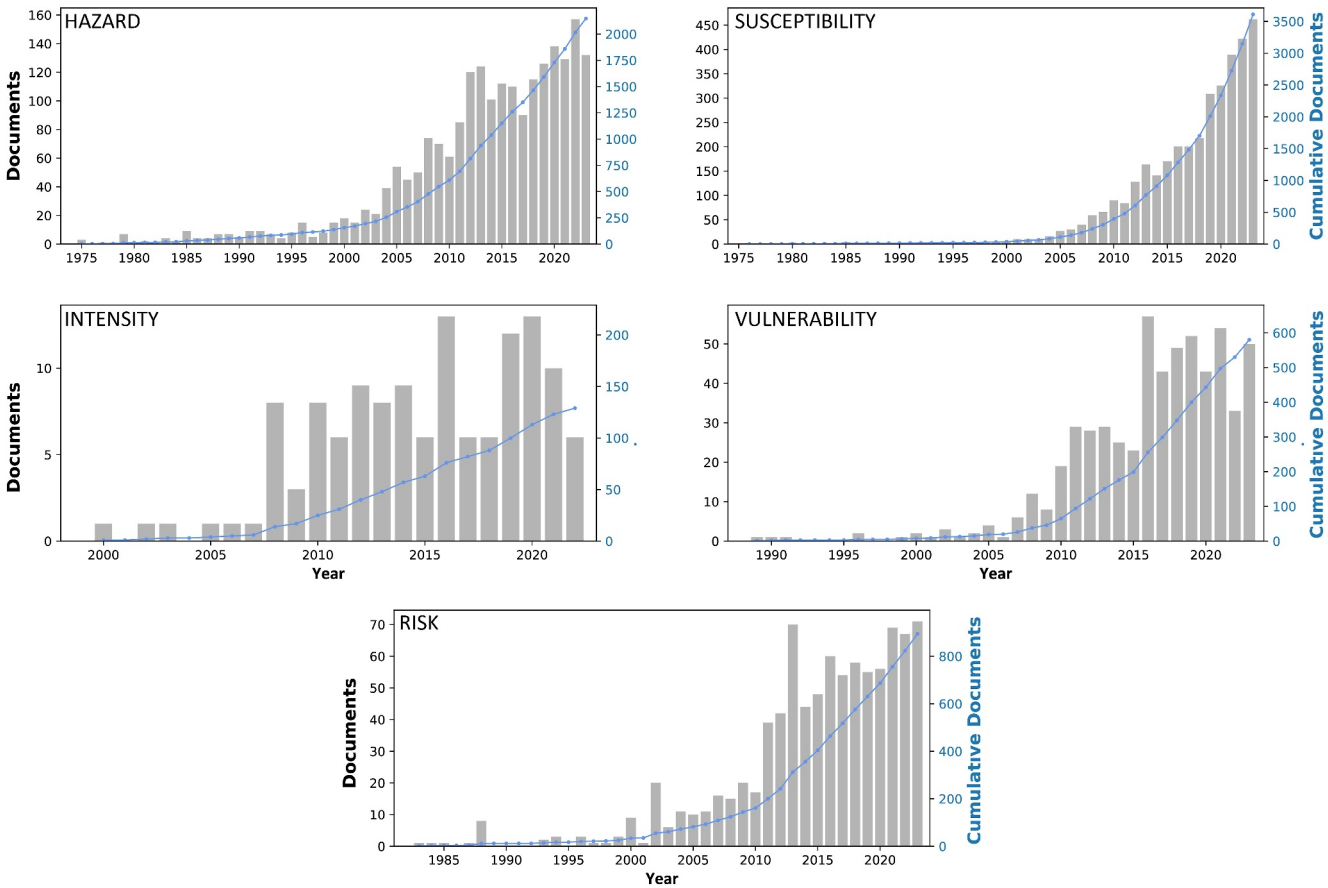

Figure 1. Temporal distribution of scientific contributions on landslide hazard, landslide susceptibility, landslide intensity, vulnerability, and landslide risk. The data collection is realized on the Scopus database by using specific criteria. For landslide hazard, data are filtered using "landslide hazard" in the title or keywords. For landslide susceptibility, data are obtained using "landslide susceptibility" in the title or keywords. For landslide intensity, data are retrieved using "landslide intensity" or "landslide magnitude" or "landslide destructiveness" in the title or keywords. For vulnerability, data are filtered using "vulnerability" and "landslide" in the title or keywords. For landslide risk, data are obtained using "landslide risk" in the title or keywords.

In this context, these aspects do not belong to the geomorphological sphere but rather represent an interdisciplinary topic (Gill et al., 2021). Specifically, the estimation of exposure and vulnerability should also take into account socio-economical dimensions as well as elements of structural engineering and urban planning. Overall, each risk component and the risk itself should be estimated separately depending on the landslide type. Notably, each landslide type, whether rockfall, debris flow, or rotational slide, presents distinct characteristics in terms of their mechanic, triggers, velocity and materials involved. Given these differences, the definition of the risk components should theoretically require tailored assessments.

However, due to the difficulty in collecting information required to identify each of these elements, small-scale landslide risk studies mostly exploit simple indicators or are based on some assumptions simplifying the given risk definition (Abella & Van Westen, 2007; de Almeida et al., 2016; Pereira et al., 2020; Segoni & Caleca, 2021). Below, we provide an overview of each of these elements required to assess the landslide risk.

2.1. Review of Landslide Hazard Assessment

Analyzing where a landslide will occur (spatial component), when it will be triggered (temporal component) and how large (magnitude or intensity component) it will be, represent the necessary requirements to assess landslide hazard (Guzzetti, 2005; Guzzetti et al., 2005). Many approaches have been proposed by the geoscience community to quantify hazard and each of its components. However, the term "hazard" has been historically confused with "susceptibility," as explained in details by Reichenbach et al. (2018). In short, the first definition of landslide hazard is what later became known as susceptibility. This, in turn, has led to some confusion (Corominas et al., 2023), especially in the early transitioning years from the old definition to the latest one. In Figure 1, we

provide an overview regarding the scientific trends from the earliest documents in landslide literature until today, reporting all the contributions per year of each individual risk components. To do so, we searched on Scopus the contributions related to landslide hazard, susceptibility, intensity, vulnerability, and risk. Notably, we do not report exposure because the associate distribution through time is essentially the same as landslide risk, because whenever exposure is assessed, this is done specifically for risk purposes.

2.1.1. Review of Landslide Susceptibility Assessment

The component pertaining to the spatial occurrence probability, or susceptibility, is the most studied one (Figure 1) and its quantification has witnessed a substantial improvement over the last decades. Expert-based mapping (Brabb et al., 1972) has been initially superseded by heuristic approach (Stanley & Kirschbaum, 2017b), and later by physics-based (Formetta et al., 2016) and statistical analyses (Pardeshi et al., 2013), or machine (Marjanović et al., 2011) and deep learning approaches (Dahal et al., 2022). Expert-based mapping depends on the skills of the investigator, and therefore it might not provide objective products. In heuristic approaches, the investigator weighs specific properties related to the landslide-triggering and provides a semi-quantitative mapping (Leoni et al., 2009). Despite the possibility of obtaining reliable zonations, these approaches can not be reproduced over large areas (Crozier & Glade, 2005; C. Van Westen et al., 1999). Physically-based models rely on understanding the mechanism behind failure conditions, and thus, they could provide accurate assessment regarding slope stability or amount of displacement for a given set of conditions if the relevant geotechnical parameters are available (Alvioli & Baum, 2016; Medina et al., 2021; G. Rossi et al., 2013). They need a large and detailed data set describing mechanical and hydrological properties (Tofani et al., 2017), which restricts their use to a limited geographic extent (Formetta et al., 2014; Seyed-Kolbadi et al., 2019). Nevertheless, few examples do exist in the literature where such limitations are suitably addressed (Cuomo et al., 2021; Medina et al., 2021; Salvatici et al., 2018). Lastly, statistical and machine/deep learning approaches belong to the family of data-driven methods. These techniques statistically evaluate the combination of factors that have triggered landslides in the past. This is done by analyzing the relationship between those factors and the past/present distribution of a landslide population through a landslide inventory (Carrara, 1983; Guzzetti et al., 1999; Ohlmacher & Davis, 2003; Reichenbach et al., 2018; C. J. Van Westen et al., 2008). In data-driven methods, the dependent variable is usually represented via a binary structure (i.e., landslide presence or absence) in each mapping unit. Therefore, the fitted model is used to predict whether a mapping unit will trigger (or not) a landslide. The output may be expressed in terms of probability or classified into different susceptibility levels. However, data-driven methods can also be affected by several shortcomings: (a) the general assumption that future landslides can occur under the same past conditions (Guzzetti, 2021), (b) the effect of some factors can vary with complex settings (Lombardo & Mai, 2018), and (c) the propagation of uncertainties and systematic errors of landslide inventories can lead to biased outputs (Steger, Brenning, Bell, & Glade, 2016; Steger, Brenning, Bell, Petschko, & Glade, 2016). Evidently, no single approach exists, nor is it universally accepted. The choice mainly depends on the scale of analysis and the availability of data on landslide occurrence and triggering conditions.

In recent years, researchers have extended this susceptibility framework to account for the temporal aspects in a single space-time modeling solution (Lombardo et al., 2020; Nocentini et al., 2023). These models differ from the traditional susceptibility because they simultaneously predict landslides both over the geographical space and the time of interest, which can vary from years (Finlay et al., 1997) to days (Mondini et al., 2023) and even down to the hour resolution (Cao et al., 2022). Whenever the temporal unit corresponds to a large interval, the corresponding landslide prediction is usually generated with the purpose of supporting master planners to optimize long-term investments (Ko & Lo, 2018). Conversely, whenever the prediction involves short-term intervals, the output of such models is typically integrated as part of early-warning systems (Segoni et al., 2018). Despite individual differences, the element in common among these temporal models lies in the ability to capture the dynamic changes in landslide distributions across different time windows by integrating various spatiotemporal predisposing, preparatory and triggering factors (Steger et al., 2023). As a result, they provide valuable insights into potential landslide occurrences and their patterns over specific regions and periods (N. Wang et al., 2022). These models offer a comprehensive approach to understanding the complex interactions between geological, meteorological, and environmental factors that influence landslide events, ultimately enhancing our ability to predict landslide occurrences. The main limitation in creating such models corresponds to the acquisition of data on past landslides because most landslide inventories unfortunately still do not report occurrence dates (Guzzetti et al., 2012). This lack of temporal information is not only due to omissions during the mapping phase but also

stems from the challenges of accurately defining these dates, even when using remote sensing products. Therefore, it is a common practice to assume that failure conditions may not change during the time and approximate the landslide hazard to the simple spatial probability of occurrence. In other words, the landslide susceptibility is often used as a proxy for hazard (Caleca et al., 2022; Corominas et al., 2014).

2.1.2. Review of the Assessment of Landslide Temporal Occurrence

The development of space-time predictive models is a recent solution in the context of landslide hazard assessment (Fang et al., 2024). Despite this step forward, the evaluation of the temporal probability of landslide occurrence still represents a challenge. This component is generally represented in the form of frequency (i.e., number of events per time interval), return period, or exceedance probability (Corominas et al., 2014). The literature proposes different approaches for assessing the temporal occurrence of landslides, and they essentially follow a similar structure to that of the susceptibility case. They can, in fact, be grouped into distinct families: heuristic, probabilistic, indirect, and physically-based methods. Heuristic methods rely on the investigator's judgment, with interpretations that can be quantified through probability assignments (Wong, 2005).

Probabilistic techniques seek to model the probability of an event occurring within a given time frame. These approaches involve the analysis of time series of past landslide events, allowing for frequency extrapolation. The temporal probability of occurrence is then defined by employing suitable models, such as the binomial or Poisson model (Catani et al., 2005; Corominas & Moya, 2008; Crovelli, 2000; Guzzetti et al., 2005; X. Li et al., 2023). The main drawback of these approaches lies in the assumption that landslides are random and independent occurrences. This assumption is inadequate for landslides, given their inherent dependence on a multitude of factors, such as climatic or anthropogenic conditions, but also in the fact that the same slopes may present characteristics that promote or reject future slope failures. For instance, if a debris flow mobilizes all the soil columns, the very same slope will not be susceptible to the same process until the weathering has generated enough potentially unstable material in the future (Parker et al., 2016). Similarly, a deep-seated landslide is a phenomenon that not only persists for long periods on the same slope but also affects the slopes nearby. Thus, there may be some degree of dependence between one landslide and the next, both in space and in time (Lombardo et al., 2020). Another limitation is related to the requirements of such models. Landslide inventories have to contain temporal details for temporal probabilities to be obtained. However, this is a condition which is not met in many areas around the globe (Guzzetti et al., 2012).

The indirect modeling of landslide temporal occurrence relies on the assumption that the return period of a trigger (e.g., rainfalls or earthquakes) might be the same as the landslide (Chau et al., 2004; Grant et al., 2016; Martino et al., 2020; Peres & Cancelliere, 2018). As a result, after selecting the magnitude of the reference trigger and its relative return period, it is possible to assume the same for landslides (Frattini et al., 2009; Jaiswal & van Westen, 2009; Tsunetaka, 2021). This allows for estimating how frequently landslides may occur in the study area but not which slope will be unstable.

Physically-based approaches are the only ones to consider slope instability conditions by accounting for both spatial and temporal dependence (Alvioli & Baum, 2016; Aristizábal et al., 2016; Salvatici et al., 2018; Schilirò et al., 2016). However, they are only applicable to limited areas (e.g., slope or catchment scale) and short time intervals (a few hours to a few days), mostly because required parameters such as geological and geotechnical data are prohibitive to reliably collect over larger areas. Ultimately, assessing the temporal occurrence of landslides lacks a universally accepted approach. The selection of the more appropriate technique depends on the scale of analysis as well as the availability and quality of historical landslide data.

2.1.3. Review of Landslide Intensity Assessment

A further component related to landslide hazard, especially when the study case is limited in its extension, is represented by the intensity of the phenomena. Landslide intensity expresses the destructiveness power of the event. Therefore, it is mainly associated with the energy released by the landsliding event (Ferro et al., 2020) and depending on the type of landslide, it can be represented by a function of landslide's movement velocity and depth, deposit thickness, impact pressures, depth of erosion, differential movements, or strain (Hungr, 1997). Similarly to the occurrence probability case, even the intensity has been addressed in a number of different ways. Specifically, researchers have attempted to define the destructive potential of landslides by employing a range of parameters: planimetric area (Moreno, Steger, et al., 2023), initial (Jaboyedoff et al., 2020) or total (Brunetti et al., 2009)

volumes, number of events (Lari et al., 2014), runout (Jakob et al., 2005), or velocity (Pudasaini & Krautblatter, 2022). These parameters are listed above, and thus, the intensity assessment could vary for different landslide types. In fact, the definition of landslide includes very different phenomena (Hungr et al., 2014). Therefore, each landslide class requires a different approach to identify the corresponding intensity component. For instance, in the case of slow-moving landslides, either the differential displacement or the total displacement is utilized to assess the potential damage or disruption to structural elements (Corominas et al., 2014) using the magnitude of the event as index (Guzzetti, Galli, et al., 2006). Especially when dealing with these types of movements (Lacroix, Handwerger, & Bièvre, 2020), the intensity can be estimated by utilizing data on ground deformation as a proxy for velocity (Tofani et al., 2014). This data can be obtained through in-situ measurements (Artese & Perrelli, 2018; Corominas et al., 2000; Moss, 2000) or remote sensing techniques, the most common making use of Interferometric Synthetic Aperture Radar (Caleca et al., 2022; Raspini et al., 2018; Solari et al., 2020). Conversely, fast-moving landslides (e.g., debris flows, shallow landslides) cannot be monitored through remote sensing and they rather require numerical scenario-based simulations (D'Ambrosio et al., 2003; Van den Bout et al., 2021).

2.2. Review of Exposure Assessment

Exposure is also a fundamental component that explains the interaction between hazard and elements at risk. This refers to the characteristics of individuals, assets, infrastructure, or any other elements within the areas that could be affected by landslide impacts (Emberson et al., 2020; Lee & Jones, 2004). This aspect is likely the least explored in the landslide literature (Maes et al., 2017; Pellicani et al., 2014), although it is well represented for other natural hazards, for example, storms or earthquakes (see, Crowley & Bommer, 2006; Dell'Acqua et al., 2013; Liao et al., 2019). The exposure of an element is determined by its position relative to the path of the landslide, which varies depending on the landslide kinematics (Corominas et al., 2014). As a result, the number and location of elements at risk differ depending on the type of expected landslide, be it a rockfall, a debris flow or a slow-moving landslide (Cánovas et al., 2016; Hantz et al., 2021; X. Wang et al., 2014). Due to this dynamic characteristic, quantifying the exposure to landslides involves a pre-required categorizing step where elements at risk are labeled as static or dynamic (Y. Li et al., 2021). The exposure evaluation of static elements, such as buildings, infrastructure, and agricultural areas, typically requires no extensive investigation because their information can be generally accessed through cadastral archives (Hunter & Williamson, 1990) or through remote sensing products (C. Liu et al., 2019). Conversely, assessing the exposure of moving elements, including people and vehicles, presents significant challenges and entails estimating conditional probabilities (spatial and temporal) of their presence at the time when a given landslide might occur (Fell et al., 2005; C. Van Westen et al., 2006). For the assessment of population exposure, the quantification is based on the number of human lives exposed (Maes et al., 2017), whereas, for physical assets (e.g., buildings, infrastructure, or agricultural areas) their exposure is determined by their monetary value (Burns et al., 2017). Therefore, the accuracy of exposure assessment heavily relies on the quality of such data (Di Napoli, Miele, et al., 2023). However, recent advancements have seen an increase in high-resolution data covering extensive regions and even global scale. This improvement in data availability has facilitated more refined and comprehensive exposure assessments in risk studies (De Bono & Mora, 2014; Emberson et al., 2020; Pittore et al., 2017; Scaini et al., 2023).

2.3. Review of Vulnerability Assessment

Aside from all these nuances, the vulnerability of exposed elements is related to the impact of an adverse event on them. Therefore, its assessment is largely dependent on the estimation of landslide intensity and related effects on exposed elements (Promper et al., 2015). Such consequences are expressed in terms of damages or losses on a continuous numerical scale ranging from zero (no damages/losses) to one (total damages/losses) (Alexander, 2005; Galli & Guzzetti, 2007).

Vulnerability can be split on the basis of the exposed elements: leading to a division in physical and social vulnerability. Physical vulnerability refers to the impact on buildings, infrastructures and utilities (Papathoma-Köhle et al., 2011). Conversely, social vulnerability determines whether a landslide event will cause injuries or fatalities (Antronico et al., 2020). Ideally, social vulnerability should also take into account the inequalities that inevitably predispose specific social groups in the context of a potential disaster (Hewitt, 2014; Tapsell et al., 2010). Because of this dual aspect, vulnerability analysis is a research topic that has been addressed via multiple communities, involving engineers, as well as natural and social scientists (Glade, 2003b). As a result, its

quantification has also been tacked with a proportional number of approaches, featuring two main approaches: judgmental/heuristic as well as data-driven or analytical methods (Corominas et al., 2014).

On the one hand, judgmental/heuristic approaches use expert opinion to evaluate the potential degree of damages or loss (Bell & Glade, 2004; Kang & Kim, 2016). As a consequence, they are somewhat subjective and strongly dependent on the specific case study (Ngadisih et al., 2014). On the other hand, data-driven methods represent a quantitative approach to evaluate vulnerability as a function of the landslide intensity and are frequently applied thanks to their simplicity, reliability and lower degree of subjectivity (Fuchs et al., 2019; Singh et al., 2017).

A careful assessment of the available literature shows that buildings are the most addressed typology of elements at risk considered in vulnerability studies (Luo et al., 2023). The reason lies in the fact that it is much easier for buildings to gather damage data based on the intensity of past events and consequently lay the foundations for building data-driven models. These are generally expressed in terms of vulnerability curves, whose estimation comes from regression analyses aimed at linking the hazard intensity to the losses (Agliardi et al., 2009; Peduto et al., 2017). Alternatively, some models opt to estimate fragility curves. These boil down to functional relations between landslide intensity and the probability of exceeding a specific building damage state (Del Soldato et al., 2019; Fotopoulou & Pitilakis, 2013; Mavrouli et al., 2014).

Differently from the physical vulnerability case, assessing social vulnerability poses greater challenges due to our society's diverse and distinct characteristics, leading to social imbalances in various parts of the world (Cutter et al., 2013). Despite its complexity, social vulnerability analysis is an essential component of landslide risk assessment, and a commonly used method for this purpose is the Social Vulnerability Index (SoVI; Y. Xiao et al., 2022). SoVI is a quantitative tool that combines multiple indicators related to social factors, such as income, education, age, access to resources, and population density (Nor Diana et al., 2021). These indicators are often weighted according to their influence on vulnerability levels. The resulting SoVI value calculates the degree of vulnerability for a specific area or community (Guillard-Gonçalves & Zêzere, 2018; Wijaya & Hong, 2018).

2.4. Historical Development: An Overview Across Spatial Scales

The combination of all elements described above (landslide hazard modeling, exposure, and vulnerability analyses) constitutes the foundation of a complete landslide risk analysis (Fell et al., 2005). Notably, the complete application of Equation 1 and Equation 2 allows for estimating landslide risk in quantitative terms. However, landslide risk assessments are heavily related to the scale of analysis (Corominas et al., 2014). Therefore, it is not always feasible to estimate the risk components in a strictly quantitative manner. For instance, in a risk analysis of a specific landslide event, it is possible to conduct a detailed assessment of the landslide hazard and to model its run-out. This implies a fully understanding of what elements are exposed and how vulnerable they are to the given landslide (L. Xiao et al., 2020). Accordingly, landslide risk may be expressed through multivariate approaches and diagrammatic representations. In the multivariate context, it is essential to establish representative risk scenarios (Guo et al., 2020). In turn, this refers to risk values associated with an object or geographical region that can be visually depicted through risk curves. These curves express the relation between all probabilistic events and the corresponding losses (Fu et al., 2020; Martha et al., 2013). In the context of human lives, landslide risk is often expressed through F-N curves (Jaiswal et al., 2011; Morgenstern, 2018). These curves illustrate, in graphical form, the cumulative frequency of N or more fatalities (F) against the number of fatalities (N), typically plotted on a log-log scale (Reeves et al., 1999; Sim et al., 2022). However, when the extent of the study area increases (e.g., regional or even larger spatial extents), Equations 1 and 2 cannot be completely solved because not only is the required data often unavailable, but spatial variance also becomes a limiting factor. In such cases, the results of landslide risk assessments can be presented in a univariate format, typically as economic losses per year (Peng et al., 2015; Remondo et al., 2008) or per mapping unit (Bednarik et al., 2012; Erener & Düzgün, 2013; Pereira et al., 2017).

To summarize, the literature on landslide risk from 2000 showed remarkable growth (Figure 1) in the number of scientific contributions (Lei et al., 2023). The observed rise can be ascribed to the widespread adoption of Geographic Information System (GIS) techniques, which have been extensively utilized as a tool for conducting spatial data analysis and graphical depiction in diverse fields, encompassing the domain of landslide risk assessment (Carrara et al., 1991; Rautela & Lakhera, 2000; C. Van Westen, 2004). Building upon the foundations laid during the previous years, the field of landslide risk assessment further experienced consistent advancements from 2005, mainly in the form of high-resolution data inclusion and the development of new approaches

(Caleca et al., 2022; Novellino et al., 2021; Peng et al., 2015; Remondo et al., 2008; Saleem et al., 2019). Focusing on the spatial scale at which these risk studies have been applied, what emerges is that the analyses are vastly site-specific and hardly go beyond this level (Corominas et al., 2005; Ferlisi et al., 2012; Karantanellis et al., 2020), with very few regional-scale contributions (Catani et al., 2005; Hidalgo & Vega, 2021; Remondo et al., 2005; Vranken et al., 2015). Similarly, contributions addressing national cases are rare in the literature (see; Dorren et al., 2009; Gaprindashvili & Van Westen, 2016). Conversely, when dealing with continental scale, the analysis boils down to a rough identification of regions where landslide hazard and the corresponding risk might be elevated (see; Jaedicke et al., 2014). More generally, risk analyses involving large landscapes are usually implemented by means of simple indicators (see; Abella & Van Westen, 2007; de Almeida et al., 2016; Pereira et al., 2020; Segoni & Caleca, 2021). This is the current state of the literature and in this context, we see the potential for risk assessments encompassing extensive geographical domains. This should be achievable, especially in light of recent developments in impact-based digital archives. Such data sets offer the potential for conducting—at least—preliminary regional scale studies aimed at identifying areas likely to suffer losses and obtain rapidly updatable and easy-to-understand results.

3. European Mountain Ranges and Mapping Unit Partition

The Baltic Shield, the Hercynian Massif, the Alpine System, and the Carpathians are the principal geological settings across the European continent. Geomorphologically, Europe hosts different landforms ranging from rugged mountain ranges to coastal plains, river valleys, and glacial landscapes, a product of various erosional and depositional processes over time (Meeus, 1995). The Pleistocene glaciations have left a significant signature on the European landscape, with large ice sheets covering northern Europe, forming fjords in Norway, U-shaped valleys in the Alps and Scotland, and moraines and drumlins in places like Sweden and the British Isles (Buggle et al., 2013; Mahaney & Andres, 1991). Alongside these processes, the European landscape also underwent a post-deglacial phase when a prominent uplift and subsequent relief growth took place in response to isostatic adjustments. This is particularly evident across the Scandinavian landscape (Nielsen et al., 2009).

To perform our analyses, the study area is divided into 13 mountain zones (Figure 2a), each reflecting different geological settings. In this work, we use the *r.slopeunits* software proposed by Alvioli et al. (2016) to further partition the 13 mountain ranges into SUs. This decision follows an initial criterion where we set out to assess landslide risk across the main morphotectonic features of Europe. In this sense, focusing on these 13 zones satisfies the initial objective, leaving out only small and individual hills. As for the SU choice, we opt for these units for geomorphological, statistical and purely computational reasons. Geomorphologically, SUs successfully approximate the slope response. In other words, if a landslide occurs, its initiation (and in most cases also its propagation) will be confined within a single slope, or SU, with the exception of extremely large ones. Statistically, this also implies that labeling an individual SU as unstable will be largely independent of the stable/unstable condition of the adjacent units, a requirement of most data-driven models (Bergtold et al., 2010). Conversely, when using grid cells, assigning an unstable label to a small unit will most likely be dependent on its neighboring units. Computationally, an SU partition also ensures generating a relatively small data-matrix and, with it, limits the final computational burden. Continuing the parallelism with the grid-cell case, the choice of a small pixel may lead to data matrices thousands or even millions of times larger than an SU counterpart. In the case of a comparatively coarse grid-cell choice, then km-wide grids will span over contrasting morphometric characteristics, making the resulting model mostly unreliable.

The way *r.slopeunits* operates is for it to make exclusive use of a Digital Elevation Model as data entry. From it, the aspect (Zevenbergen & Thorne, 1987) is generated, and SUs are obtained by clustering slope exposition pixels following a hydrological criterion. In short, SUs are delineated between stream and divide lines, creating a fractal representation of sub-catchments. The notions summarized above are numerically translated into a number of parameters, which *r.slopeunits* requires. Specifically, the fractal representation of sub-catchments is expressed with the flow accumulation threshold and minimum surface area, two parameters that regulate the starting and ending planimetric extent targeted by the user. As for the aspect clustering procedure, this is regulated by the circular variance, a parameter that controls how rigidly (values close to 0) or flexibly (values close to 1) the calculation should allow for variations in aspect values within a single SU polygon. Notably, because of its relatively simple requirements, *r.slopeunits* has seen significant use in recent years (Amato et al., 2023; Schlögel et al., 2018). This has even stimulated other scientists to produce alternative SU generators (Al-Thuwaynee et al., 2023; F. Huang et al., 2021; K. Wang et al., 2019). More generally, this has been translated into several

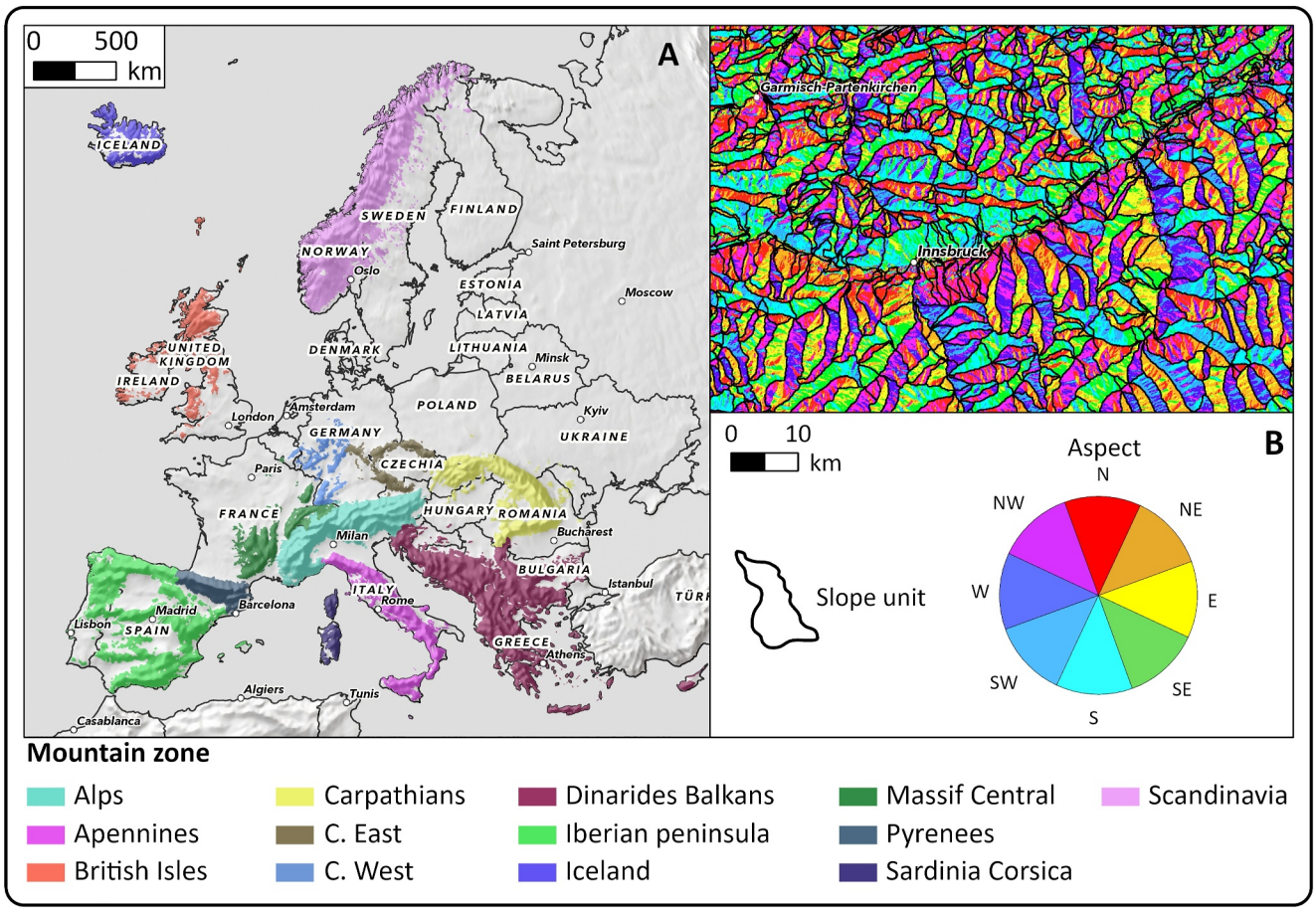

Figure 2. Panel (a) illustrates the different mountain zones in Europe. Panel (b) shows a detail of the Slope Unit partition using examples from Innsbruck.

contributions interest in the field of landslide occurrence modeling studies (Amato et al., 2019; Domènech et al., 2020; Lombardo et al., 2020).

In our case, the *r.slopeunits* configuration we adopt led to 570,635 SUs, with a mean surface extent of 3.6 km^2 and a variability of 4.2 km^2 measured in a single standard deviation. The exact parameters are: minimum area = 400,000; circular variance = 0.4; clean size = 200,000; threshold = 10,000,000; reduction factor = 10. For further explanation of what each of these parameters implies, we refer the reader to Alvioli et al. (2016).

3.1. Landslide Inventories

Landslide inventories are crucial to support any consideration or assessment involving susceptibility, hazard, and risk analyses (Corominas et al., 2014; Fell et al., 2008). In the current state, no unique and comprehensive European landslide inventory exists. Individual countries respectively host and maintain their own databases, which in most cases are either inaccessible or limitedly accessible (Foster et al., 2012; Jaedicke et al., 2009; Rosser et al., 2017). This leads to an overall scenario where the digital information on slope failures at the European scale is mostly incomplete. As a result, the true landslide occurrence can be largely underestimated in specific locations (Herrera et al., 2018). Exhaustive information on the structure and availability of landslide inventories among European countries has been widely analyzed by different authors in the last decade. For instance, Van Den Eeckhaut and Hervás (2012) and Herrera et al. (2018) summarized the state-of-art on this topic. The very same data set was used here to model the landslide occurrence probability over Europe. Specifically, we collected 17 inventories among national, regional and local European administrations intending to cover the main mountain ranges. The information on the collected data is summarized in Table 1.

Table 1
Overview of the Collected Landslide Inventories Across European Countries

Country/Region	Mountain domain	Repository
Austria	Alps	Link-At
Bavaria (Germany)	Alps and Central West	Link-De
Chania, Karditsa (Greece)	Dinarides - Balkans	Link-Gr
Czechia	Central East and Carpathians	Link-Cz
France	Alps, Massif Central, Pyrenees and Sardinia-Corsica	Link-Fr
Great Britain	British Isles	Link-Uk
Iceland	Iceland	Link-Is
Ireland	British Isles	Link-Ie
Italy	Alps, Apennines and Sardinia - Corsica	Link-It
Norway	Scandinavia	Link-No
Portugal	Iberian peninsula	Link-Pt
Romanian Carpathians (Romania)	Carpathians	Link-Ro
Slovakia	Carpathians and Central East	Link-Sk
Slovenia	Dinarides - Balkans	Link-Si
Spain	Pyrenees and Iberian peninsula	Link-Es
Sweden	Scandinavia	Link-Se
Switzerland	Alps, Massif Central and Central West	Link-Ch

Overall, we collected 1,034,700 landslides. These landslides geographically fall inside 66,764 SUs, or 11.7% of the total units. Out of all the European mountain ranges, the Apennines and Alps are the ones that host the largest amount of landslides, with 87.3% of all the ones we collated. Such observation is already an indicator of a substantial unbalance in the European database we collated. One may argue that this may be a natural distribution. However, it is much more logical to assume that the human factor controls the spatial distribution and frequency of landslide occurrences in the data, expressed explicitly in how geological surveys operate in landslide mapping or in how they transfer the mapping responsibilities to other agencies or professional groups. This is, for instance, the case highlighted by Loche et al. (2022) among different regions in Italy. Therefore, the situation can only be more diversified when different countries are involved. As a result, if one would generate a susceptibility model trained over SUs labeled as stable and unstable based on the landslide distribution over Europe, the results would potentially reflect heightened occurrence probabilities at locations where more landslides are reported but not necessarily where the susceptibility is actually high. In the context of susceptibility modeling, these issues are typically addressed by including some bias-removal procedure in the modeling, which is also the strategy adopted in this work. Further technical explanations on this topic will be provided in Sections 3.2.2 and 4.

Notably, in this specific case where we do not have access to consistent temporal information for each European landslide, we simply focus on estimating and removing spatial biases. However, temporal biases are also to be generally expected over wide regions (Steger et al., 2024). In the literature, this is mostly mentioned in relation to recent improvements in the quality and frequency of orthophoto and satellite data acquisition, in contrast to older inaccurate reports and low-quality aerial cartographic support (Niyokwiringirwa et al., 2024).

3.2. Covariates

The selection of an appropriate set of covariates to explain the distribution of stable/unstable slopes is a fundamental requirement that should always have a dual connotation in any data-driven model. The first (qualitative) aspect concerns choosing a covariate set that follows a geomorphological criterion (Budimir et al., 2015). In other words, an initial screening is performed by any user, who typically opts for a set of predisposing and triggering factors, whose role in the model is to explain directly or as proxies some parameters or quantities tied to the physics of the process under consideration. The second (quantitative) aspect in selecting a

Table 2
Covariates' Overview: Names, Description and Acronyms

Covariate	Description	Acronym
Country	Country to which the SU belongs	*Zone*
Length of infrastructures	Total length of infrastructures within SU	I_L
Slope μ	Mean of slope steepness within SU	SL_μ
Slope σ	Standard deviation of slope steepness within SU	SL_σ
Distance to active faults	Distance between the SU centroid and nearest seismogenic active fault	*D2F*
% Land use change	Total percentage in terms of land use change within SU	LU_C
NDVI μ	Mean of NDVI over 20 years within SU	$NDVI_\mu$
Cumulated yearly rainfall μ	Mean of cumulated yearly rainfall over 20 years within SU	AR_μ
Profile curvature μ	Mean of profile curvature within SU	PrC_μ
Planar curvature μ	Mean of planar curvature within SU	PlC_μ
Lithology	Dominant lithology class within SU	*LIT*
Northness μ	Mean of northness exposure of SU	NN_μ
Eastness μ	Mean of eastness exposure of SU	EN_μ

suitable set of covariates should follow a numerical criterion directed to removing any redundant information (Van Der Linde, 2005).

In this manuscript, two additional elements conditioned the strategy for the choice of a suitable set of covariates. These correspond to the lack of information on the type of landslides, due to the continental nature of the inventory we collated. And, the second boils down to the geomorphological complexity of the mountain regions under consideration. For this reason, we decided to collect a very large data set of independent variables expressing the general environmental characteristics, and the meteorological conditions (e.g., slope steepness, rainfall data). From this large set, we plan to isolate the most relevant covariates by undertaking a penalized variable selection (Marra & Wood, 2011).

However, such a scheme would not work in a situation where a strong bias affects the data. In fact, one or more variables in the set could be partially sensitive to the bias (share part of the spatial patterns with it). As a result, the estimation of the regression coefficients could be influenced and ultimately lead to classification results whose performance may seem high, but whose susceptibility patterns would reflect artifact trends. This topic is extensively discussed in the following articles, and we refer the reader to these for understanding multi-scale bias propagation issues in landslide susceptibility studies (Lima et al., 2021; Lin et al., 2021; Loche et al., 2022; Stanley & Kirschbaum, 2017b; Steger et al., 2021; Steger, Brenning, Bell, & Glade, 2016).

The same articles mentioned above offer solutions to minimize the propagation of inventory biases into any susceptibility model. Among them, the most elegant and accepted solution consists of the introduction of a covariate that has a strong association with the bias. Its role would be to capture all the spatial dependence related to the incompleteness of the landslide inventory, leaving the estimation of the remaining covariate effects unaffected. As a result, one can then remove the bias covariate from the additive structure of the model and produce bias-removed probability estimates. It is for this reason that the following two subsections will separately present the covariates that we choose to carry the susceptibility signal (see, Section 3.2.1) and the covariates that we chose to capture and remove the bias from the model (see, Section 3.2.2). A generic list of all tested covariates can be found in Table 2. As for how we performed the penalized variable selection, the relative explanation is presented in Section 4.1.

3.2.1. Bias-Unrelated Covariates

The covariates we choose to explain European landslides' predisposing and triggering factors include geomorphological, geological, meteorological and land use properties. The morphometric ones are obtained

from the Copernicus GLO-90 DEM (https://doi.org/10.5270/ESA-c5d3d65), namely: (a) slope steepness (Zevenbergen & Thorne, 1987); (b) eastness and northness (Fassnacht et al., 2012); (c) profile and planar curvature (Moore et al., 1991). We also include a proxy for seismicity computed as the distance between the centroid of each SU from the nearest seismogenic active fault (provided by Danciu et al. (2021)). The meteorological proxy is obtained instead as the mean annual rainfall over the past 20 years of NASA global precipitation measurement data (see, Huffman et al., 2015). We also incorporate vegetation density as the mean annual Normalized Difference Vegetation Index (NDVI; Pettorelli et al., 2005), referred to the last 20 years of LANDSAT 7 imagery (Masek et al., 2006). As for the lithological signal, each SU is assigned the dominant class, whose information was accessed through the map made by Wilde et al. (2018). We also include land use, not in its raw expression but rather in terms of land use change (Glade, 2003a). We do so by computing the percentage change of each land use class per SU, over the last 20 years of MODIS data (Justice et al., 2002). Notably, we opt for MODIS instead of the CORINE Land Cover database (Bossard et al., 2000) because the last update of the European-specific product dates back to 2018, and also excludes information on areas such as the Ukrainian Carpathians.

During the pre-processing phase of any SU-based model, summarizing the variability of high-resolution predictors over the polygon extent of each mapping unit is required. For instance, in Section 3, we report a mean SU planimetric area of 3.6 km^2, while in this Section, we mentioned the use of a 90 m resolution Copernicus DEM. As a result, an average SU in our European delineation theoretically contains 444 grid cells (3.6 km^2 divided by 0.0081 km^2). We assign each SU the mean and standard deviation values to reflect the associated covariate distribution. This is a common procedure (Guzzetti, Reichenbach, et al., 2006), justified whenever the covariate distribution per SU is normal or close to it (see Figure 3 in Lombardo and Tanyas (2020)). Notably, alternatives do exist in the form of a quantile covariates' representation (Amato et al., 2019), but such a choice would increase the predictor space. For this reason, in the context of the large SU number we generated over Europe, the choice of a dual representation (μ and σ) ensured the least complexity.

To provide an overview, we list the predictors and their statistical properties in Table 2.

3.2.2. Bias-Related Covariates

To capture the spatial variability in the data due to national patterns of inventories' completeness rather than natural characteristics, we used two covariates. These are: (a) national country of the institutions that have generated the different inventories (see, Loche et al., 2022; Meinhardt et al., 2015); (b) total spatial distribution of transportation infrastructure per SU (see, Stanley & Kirschbaum, 2017a; Steger et al., 2017) computed using the OpenStreetMap database (Haklay & Weber, 2008). We recall once more that such properties will not be strictly used for susceptibility modeling. They will enter the regression procedure only during the initial stage, with the aim of capturing the effect of various mapping organizations (the i^{th} case mentioned above) or the greater tendency to report landslides along transportation lines (the ii^{th} case mentioned above). For predictive/mapping purposes their contribution to the model will be forced to zero, effectively removing the bias.

4. European Landslide Susceptibility Modeling

Below, we briefly provide a comprehensive overview of the model adopted to estimate landslide occurrence probabilities across the main European mountain belts, the choice of validation routines and the related performance assessment.

4.1. Generalized Additive Models

Generalized Additive Models (GAMs) represent a class of statistical models that extend the Generalized Linear Model (GLM) by allowing for the incorporation of non-linear relationships between independent and dependent variables. These non-linear associations are accommodated using smoothing functions in the form of splines (Hastie & Tibshirani, 1987). Thus, independent variables can be employed in either linear or non-linear forms, leading to high flexibility and associated performance. This characteristic enables the approach to be categorized within the interpretable machine learning family (Molnar, 2020). Consequently, owing to their transparency and interoperability, GAMs have found extensive application in geomorphological studies, mainly in the form of landslide susceptibility (Brenning et al., 2015; Goetz et al., 2015; Loche et al., 2022; Steger, Brenning, Bell,

Petschko, & Glade, 2016). GAMs are versatile in handling various statistical distributions, including but not limited to binomial, Poisson, and Gamma (see, Yadav et al., 2023). In the context of landslide susceptibility, where the response variable indicates the presence or absence of landslides for each mapping unit, a Binomial GAM is often chosen, this being also the case for the present contribution. The general structure of the Binomial GAM we implement can be expressed as follows:

$$\log\left(\frac{p}{1-p}\right) = \beta_0 + \beta_{NN_\mu} NN_\mu + \beta_{EN_\mu} EN_\mu + \sum f_1(Zone, LIT) + \sum f_2(SL_\mu, SL_\sigma, NDVI_\mu, I_L, AR_\mu, PrC_\mu, PlC_\mu, LU_C, D2F) \quad (3)$$

where $\log\left(\frac{p}{1-p}\right)$ is the Binomial probability we aim to estimate via a logit link function, p being the actual probability of landslide occurrence. The right side of the equation shows the additive structure of a GAM, listing the covariates we selected and the related effects. Specifically, β_0 is the global intercept, NN_μ and EN_μ correspond to two linear cases, and the remaining ones represent the random effects. Overall, f_1 indicates two categorical effects, and f_2 indicates splines used for nine ordinal covariates.

As elaborated in Section 3.2.2, our objective is to construct a model that effectively addresses the spatial incompleteness present in landslide inventories. To achieve this, we equipped our Binomial GAM with a bias-removal step. We recall here that the aim of any statistical model is to explain the variability of a given response variable according to the selected probability distribution. In our case, the spatial distribution of landslides across Europe is what our model would attempt to explain according to the set of covariates we chose. Therefore, if the variability of landslide presence/absence is controlled by external factors such as different reporting protocols across European countries or simply the task of mapping being exclusively executed by road management agencies, using such covariates would heavily bias the resulting susceptibility (Loche et al., 2022). However, it is possible to turn this around and make use of such biased covariates to capture the variability in the landslide inventories and then set, a posteriori, the estimated regression coefficients of biased covariates to zero (Steger et al., 2017). In such a way, the remaining covariates would not be affected negatively in their effects' estimation, and the final susceptibility map would remain unbiased (e.g., Lin et al., 2021; Steger et al., 2021). For this reason, we introduced a covariate we referred to as *Zone*, this being responsible for capturing the bias in the European inventories associated with the differences in landslide mapping protocols. Similarly, we also introduced an additional covariate we refer to as I_L, with the aim of capturing the variability in the European inventories due to the dominant mapping along roads.

In our model, we introduced the covariate *Zone* as a categorical random effect (see, f_1 in Equation 3). This means that one random intercept will be estimated independently for each country listed in the vector *Zone*. In other words, we used *Zone* as an *i.i.d.* effect, or "independent and identically distributed random variable" (Wood, 2013). For reasons not related to bias-removal actions, we also included an additional *i.i.d.* covariate, this being the predominant lithotype per SU, or *LIT*, as per notation in Equation 3. Similarly to the *Zone*, a categorical use of the *LIT* implies an estimation of a random and independent intercept for each lithological class. The effects of the remaining covariates were considered nonlinear and fitted via smoothing functions (f_2). To control their maximum flexibility, a constraint was imposed on these functions by setting a k-value of 5. Conversely, for the covariate I_L the value was set to 3 after numerous tests. In analogy to the *Zone* case, the I_L function will be set to zero to remove any bias accordingly.

The Binomial GAM we set up incorporates an automatic variable selection procedure utilizing the double penalty technique. A comprehensive technical description of this technique is provided in Marra and Wood (2011), to which we refer the reader for further details. Ultimately, the implementation of our Binomial GAM was carried out in the *R* environment (Ihaka & Gentleman, 1996) by using the *mgcv* package (Wood, 2017).

4.2. Performance Assessment

To evaluate the performance of our model, we employed three distinct cross-validation routines. The initial approach involved a classical random cross-validation (RCV), partitioning the data set into 10 mutually exclusive subsets. Therefore, the model was iteratively trained and tested 10 times, with each 10% subset serving as the test set once. However, the RCV often produces limited variations in performance with respect to the fit, whenever the

given data set exhibits some degree of spatial clustering. A complementary and even more relevant cross-validation routine has been suggested in the literature to break down any spatial coherent structure in the data. We refer the readers to the spatial cross-validation (SCV, hereafter) explained by Brenning (2012), or to the leave-group-out recently introduced by Z. Liu and Rue (2022).

In this manuscript, we opt for implementing a SCV (Pohjankukka et al., 2017), to explore the predictive results of our model without obtaining overly positive metrics due to residual clustering effects. SCV results can offer valuable insights into spatial robustness as they allow for monitoring of how model performance may vary across different spatial regions. Thus, one can recognize specific sectors of a given study area associated with the worst predicting scenario. Building upon these principles, we implement two different SCVs. We refer to the first as a domain-oriented SCV strategy, wherein the data set is partitioned into n distinct subsets based on the different mountain regions ($n = 13$). The model is subsequently trained on $n - 1$ subsets and tested on the remaining region. We then iterate the process for all 13 mountain regions, ensuring comprehensive coverage and assessment of the model performance across diverse geomorphological domains. Conversely, we implement the second SCV approach based on a more conventional k-means clustering routine, as per the *sperrorest* package. For technical details about the implementation, we refer the reader to Brenning (2012). In short, *sperrorest* uses the x and y coordinates of the mapping unit of choice (here corresponding to the centroid of each SU), and clusters them into a number of groups defined by the user using a k-mean technique. The interesting aspect of *sperrorest* is that one may obtain high or low predictive performances due to the initial spatial arrangement. To avoid such effect, *sperrorest* offers an additional option to randomize the clustering procedure. As a result, one can obtain any number of subsets, each one further clustered differently from the previous. Here, we opt for a ten-by-10 partition, creating 10 random subsets, each one divided into 10 clusters. As a result, we train at each fold over nine clusters and validate onto the remaining one, repeating this operation across the random subsets for a total of 100 SCV replicates.

Variations in performance are evaluated via cut-off independent metric, opting for the Area Under the Receiver Operating Characteristic curve (AUROC, Hosmer & Lemeshow, 2000). The AUROC is a common evaluation metric used to assess the performance of binary classification models (Hanley & McNeil, 1982). The AUROC is derived from the Receiver Operating Characteristic (ROC) curve, which is constructed by graphing the True Positive Rate (TPR) against the False Positive Rate (FPR) over a range of classification thresholds. Notably, AUROC values range from 0.5 (no realistic classifier should report values below 0.5) to 1, where the former points out a purely random classifier, while an ideal classifier attains a value of 1 (Fawcett, 2006).

5. European Landslide Risk Modeling

In the forthcoming sections, we delineate the methodological procedures adopted for modeling landslide risk across the diverse landscapes in Europe. Leveraging the findings obtained by the previous susceptibility step, together with high-resolution data on elements at risk, below, we propose a protocol to quantify the potential risk posed by landslides. We express risk in terms of expected losses for potential human lives, settlements and agricultural regions within each SU. To the protocol presented below, we will also add considerations regarding the inherent uncertainties and approximations (see, Sections 5.1 and 5.2.1) that arise when dealing with regional scale studies.

5.1. European Exposure

5.1.1. Human Settlements and Agricultural Areas

In the context of risk analysis, exposure is a component that describes the interaction between the dynamics of the phenomenon at hand and the elements at risk, as well as vulnerability (Corominas et al., 2014). Specifically, the exposure of an element exhibits a strong dependence on its spatial proximity to the landslide runout (Pellicani et al., 2014). Nevertheless, constrained by the limitations of regional to continental scale studies, the precise modeling of this intricate relationship remains elusive. This has mostly to do with the impossibility of simulating landslide runout over large geographic areas. Consequently, in our risk model, we assume that, in the event of a landslide, all elements placed within a SU will be affected.

Our analysis does not account for transportation infrastructure among the exposed elements due to the un-availability of a comprehensive European database enabling the extrapolation of the monetary values or

reconstruction costs. We express exposure in monetary units (€), necessitating a preliminary computation of the spatial extent occupied by the distinct categories of elements at risk within each spatial unit (SU).

To calculate the extent of land occupied by human settlements in our mapping unit, we use the GHS-BUILT-S database (Pesaresi & Politis, 2022). This database is represented as a spatial raster available with different spatial resolutions (e.g., 10, 100, and 1,000 m), providing a detailed representation of the global distribution of built-up surfaces. Furthermore, the data are spatio-temporal interpolated or extrapolated from the period between 1975 and 2030. This aggregation is performed on a 5-year interval basis, allowing for potential studies with future scenarios. For further details related to this product, we refer the readers to Schiavina et al. (2022). In our context, we opt to utilize the 100-m spatial resolution data set, as opposed to the more detailed 10-m data set. While the latter offers greater spatial information, it is constrained by its data availability, with the most recent update dating back to 2018. As a result, we derive the extent of the built-up area within each SU by summing the values of each 100 m $\times$ 100 m grid cell, quantifying the surface area covered by human settlements for each mapping unit. Concerning the economic evaluation of human settlements, we employ an exposure database specifically designed for seismic risk analysis in Europe (Crowley et al., 2020), whose information is available in the repository provided by Crowley et al. (2021). The exposure database describes the spatial distribution of residential, commercial and industrial building classes in terms of building count, covered area m^2, occupants and reconstruction cost (€) for 44 European countries. The database can be accessed at various resolutions; however, in our specific context, we employ the higher resolution characterized by a hexagonal grid with a spacing of 0.30 $\times$ 0.34 decimal degrees. Despite being relatively coarse, this resolution represents the best description of building exposure in Europe among the available products. Consequently, we calculate the mean value in €/m^2 for each hexagonal grid by dividing the relative total reconstruction cost and the covered area by buildings. As a result, we determine the mean building economical value for each hexagonal grid and further aggregate this information at the SU level by taking the mean of the cost distribution. The quantification of human settlement exposure within each SU is then achieved by multiplying the relative mean monetary value (€/m^2) with the corresponding built-up surface area (m^2).

As for the spatial distribution of agricultural areas, we derive this information from the CORINE Land Cover 2018 (CLC 2018) database. In contrast to the approach used for land use covariate in the landslide susceptibility modeling (see, Section 3.2.1), we use the CLC 2018 database instead of the MODIS database. The choice is due to the CLC 2018 database's superior spatial resolution of a 100-m grid side compared to the 500-m resolution offered by the MODIS database. Additionally, the CLC 2018 database provides more comprehensive and detailed information regarding the various classes of land use. This enhanced level of detail and resolution in the CLC 2018 database is crucial for capturing the heterogeneity of agricultural areas, making it the preferred choice for our analysis, although it does not provide information for Ukrainian Carpathians. Due to our focus on specific land uses and relative risk assessment, we adopt a proxy to represent the spatial coverage of agricultural areas within each SU. Specifically, we consider Group 2, denoted as "*Agricultural Areas*" and subgroup 3.2.1, identified as "*Natural Grasslands*" from CLC 2018 database. The monetary valuations of agricultural areas across Europe are derived from the Land prices and rents (APRI-LPRC) database, meticulously curated by the statistical office of the European Union - EUROSTAT (Eurostat, 2012). This comprehensive database serves as a reliable source of land prices expressed in euros per hectare (€/ha) for diverse regions and countries within Europe. By leveraging this database an economic value for agricultural areas is defined for each SU. Unfortunately, the database does not encompass certain countries such as Germany, Norway, Portugal, Austria, Iceland, and Switzerland. As a consequence, "No Data" is encountered in our assessments for these countries. Nevertheless, previous regional scale investigations have indicated that the influence of the agricultural area component in risk modeling is significantly less compared to urban centers (Caleca et al., 2022). Considering this insight, the uncertainty arising from the absence of land cover or land price data in these specific countries is deemed acceptable within the scope of our analysis, especially because the present contribution serves mostly as a review and example basis. As a result, for SUs with a complete description of agricultural areas, their exposure is quantified by multiplying the market value (e/ha) and the corresponding surface extent (ha), resulting in an exposure value expressed in euros (€).

An overview of the data we use to evaluate the exposure components for both human settlements and agricultural areas, we refer the readers to Table 3.

Table 3
List of the Exposure Components and Database Employed for Their Assessment

Exposure component	Input data	Repository
Spatial distribution of human settlements	GHS-BUILT-S	Link-GHSL
Spatial distribution of agricultural areas	CORINE Land Cover 2018	Link-CLC
Economic value (€/m^2) of buildings	Exposure model data for European seismic risk assessment	Link-EMD
Economic value (€/ha) of agricultural areas	Land prices and rents (APRI_LPRC)	Link-APRI

5.1.2. Population

Ultimately, we also make use of population density data. Notably, the time scale for which our susceptibility model is valid and the time scale for which population density changes its spatial distribution is very different. Therefore, formally defining a numerical life loss estimator is not possible. In fact, to match the two data and estimate losses, one should model landslide dynamics (initiation and propagation) together with the spatio-temporal distribution of the people potentially affected (M. Rossi et al., 2019). This information for most of Europe has been recently made available with a monthly resolution in time (for the reference year of 2011), and with a spatial resolution of 1km^2. This data set has been published by Batista e Silva et al. (2020) and highlights differences in the distribution of population on a sub-daily basis, showing patterns for both day and night. This is the only regional scale data set with analogous characteristics, this being the reason for our choice (further explanation will be provided in the following section).

5.2. European Risk

5.2.1. Risk of Human Settlements and Agricultural Areas

The landslide risk assessment relies on the theoretical framework outlined by Equation 2. We recall here that when dealing with regional scale studies, it becomes necessary to incorporate certain assumptions into the methodology. This is mainly attributable to the lack of data, which hinders an overall evaluation of risk components at the large extent of the study area. Specifically, the characterization of the hazard component is delineated by means of spatial probability of occurrence (susceptibility), owing to the intrinsic limitations precluding the quantification of its distinct temporal and intensity dimensions (Guzzetti et al., 2005). The inherent impracticability of amassing comprehensive data pertaining to landslide kinematics, frequency, and magnitude at a continental scale imposes the need for simplifying the hazard information to the available susceptibility. Furthermore, an additional assumption is incorporated regarding the vulnerability assessment. To elaborate, evaluating vulnerability is a complex task, even for site-specific investigations, as it requires assessing the reaction of exposed elements to the phenomenon (Z. Li et al., 2010; Tapsell et al., 2010) and its intensity (Promper et al., 2015). These challenges are even more accentuated when dealing with regional scale analyses. As a result, we hypothesize that in the event of a landslide, any element intersecting its trajectory would incur irreparable damage, thereby implying a vulnerability value of 1, with the due uncertainty that such a hypothesis brings into the analyses. As a result, Equation 2 can be re-written to suit our analysis, specifically in relation to a singular SU, as follows:

$$R = \frac{S \times (E_{hs} + E_{aa})}{A_{SU}}, \tag{4}$$

where R is the landslide-induced risk expressed in euros per square meter (€/m^2); S is the spatial probability of occurrence of landslides (susceptibility); E_{hs} is the human settlements exposure (€); E_{aa} is the agricultural areas exposure (€); A_{SU} is the planimetric area (m^2) of the reference SU.

The application of Equation 4 expresses risk in terms of expected economic losses across the European landscape, on a continuous scale. Notably, we opt to conceptualize risk in terms of €/m^2; this selection is made to facilitate both comprehensive SU comparisons and disseminate insights concerning areas that might be predisposed to experience more substantial damages.

5.2.2. Population at Risk

For a continental-scale study, population risk dynamics are currently largely unfeasible to estimate. However, one can still obtain a general overview of the risk the population may be exposed to by exploiting the demographic census and matching it against the landslide occurrence probabilities. In turn, this information may be used for master planning purposes. Interestingly, if a landslide or a population of landslides would take place during the day or night times, the risk pattern will inevitably assume very different spatial characteristics. The nighttime mainly sees the population clustered in residential areas, whereas the daytime highlights a distribution clustered in commercial and/or urban areas. Here, we try to capture and exemplify such differences by plotting two separate maps, one where our European landslide susceptibility is spatially joined to the daytime population density and one where the same is produced for the nighttime. This is done by taking the year 2011 as the reference period, mainly due to reasons of data availability. The data set produced by Batista e Silva et al. (2020) offers a day and night representation aggregated on a monthly basis. To summarize this information, here we take the annual mean over day and night. Thus, rather than generating a formal life loss estimator, we produce an overview of the potential population at risk during the two main phases of a daily cycle.

6. Results

6.1. European Susceptibility Overview

This section is divided into three main components. We initially present a summary of the covariate effects estimated in our landslide susceptibility model (see, Section 6.1.1). Subsequently, we provide a summary of the model performance (see, Section 6.1.2). And finally, we conclude the susceptibility overview by comparing two (biased and unbiased) probabilistic maps (see, Section 6.1.3).

6.1.1. Covariate Effects

We present the estimated covariate effects expressed at the scale of the response. We recall here that one may express covariate effects at the scale of the regression coefficients or directly in terms of occurrence probabilities. We consider the latter to be slightly more readable, although the overall meaning is essentially the same. The visual representation of such effects is reported in Figure 3. There, one can notice that the ordinates are expressed as the logistic cumulative density of the respective regression coefficient's distribution. In other words, the regression coefficients are transformed by taking their exponential divided by 1 + their exponential. We recall here (see, Section 4.1) that other than EN_{μ} and NN_{μ}, all other covariates have been passed to the model as random effects, either in a categorical form (as *iid*) or in an ordinal form (as splines). For reasons of conciseness, we limit our interpretation focus to the covariates discussed below.

The categorical effects are displayed in Figures 3a and 3b. The former depicts the random intercepts estimated for the countries responsible for compiling the landslide inventories. An in-depth analysis of the outcome derived from the application of these effects reveals a discernible trend, wherein the countries can be categorized into two distinct groups. These are clearly shown to be clustered far above the 0.5 probability mark and far below the same. Their respective countries are deemed highly susceptible to landsliding. For instance, Italy (ITA) and Switzerland (SWI) are clear examples, with assigned marginal probabilities of 0.94 and 0.93, respectively. It is essential to reiterate that the incorporation of random effects within our modeling framework facilitates the evaluation of the completeness of the various landslide inventories at our disposal. Based on this consideration, it becomes evident that the countries falling within the first group primarily correspond to those possessing comprehensive information regarding the presence or absence of landslides at the national level. Other examples include Slovakia (SLK), France (FRA), Austria (AUS) and the United Kingdom (UK). Conversely, the second group falls below the 0.5 probability threshold, and lists countries with only available regional inventories or, in general, with limited information on landslide occurrences. Notable members of this group encompass Slovenia (SLO), Greece (GRE), Portugal (POR), Spain (SPA), Sweden (SWE), and Romania (ROM).

Another covariate we modeled with a random categorical effect is the lithology. The effects of lithological classes on the probability of landslide occurrence are reported in Figure 3b. There, examining the resulting effects shows that the class *LIT*19, or claystones and clays, underlays areas very prone to landslide occurrence, being estimated with a marginal probability of approximately 0.8. This is an aspect of particularly relevance that has always separated machine learning from statistical studies, as the second type offers a clear interpretation. For instance,

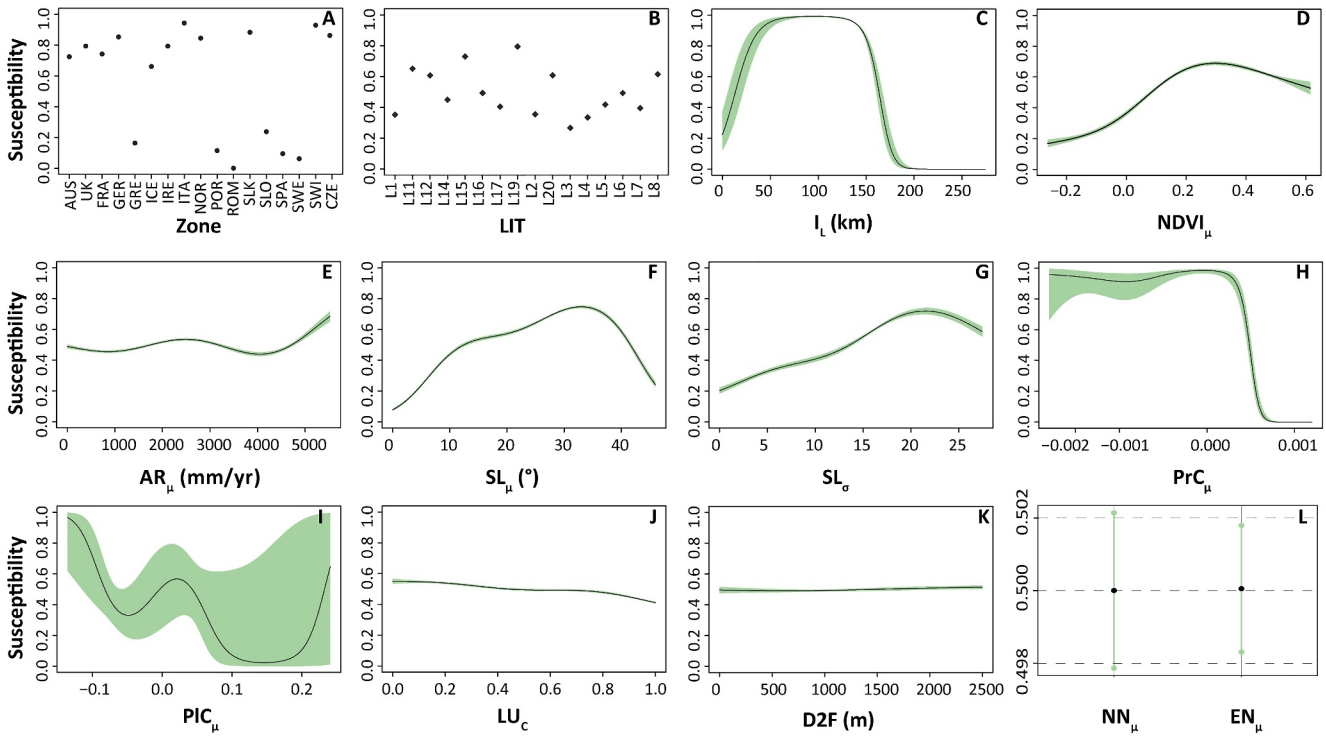

Figure 3. Marginal plots of the estimated covariates' effects: panels (a) and (b) show the effects of covariates modeled as random effects. Panel (c)–(k) report the summary of ordinal nonlinear effects. Panel (l) highlights the linear effects. For the acronyms, we refer the reader to Table 2. Notably, the *y*-axes are expressed at the scale of probability of landslide occurrence (Susceptibility) rather than at the scale of regression coefficients.

here we can assume that such a strong and positive contribution to the overall susceptibility may be due to claystones and clays having high water retention capabilities. In turn, this means they can absorb and retain water for extended periods. When these materials become saturated, their weight increases significantly, potentially bringing slopes to the brink of failure (Yalcin, 2007). Additionally, clay layers often have low permeability, which hinders the rapid drainage of water. This can lead to increased pore water pressure within the slope, reducing the effective stress and shear strength of the material and making the slope more prone to sliding. Another reason supporting the positive influence of this lithological class lies in the tendency of claystones to lose strength due to weathering. Notably, physical and chemical weathering can alter the mechanical properties of these layers leading to a strength degradation (Alonso et al., 2010; Miščević & Vlastelica, 2014). Conversely, the effect of the lithological class corresponding to plutonic rocks (*LIT*3) reveals a low marginal probability of landslide occurrence (i.e., 0.29). This may be attributed to several geological and geotechnical characteristics that make these rocks more stable compared to other lithological classes. First, plutonic rocks are typically hard and have low porosity. This means they have high shear strength and are less prone to water infiltration. Their inherent strength and low water retention properties make them relatively stable (Fell et al., 2012). Moreover, they often lack foliations and weak planes that are present in sedimentary rocks and some metamorphic rocks, which can act as failure surfaces during landslides. However, it is noteworthy that in non-glaciated mountainous sectors under humid temperate climates, plutonic rocks (especially granitoids) are often recognized as geological conditions highly prone to shallow landsliding (Borrelli et al., 2018; Durgin, 1977; Ietto et al., 2016; Regmi et al., 2014). These conditions are associated with discontinuous weathering profiles between soil and bedrock layers. Although the robustness of plutonic rocks in the European mountain domains is well documented, the estimated low influence on landslide susceptibility may also reflect their geological history, and climatic environment as well as their changes over time.

In Figure 3c, the covariate' effect related to the total length of infrastructures within each SU (I_L) is reported. We recall once more that this covariate, together with *Zone* was included in our modeling for the purpose of a bias-capture action (see, Section 4.1). Through the examination of the covariate in question, three discernible trends can be extrapolated. First, there is a notable positive influence of the variable I_L within the spatial range of

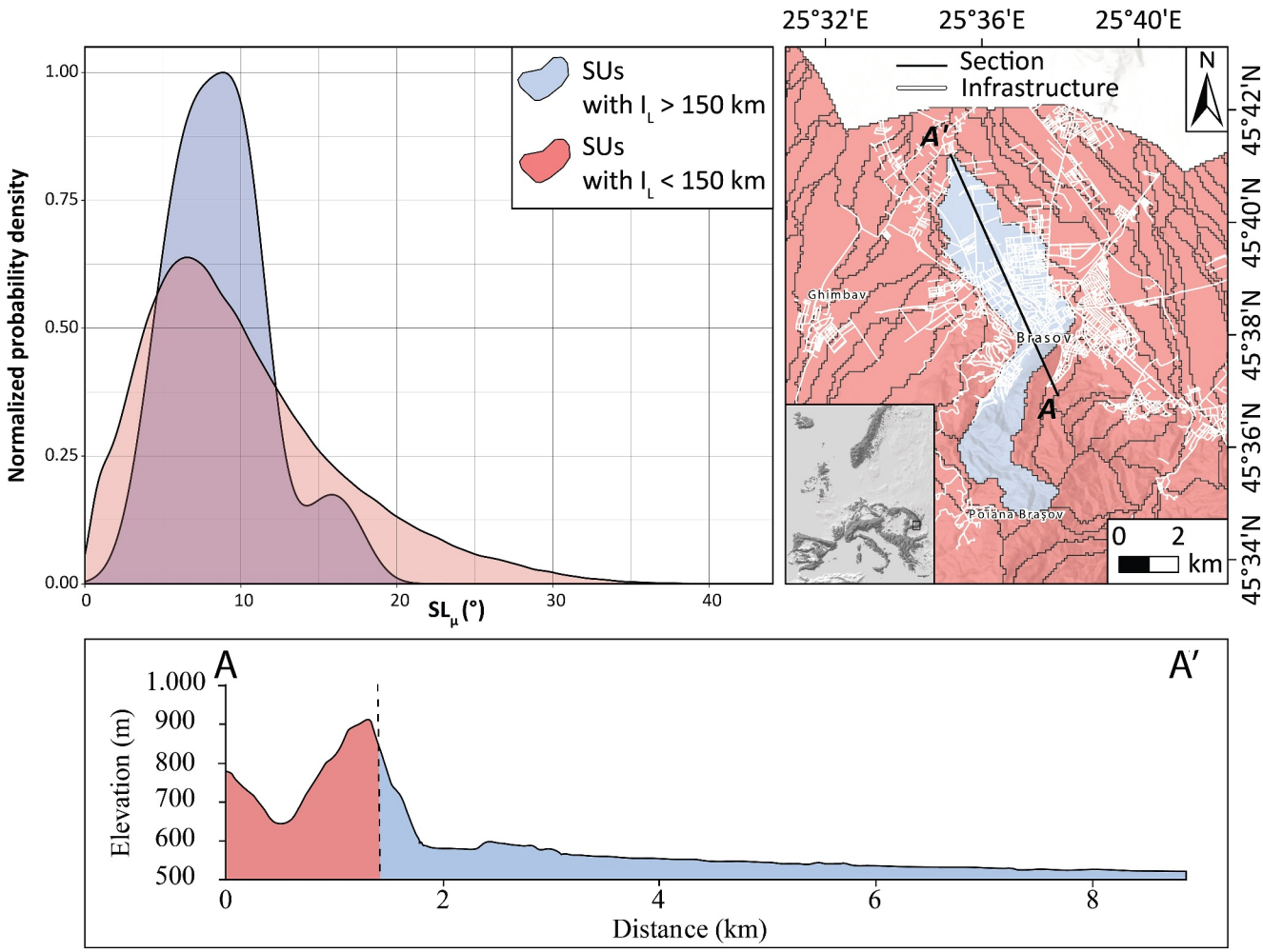

Figure 4. Distribution of the mean slope steepness (SL_μ) for Slope Units (SUs) with I_L less than 150 km (light red curve) and SUs with I_L greater than 150 km (light blue curve). On the right side a detail of these conditions and the relative cross profile (bottom figure).

0–50 km. Second, this positive trend stabilizes within the interval of 50–150 km. Lastly, beyond the latter boundary, there is a significant decline in the marginal probability, leading to 0. One plausible interpretation of these observed patterns, considering the underlying hypothesis that the inclusion of I_L aims to capture the bias related to number of mapped events, is as follows: within SUs characterized by I_L values falling within the range of 0–150 km, there appears to be a potential overrepresentation of landslide occurrences, consequently leading to an elevation in the likelihood of such events. Conversely, when I_L exceeds the threshold of 150 km, the related trend suggests the underrepresentation of mapped events, and it is reflected by the substantially diminished probability of landslide occurrence. In former studies, this bias descriptor is commonly represented by the distance between the mapping unit and the nearest infrastructure (Stanley & Kirschbaum, 2017a); therefore, the overrepresentation in the proximity of such structures is directly reflected in a very high predicted probability of occurrence in those areas (Steger et al., 2021). Differently, in this work, the bias descriptor is represented by the total spatial covering in the mapping unit. Consequently, a logical interpretation of the obtained trends would imply that bias propagation in the estimated probabilities exhibits nearly continuous growth as the variable I_L undergoes variation (i.e., higher values of I_L correspond to higher predicted probability). However, as described above, our analysis reveals a distinct probabilistic trend. Upon inspection (see Figure 4), it becomes evident that the potential bias propagation may primarily occur within the spatial interval of 0–150 km, which predominantly encompasses more steep slopes. Conversely, areas characterized by I_L values exceeding 150 km are mainly associated with partially flat areas, which, from a geomorphic perspective, are less prone to trigger landslides, but where infrastructure construction is easier to realize (higher values of I_L).

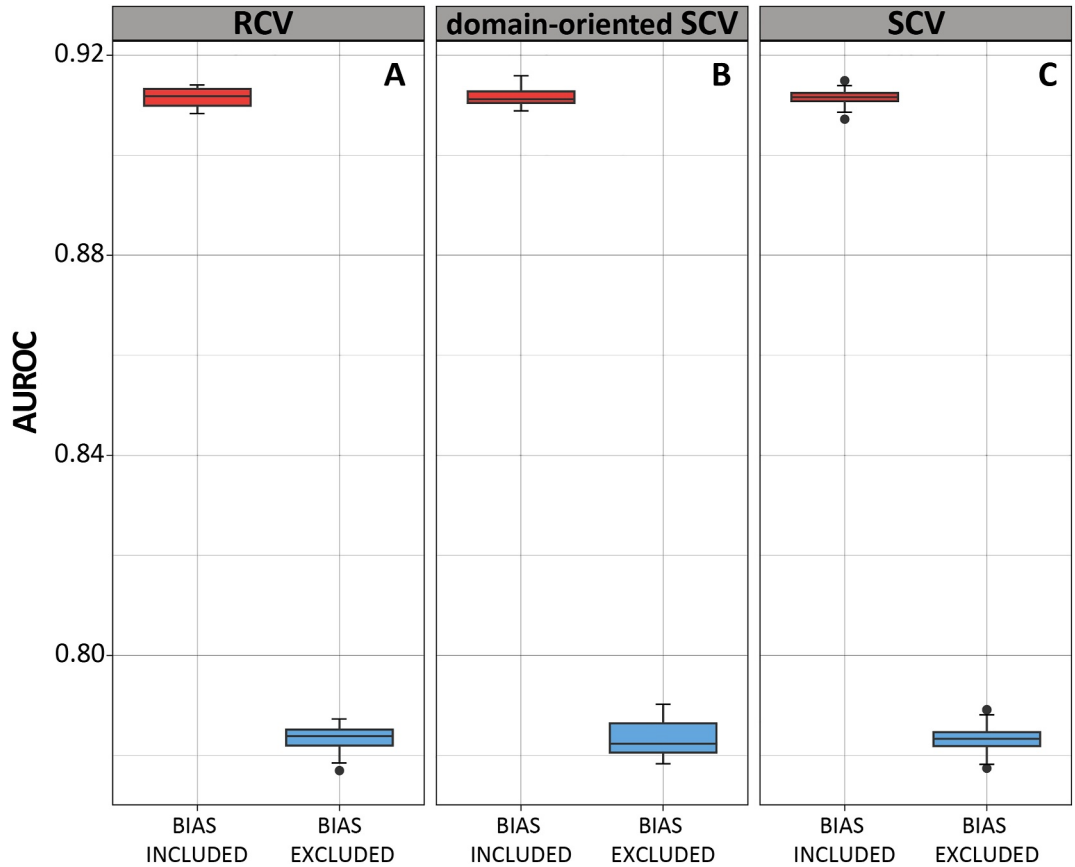

Figure 5. AUROC values estimated for the purely random cross-validation (a), domain-oriented spatial cross-validation (b) and purely spatial cross-validation (c). The AUROC values were estimated both ignoring and excluding the bias propagation within the prediction.

Figure 3f reports the contribution of SL_{μ}, which appears to follow an overall positive trend up to approximately 35°. Beyond this threshold, the likelihood of landslide events exhibits a decline. From a geomorphological point of view, the results is reasonable as SUs exceeding a critical threshold of 35° are deemed excessively steep to support the presence of potentially unstable soil columns. Notably, in light of this interpretation, we remind the reader that most of the European data set we compiled lacks information on landslide types. As a result, we hypothesize that phenomena such as rockfalls, which are more frequent in very steep areas, are less reported with respect to other types.

6.1.2. Performance

The model performance is summarized in Figure 5. We recall here that the model has been challenged through three different cross-validation routines. Each of these has been further differentiated according to the presence of the bias in the model or, by removing it (i.e., zeroing-out the contributions of the *zone* and I_L effects). Overall, we observe that when bias propagation is ignored, the AUROCs tend to exhibit much higher values, almost to the point of reaching a perfect prediction. This is already a hint that should make any user exposed to similar results think twice about why this may be the case. One plausible explanation for this trend is that the model learns to exploit dataset-specific biases rather than uncovering the underlying general relationship. Here, we purposely include such bias-related covariates and remove their effect for an unbiased landslide susceptibility map. What we note is that the apparent loss in predictive power brings the AUC among all biased cross-validated models from 0.91 to 0.78 of all unbiased cross-validated models. We stress once more that this 0.13 AUC performance drop is purely apparent and its repercussions to the respective predictive maps will be presented in the subsequent section. The most important information to convey is that even when removing the bias, the model does not drop to the point of becoming non-informative. On the contrary, according to the performance classification proposed by

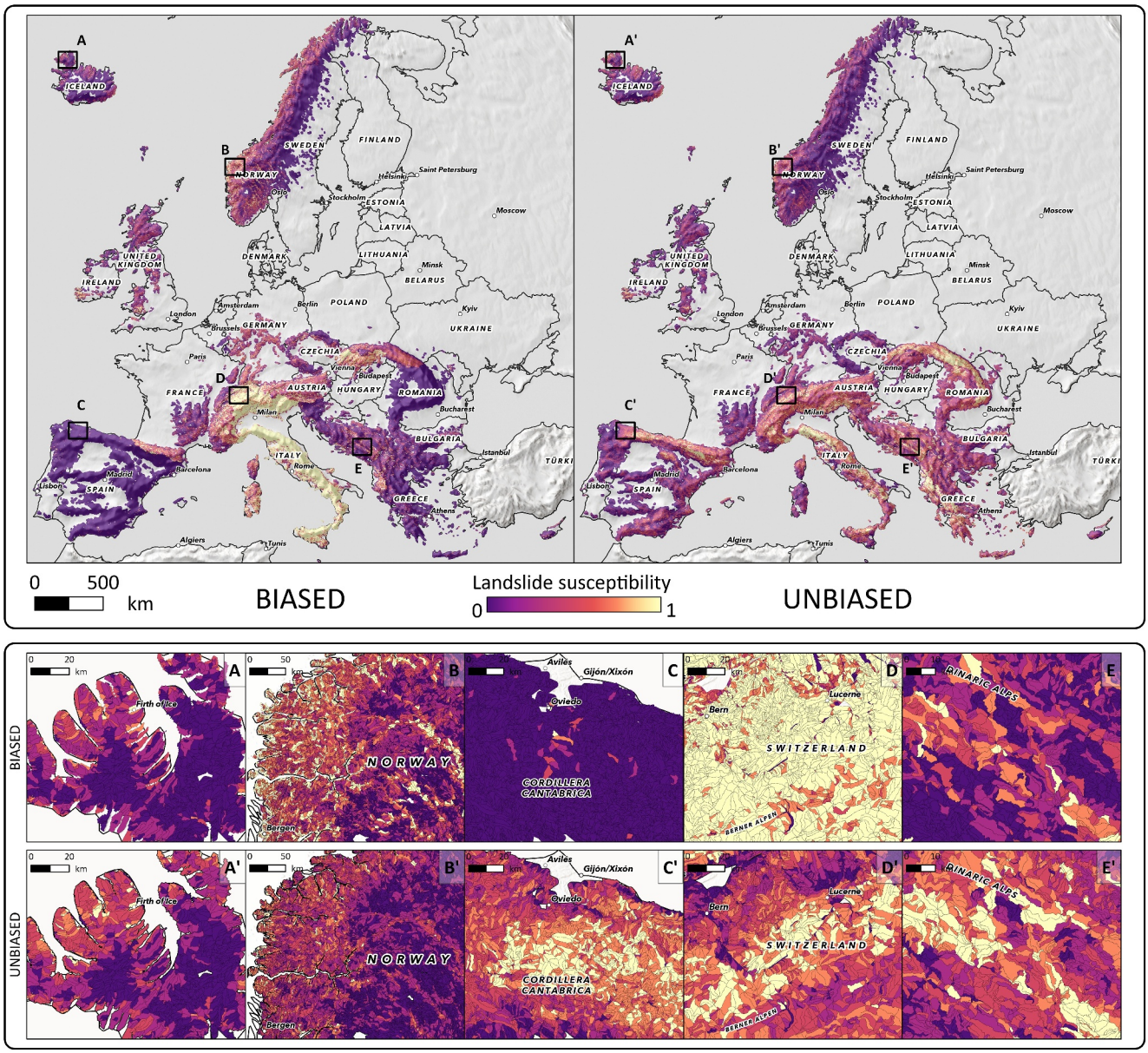

Figure 6. Biased and unbiased landslide susceptibility maps. Zooms offer a comparison between the two different maps. The first row shows details of the biased map. The bottom row displays the same locations for the unbiased map.

Hosmer Jr et al. (2013), a 0.78 of AUC corresponds to an acceptable classifier and is actually close to the excellent class boundary. This should be the true predictive power one should consider when using the outcome of such a model and when interpreting its susceptibility patterns.

6.1.3. Biased Versus Unbiased Probabilistic Maps

After showcasing the predictive power of our susceptibility model, in this section, we convert the model results into maps. We choose to preserve the continuous spectrum of probabilities rather than classifying it into distinct susceptibility levels. This is a choice we make to use probabilities later in support of the risk evaluation. Therefore, the spatial representation of the model outputs still ranges from 0 to 1, where the former indicates non-susceptible conditions and the latter indicates SU prone to failure. However, to illustrate the issues related to the inclusion of bias sources into susceptibility models, we opt to follow the same structure presented above in Figure 5. In other words, we present both the biased and unbiased susceptibility maps (Figure 6). As it appears

quite clearly in the left panel as well as in the first row, where we report few dedicated zooms, the bias mainly contributes to elevating/reducing the susceptibility patterns to the point of saturating the scale. For instance, the left panel shows susceptibilities that follow the geographic distribution of administrative boundaries. This is an artifact brought into the model by the various organizations responsible for landslide mapping. Specifically, regions such as the Alpine and Apennine environments are ranked almost homogeneously with the highest probabilities; however, when the effects of bias propagation are removed from the analysis, these mountainous areas display a more heterogeneous distribution of landslide probabilities, which turns out to be more reliable from a geomorphological perspective. Conversely, in regions where landslide data completeness is limited, such as the Iberian Peninsula and the eastern sectors, landslide probabilities tend to be closer to zero. However, following the removal of the effects of those variables that systematically describe the landslide data collection bias, the modeled propensity of trigger landslide moves to higher values in those areas. The comparison between the two different maps highlights even areas where there are no substantial changes or where they occur in a feeble intensity, as in the case of Scandinavia and Iceland. Notably, analyzing the Scandinavian environment, we notice that the Norwegian landscape experiences a weak decrease in the probabilities after the removal of data collection bias. The same situation is further showcased in the series of zooms below. For instance, the first row appears quite saturated in panels C (Iberian peninsula) and D (Alpine domain). There, almost no spatial variation can be seen across SUs, with the former appearing mostly non-susceptible and the latter being almost susceptible everywhere. This effect comes from the completeness of the original inventory, and once removed in the row below, geomorphologically reasonable patterns become evident.

Figure 7 further simplifies the identification of the most biased landscapes. There, it is possible to check the distribution of susceptibility values for each of the 13 spatial domains under consideration, with and without bias. Notably, within the Alps, Apennines, and Sardinia-Corsica regions, the complete removal of the effects of those variables responsible for the bias propagation led to a substantial decrease in the scores of the model outputs. Similarly, albeit with a less pronounced effect, the Central-West and East sectors exhibit a shift toward smaller probability values. Conversely, the Carpathians, Dinarides - Balkans, Iberian peninsula and Pyrenees present an opposite trend, with a significant increase in the respective scores when the bias is removed. Nevertheless, the mitigation of the influence of landslide data bias on model outputs does not always manifest as a conspicuous modification in score distribution. This is the case of the British Isles, Iceland, Massif Central, and Scandinavia, where the two distinct curves almost coincide, implying a minimal score distortion between the biased and unbiased maps.

6.1.4. Comparison With Existing Products

This section provides a comparative analysis of our unbiased probabilistic landslide susceptibility map with respect to existing products for the same study area. The objective of this comparison is to identify any common patterns between our probabilistic map and others. We use as first-order benchmarks the European landslide susceptibility map presented by Wilde et al. (2018) and, as the second one, the global map developed by Stanley and Kirschbaum (2017b). Notably, unlike our probabilistic methodology, these benchmark products have both been obtained via heuristic approaches and, in doing so, the respective authors have based their analyses on a gridded mapping unit. Specifically, the map from Wilde et al. (2018) has been originally expressed at a 200 m grid resolution, whereas the one by Stanley and Kirschbaum (2017b) estimates susceptibility on a 1 km pixel size. To facilitate the comparison, we had two options: either aggregate these products at the same level as our SUs, for instance, by taking the maximum or the most frequent susceptibility class within one of our polygons. As an alternative, we could avoid any aggregation and rather simply extract the respective grids, as long as they intersect our regions of interest. To respect the status and official use of these products, we opted for the second option, with the idea in mind of minimizing our interference and processing of the information they convey. As for our product, we then followed a Jenks classification scheme (Jenks & Caspall, 1971; North, 2009) to bin our continuous probability spectrum into five classes comparable to those of the two products under consideration.

The three resulting maps are presented in Figure 8. There, Panel A presents our output, while Panel B displays the product of Wilde et al. (2018), and Panel C shows the product of Stanley and Kirschbaum (2017b). Interestingly, all products highlight the Alps, Apennines, Pyrenees, and Carpathians as the most susceptible regions. However, a notable distinction exists in the range of values because the other two maps essentially showcase grids belonging either to moderate, high or very-high susceptibility classes, with no presence of the other two. Conversely, our probabilistic approach yields a more nuanced representation of landslide susceptibility across Europe, resulting in

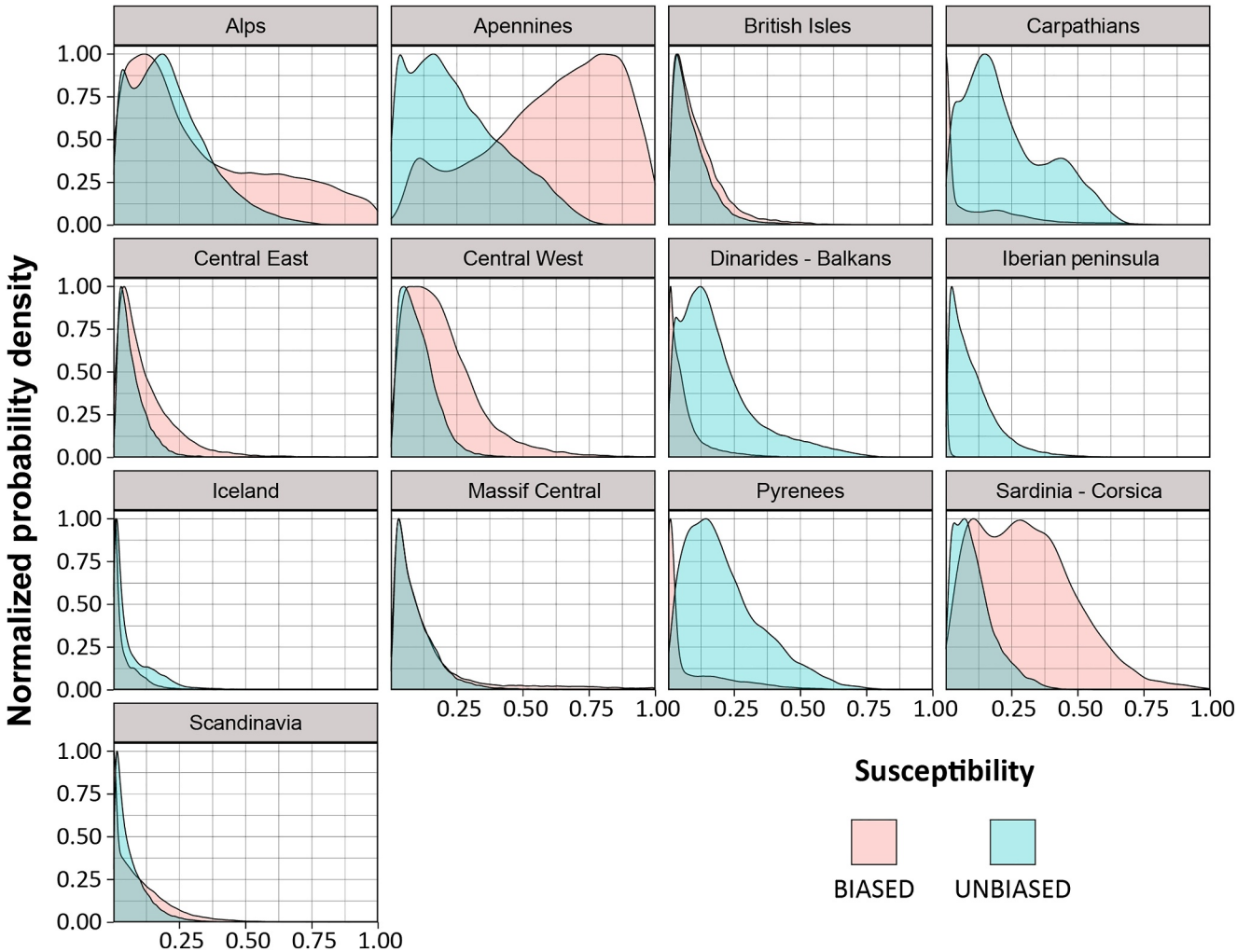

Figure 7. Distribution of the biased and unbiased probabilities of landslide occurrence for each mountain region. The light-red curve reflects the biased probabilities, whereas the light-blue reports the unbiased distribution.

a more spatially varied distribution of susceptibility classes, although the Alps appear to be generally less susceptible compared to the other two.

The issue of saturation in the available susceptibility range is something worth discussing, as it affects many susceptibility studies in the literature. In fact, these two products include also flat areas in their calculation. These are trivial zones (Steger et al., 2021), where one does not need complex susceptibility models to know that no landslides can take place because the physics of the process dictates that flat areas, for instance, are not susceptible by definition. In turn, this has negative repercussions when building complex models simply because any model simply learns to discriminate between flat and non-flat terrains rather than learning internal characteristics unique to the rough ones. The latter should be the target of any susceptibility model, through which a level of de-saturation of the probability range is obtained. As for situations where trivial areas are still part of the modeling procedure, the results are evident in panels B and C, where all the mountainous landscapes are essentially estimated as susceptible, whereas in reality, this is not the case.

6.2. European Risk Overview

In the subsequent sections, we offer an overview of our landslide risk analysis. Initially, we provide a concise summary regarding the findings of the exposure assessment framework (see, Section 6.2.1). Subsequently, we present the results of the risk analysis through two distinct modes of representation: (a) the depiction of the spatial

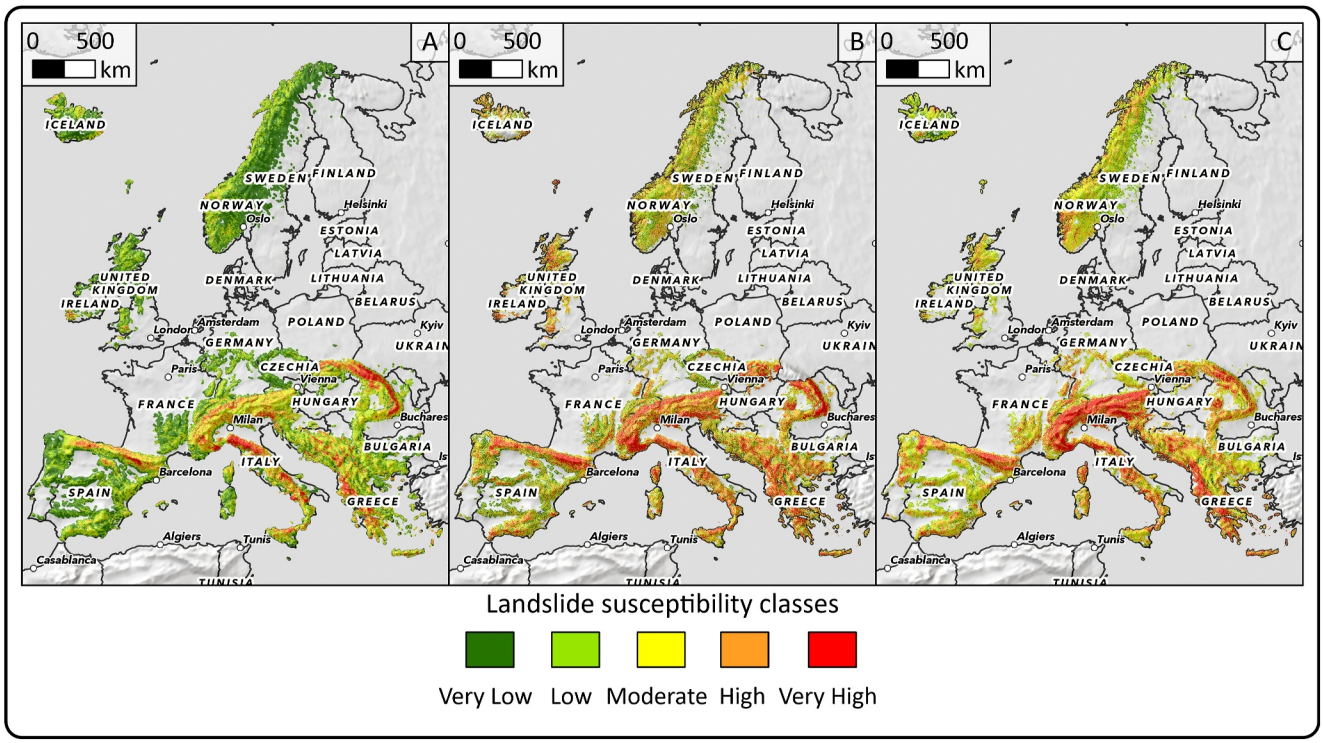

Figure 8. Comparison between the unbiased landslide susceptibility map (panel (a)) derived from this work and two previous products (panels (b) and (c)). Panel (b) depicts the landslide susceptibility map of Wilde et al. (2018), while panel (c) displays the global product of Stanley and Kirschbaum (2017b).

distribution of expected economic losses and (b) the delineation of different hotspots obtained by combining the spatial patterns of the unbiased susceptibility together with the exposure of human settlements (see, Section 6.2.2).

We also provide a cartographic representation of the population at risk by plotting two separate maps, one where our European landslide susceptibility is spatially joined to the daytime population density and one where the same is produced for the nighttime (see, Section 6.2.3). Lastly, in Section 6.2.4, we introduce and discuss the advantages associated with the dissemination of landslide risk information via WebApp.

6.2.1. Exposure

The spatial representation of economic values expressed in terms of euros (€) pertaining to human settlements and agricultural areas are reported in Figure 9. We recall that the exposure of human settlements is defined by the building footprint within each SU, whereas the one relative to the agricultural areas is computed on the basis of the spatial distribution of specific land use classes (as described in Section 5.1). The exposure of human settlements ranges from 0 to 126 Billion €, with a mean of 25 Million € and a standard deviation of 340 Million €. Overall, the sum of economic exposure relative to human settlements across our showcase study is about 14 Trillion €. Upon careful analysis of the map showing the economic values of buildings across the European landscape, we notice that the highest values are mainly located in the areas corresponding to footslope and toeslope sectors, or generally in areas close to floodplains. Notably, these regions coincide with the presence of major urban centers, thereby increasing local economic exposure. Conversely, lower economic exposure patterns are placed in sectors at elevated altitudes and steeper slopes, where the concentration of large human settlements is rare or even absent.

The economic exposure of agricultural areas ranges from 0 to 187 Million €. However, due to a lack of data regarding the market values of the land uses for a few countries (e.g., Germany, Switzerland, Portugal, Norway) in our input database (see, Section 5.1), we assign No Data to the corresponding mapping units, represented in gray in the map. Aside from these missing values, the exposure of agricultural areas can be summarized with a mean of 1.5 Million €, and a standard deviation of 3.8 Million €, for a total of 562 Billion €.

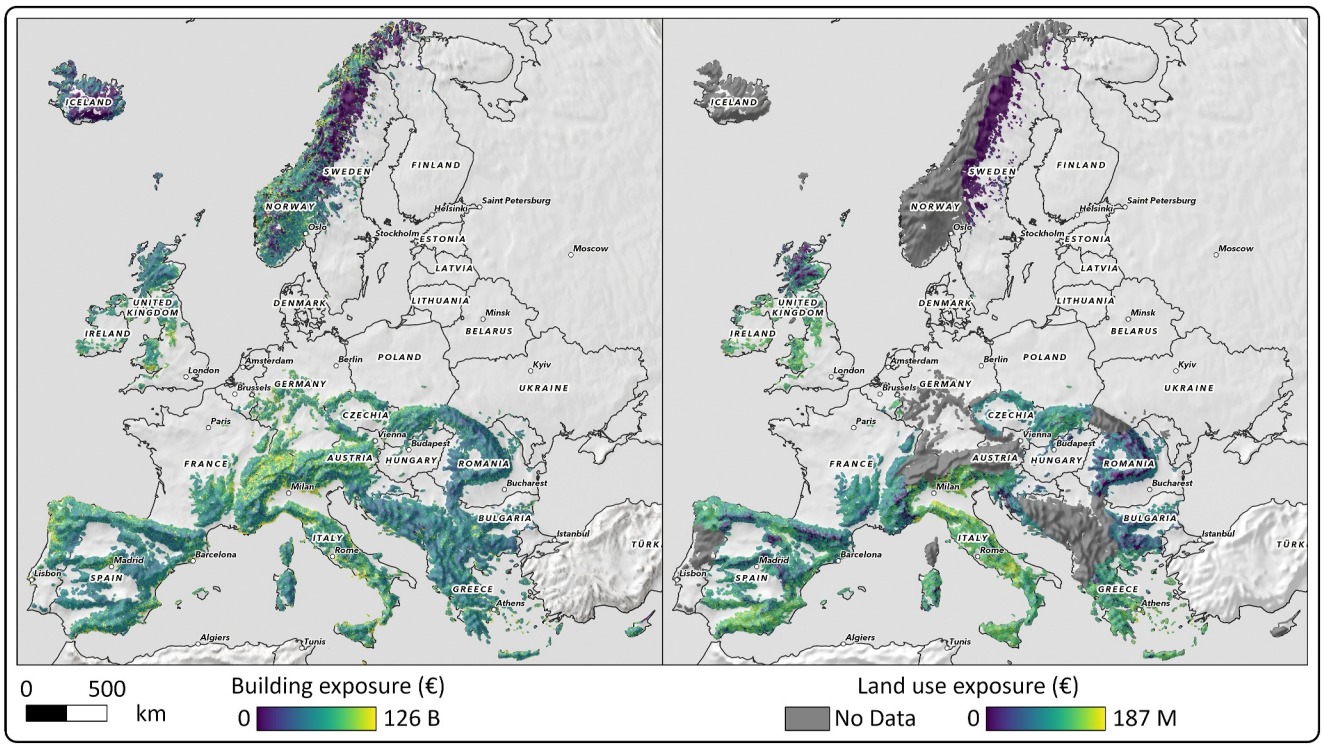

Figure 9. Exposure maps in terms of economic values (€) of human settlements (buildings) and agricultural areas (land use) respectively.

The highest agricultural values are attributed to the Apennine chain or to the eastern sector of the Alps. Furthermore, lower economic values appear to be mainly located in mapping units at elevated altitudes. This is mostly due to agricultural practices being almost absent in the highest portions of the topographic profile.

By comparing the distribution of economic exposures for human settlements and agricultural areas, landslides potentially threaten the first up to a few orders of magnitude higher than the second in terms of potential financial losses. Specifically, looking at the respective mean values, we notice a difference of one order, which increases up to two orders, when inspecting the comparison between the two total values across Europe. Obviously, the lack of data in several countries partially contributes to such enormous discrepancy. Nevertheless, such difference is acceptable when considering the different economic implications (see also, Caleca et al., 2022; Pellicani et al., 2014).

6.2.2. Risk: Expected Economic Losses and Hotspots

In this section, we present the outcomes derived from the landslide risk modeling, shedding light on expected economic losses and delineating risk hotspots throughout the European landscape.

Figure 10 displays the map translation of the results generated through the application of Equation 4 (see Section 5.2.1). We recall the prohibitive challenge of defining the vulnerability across such a geographic extent. Therefore, we assume that human settlements and agricultural areas would incur irreparable damages in the event of a landslide. Returning to Figure 10, the depicted cartographic representation illustrates expected economic losses in a continuous scale spanning from a minimum of 0 to a maximum of 8,383 €/m^2. The distribution of these outcomes is captured by a mean value of 1.04 €/m^2, accompanied by a single standard deviation of 17.2 €/m^2. When excluding areas reporting zero, these values increase up to 5.53 €/m^2 and 41.8 €/m^2 for the mean and standard deviation, respectively. The analysis of the right side of Figure 10 reveals that areas marked by high expected economic losses are mainly located in the central and southern sectors of the European landscape. A notable concentration of such values is observable in the Alpine and Apennine environments, as indicated by their respective distributions. Conversely, the lowest scores are predominantly observed in the northern and eastern sectors, delineated by the geographical domains of Dinarides-Balkans, Iceland, and Scandinavia. Specifically, the

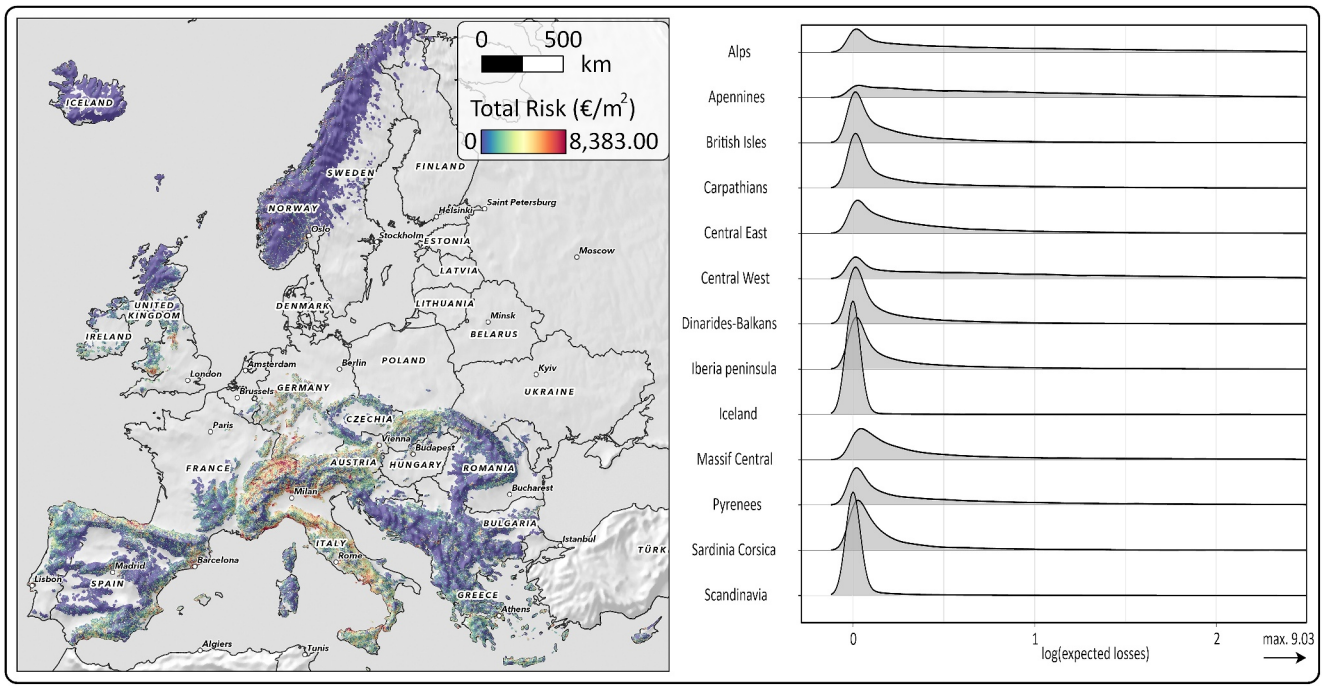

Figure 10. The left panel shows the cartographic representation of expected economic losses across the European landscape. The right panel reports the distribution of losses for each mountain domain on a logarithmic scale.

latter regions exhibit a distribution centered mainly around a domain characterized by very low expected losses (e.g., the logarithm of the potential losses is close to zero). Notably, by multiplying the potential loss per squared meter for the relative extent of the SUs, possible damages range from 0 to 20 Billion €, with a total of approximately 2.3 Trillion €. The sectors with the highest potential losses are predominantly situated in areas corresponding to footslopes or toeslopes, in proximity to floodplains, and where the major human settlements are located. Conversely, the lowest potential losses are associated with areas of higher elevations and specifically with crests or upper slope positions. The second trend might be acceptable due to the limited presence of human settlements. However, the first could be perceived as ambiguous by both geomorphologists and land use planners, since higher economic loss values are associated with areas where the probability of landslide occurrence is generally low. The ambiguity comes both from the inherent challenges in assessing expected economic losses at this scale and the significant influence of human settlement exposure. The limitations primarily arise from the difficulty of defining the vulnerability component, which may contribute to adjusting the degree of loss. Additionally, the role of large urban centers cannot be neglected, as larger settlements tend to expose greater economic value, contributing to the marked increase in expected losses we report here.

To bypass this ambiguity in the landslide risk assessment, in Figure 11, we offer an alternative representation. We opt to visualize the spatial distribution of landslide susceptibility and human settlement exposure together in a map by means of a bivariate color scheme. This allows us to compare and emphasize SUs with a high probability of landslide occurrence and high building exposure. To do so, we plot both the landslide susceptibility and building exposure on a logarithmic scale, and further classify them into three discrete classes following the Jenks method (Jenks & Caspall, 1971; North, 2009). The choice of a logarithmic scale is mainly to remove saturation due to the heavy-tailed risk distributions. Notably, this is a monotonic transformation and therefore, maintains the relative proportion in the original scale. For the exposure component, we only showcase human settlement exposure because of its predominant role compared to agricultural areas in our landslide risk assessment. In this map, Alps and Apennines are mainly characterized by the presence of those areas where both the landslide occurrence and building exposure are high (i.e., dark violet color). Conversely, areas including major urban centers are depicted with a low probability of landsliding and high building exposure (i.e., blue color). We also provide two details of such hotspots (Figures 11a and 11b) for a better visual inspection. From a geomorphic perspective, the proposed classification scheme seems reasonable since SUs with buildings located in upper slope

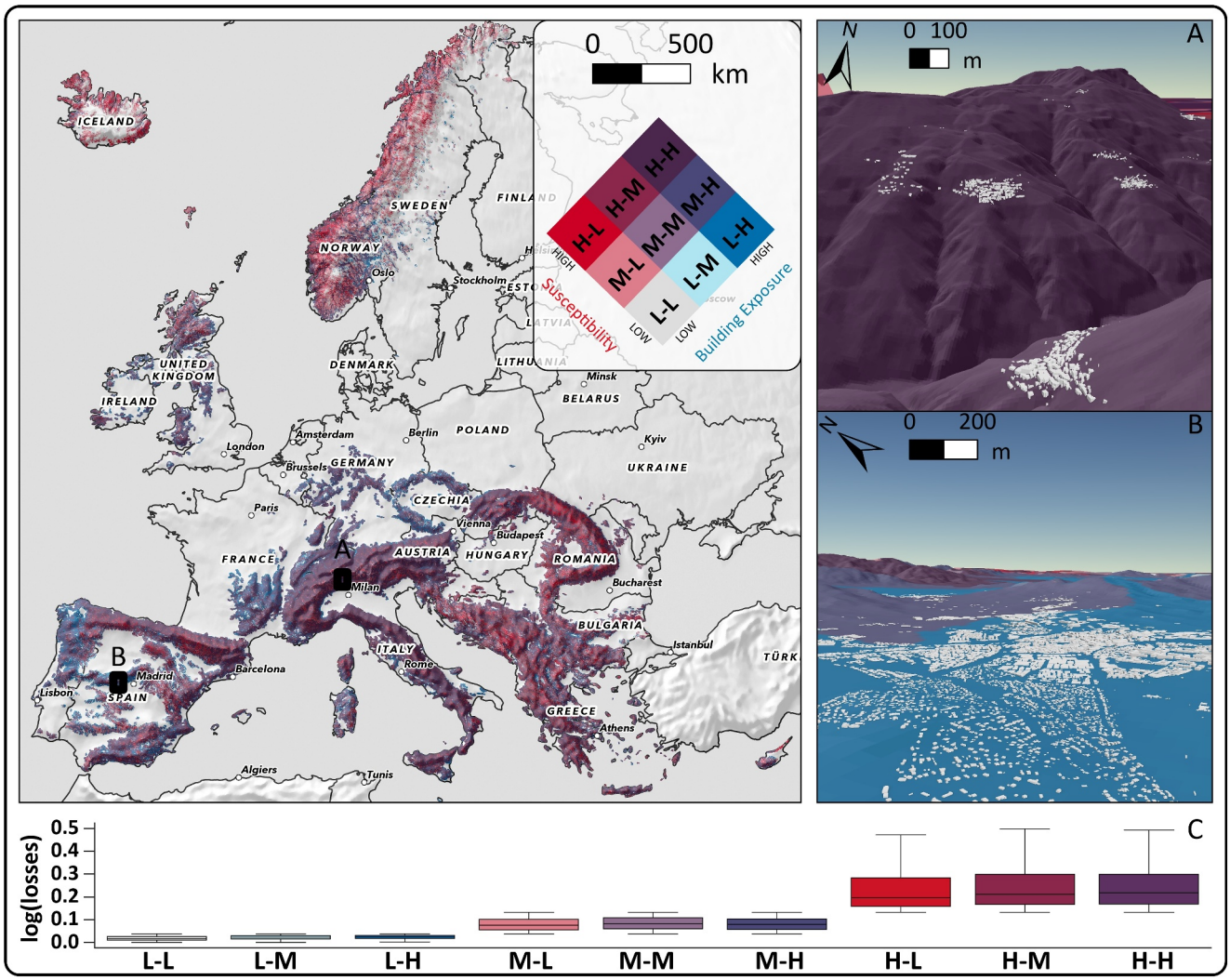

Figure 11. Landslide risk hotspots across the European landscape. Panels (a and b) present a detail of the spatial distribution of risk hotspots, where the 3D building representation is acquired from Open Street Map (LINK-3Dbuildings). Panel (c) shows the distribution of the expected economic losses, on a logarithmic scale, among the different hotspot classes. L stands for "Low," M for "Moderate," and H for "High." The first letter denotes the landslide susceptibility level, while the second letter corresponds to the exposure level of human settlements.

positions are clustered in the hotspot "high susceptibility—high exposure" (Figure 11a). On the other hand, mapping units close to floodplains are included within the class "low susceptibility—high exposure" (Figure 11b). This plotting scheme, therefore, seems to be reliable for the landslide risk analysis framework. Specifically, we notice a clear trend by analyzing the distribution of expected economic losses (Figure 11c) among the different hotspots: as the level of landslide occurrence increases, the expected losses increase.

6.2.3. Population at Risk

Here, we report the outcomes of the analysis related to the population at risk. We recall that this contribution does not provide a loss life estimator due to the challenge of modeling both the dynamics of landslides and the spatio-temporal distribution of people at a continental scale. Therefore, the analysis is essentially a spatial join between our European landslide susceptibility and the yearly population density both for daytime and nighttime. The cartographic representation of the population at risk is displayed in Figure 12. In the database of Batista e Silva et al. (2020) from which population density is extrapolated, information for some countries is not available and therefore not represented (e.g., Norway, Switzerland, Bosnia and Herzegovina, Albania, and Serbia). On the left side, we show the yearly population at risk during the daytime. The representation is built upon a bivariate scheme

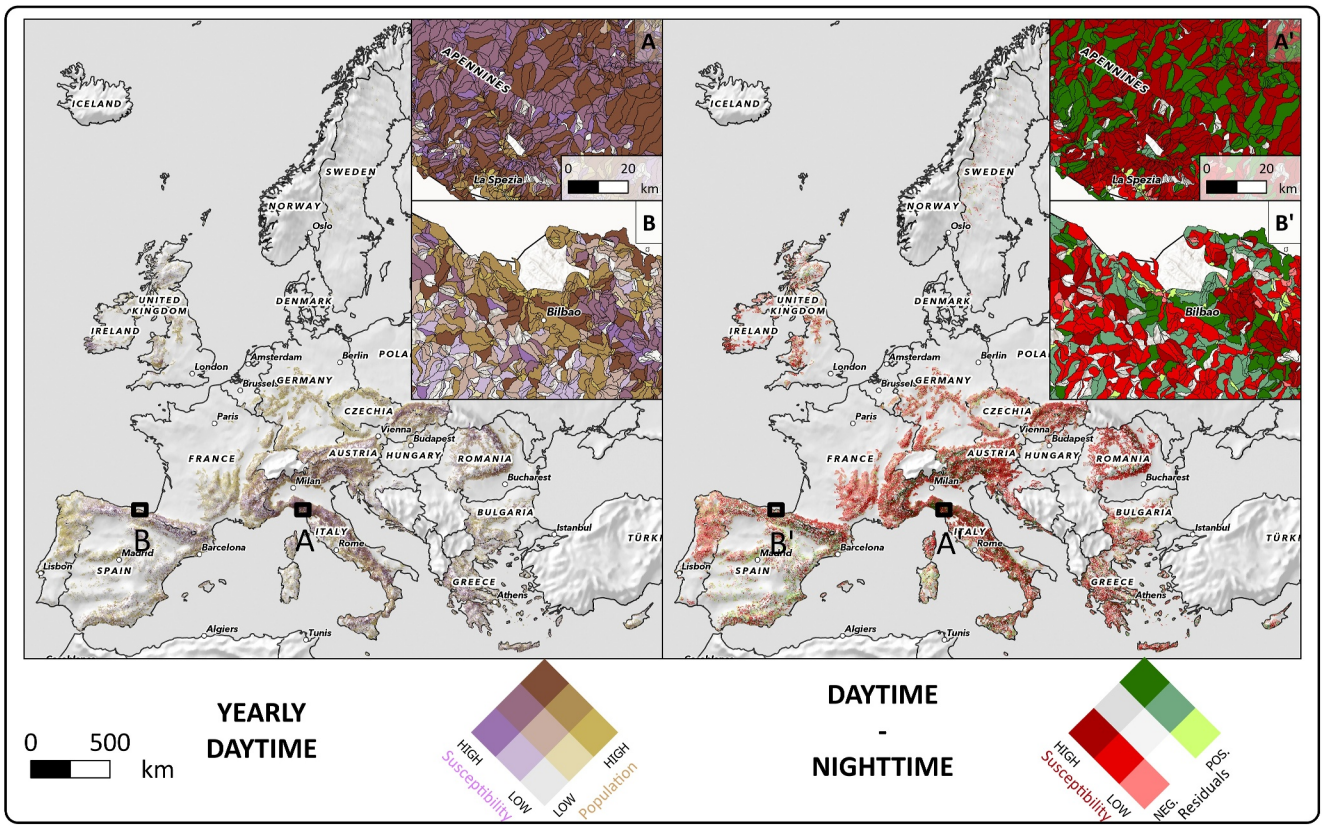

Figure 12. Cartographic representation of the population at risk. The left panel shows the spatial distribution of landslide susceptibility and yearly population density during the daytime. The right panel displays the spatial distribution between landslide susceptibility and differences during daytime and nighttime in the yearly population. Red colors indicate mapping units where the population of nighttime is greater than the one of daytime. The green colors display the opposite case. Both maps are generated with a bivariate scheme. Slope Units without population are not displayed.

where the landslide occurrence probabilities and such population density are spatially combined. We notice that the major concentration of people in high-susceptibility areas is mostly distributed across the Alpine and Appennine domains, with some hotspots in the Carpathians sectors. Conversely, the central sectors of the European landscape are mainly represented as classes where the population density is particularly high but with a low or medium probability of landslide occurrence. A possible explanation of this trend is that these sectors mainly correspond to areas close to the major human settlements, where the people are particularly concentrated and where the conditions do not promote landsliding. On the right side, we do not report the corresponding representation for the nighttime for a simple reason: we notice a slight difference in the spatial patterns between the population at risk during the daytime and nighttime. As a consequence, we opt to visualize the difference between the two daily cycles joined with the landslide susceptibility via a bivariate scheme. In this way, we can facilitate the visualization of changes in patterns between daytime and nighttime, providing a more informative product. There, SUs where the population at risk for nighttime is greater than daytime (i.e., red colors), turn out to be the majority across the landscape. The main reason might be that during the night, the population goes back to residential areas located in mountainous areas. The opposite situation is shown during the day, with the population clustering in industrial and commercial areas. These are mainly located in flat areas, which are not included in our SUs. Overall, this scheme suggests that the population in highly susceptible zones is mainly distributed, as in the case of human settlements, across the Alps and Apennines for both the daily cycles.

6.2.4. Enhancing Scientific Communication on Landslides: WebApp

In this section, we present our idea on how to enhance the sharing and communication of results derived from a landslide risk analysis. In recent years, there has been a continual expansion in the evolution of innovative interactive tools, such as WebGISs (Dahal & Lombardo, 2023). By leveraging this trend, we opt to share our

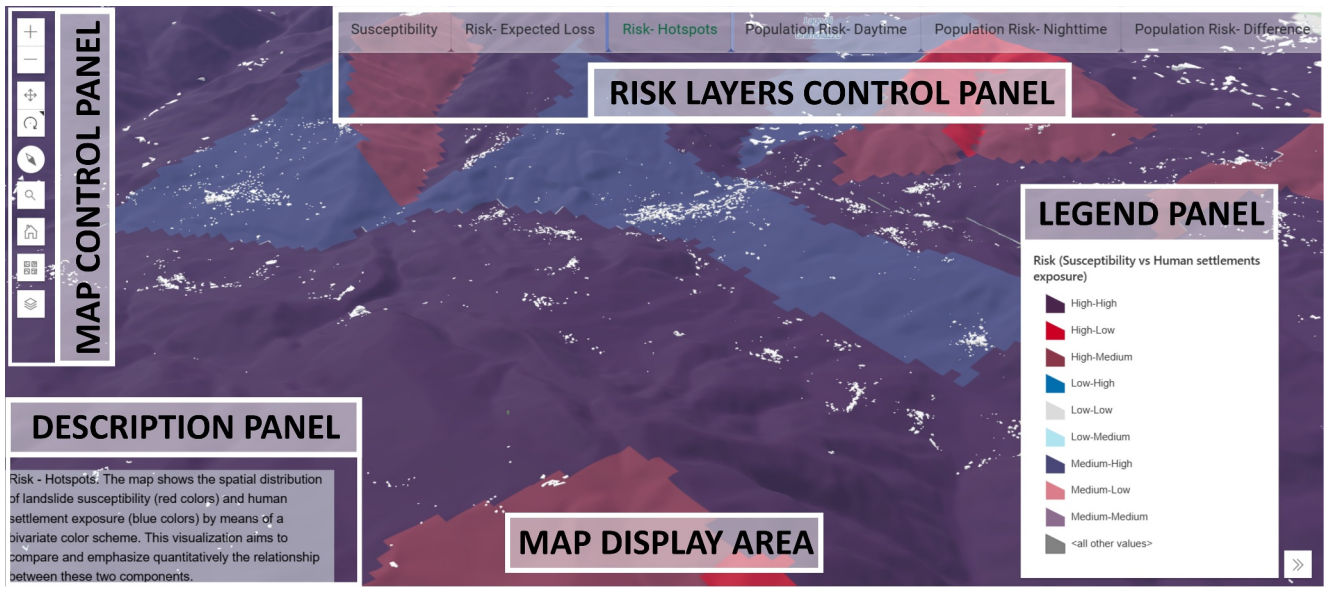

Figure 13. Overview of the WebApp interface and corresponding control panels.

results in a WebApp, which is accessible to the following link: https://pan-european-landslide-risk.github.io/. The WebApp is a client-side web interface hosted through GitHub pages, where interactive functionalities are developed using *JavaScript* combined with *ArcGIS online*. The platform presents common WebGIS functionalities such as layer selection, zoom, panning, legend visualization, pop-up, and spatial search. Users can interact with the outcomes of our landslide susceptibility modeling and risk analysis, by selecting the corresponding layers on the top of the interface. The application's structure can be divided into five control panels (Figure 13), whose corresponding positions are consistent throughout the devices and browsers. The map display is the main element and is capable of rendering 2D and 3D representations based on the user's choice. The 2D visualization is a normal stacking of layers, such as the basemap and our risk data. Conversely, in the 3D mode, the map has a base elevation layer on top of which any risk component can be displayed for a more realistic inspection. To avoid visualization lag, the requests to load layers are dynamically sent to the server based on the zoom level and extent. The description of each layer is reported in a specific panel to facilitate their understanding so that the platform can be used as a stand-alone application. The panels are also inter-connected with each other via query functions and automatically updated when users select a single layer. Notably, the map area presents common features of a GIS environment, where users can select any element and visualize its attributes. For instance, the unbiased susceptibility score or expected economic losses can be easily inspected for any SU. To promote the dissemination of these tools for landslide studies communication, we share the WebApp source code via GitHub (https://github.com/Pan-European-landslide-risk/pan-european-landslide-risk.github.io).

7. Discussion

The sections below will list the pros and cons of the analytical procedure we followed as well as offering an overview of risk dissemination platforms.

7.1. Supporting Arguments

The following sections will provide an overview of the strengths related to the two main components presented in this work.

7.1.1. Susceptibility Considerations

Our product is as unbiased as possible. Landslide susceptibility applications that have included a bias-removal step have all been expressed at the regional or national scale at best. This is the case of Moreno, Lombardo, et al. (2023) for a region in South Tyrol, or for the whole Austrian territory (see, Lima et al., 2021). The only

analogous case where a similar protocol is in place for continental susceptibility modeling is the study presented by Lin et al. (2021). Therefore, what we present here is a unique case where at such a small scale, we produce the best susceptibility estimates.

Oftentimes, landslide susceptibility studies at the continental scale make use of mapping units that are geomorphologically difficult to justify. For instance, the previous European susceptibility (see, Günther et al., 2014) is expressed at a 1 km × 1 km resolution, even though the most recent one was improved up to 0.2 km × 0.2 km (see, Wilde et al., 2018). The analogous case for South Asia has seen even a partition of the landscape with a 3 km × 3 km (see, Titti et al., 2021). As for global susceptibility products, they are all expressed at a 1 km^2 resolution (Hong et al., 2007; Nadim et al., 2006; Stanley & Kirschbaum, 2017b).

This is a justifiable approach only for computation reasons. However, it is something that neglects the underlying geomorphology. In fact, within a 1 km^2, the landscape can host both peaks and valleys, limiting the model inference and interpretation. Conversely, partitioning a given study area, even in the case of continental scales, by means of a geomorphological mapping unit makes the interpretation and the resulting map much more insightful. Here, we make use of SUs. Therefore, even if a SU would present a comparable extent of the 1 km^2 or 9 km^2 resolutions mentioned above, there would be no confusion as to why a given susceptibility value has been assigned.

Notably, we could have also taken a different route in the way we constructed our model. A separate susceptibility assessment could have been made for each mountain belt rather than putting together a single European model. We would like to spend a few words on this consideration because we consider our European approach a strength and a solution to most problems that would have arisen from a number of separate susceptibility cases. Specifically, splitting the whole European data set into a dozen of subsets would have led to a series of complications, which we will list below.

First, the issues related to individual biases would have still been there, and actually, tailoring the analyses to local products would have generated single models whose output would not be comparable to one another. Therefore, the interpretation of the covariates' effects would have suffered from the split. In fact, a smaller data set would have inflated the uncertainty of the marginal plots (see Figure 3). Therefore, splitting the data set would have returned several slightly different covariates' effects whose coherence may have been difficult to read and interpret. In our case, a single model ensures the reading of each contribution in a consistent manner.

Second, the probability would likely range from 0 to 1 in the case of rich inventories, whereas much less populated inventories would have led to much narrower probability ranges, making the comparison hard. As a result, considerations on the applicability of such a model would have also been largely limited. For instance, in our current setting, a European model ensures European-level considerations. However, single models would have led to different performances and with those, one would be unable to discriminate areas of higher ultimate risk from others.

7.1.2. Risk Considerations

The outcomes from our landslide risk analysis bring a new perspective to the current state of this topic. Notably, as discussed in Section 2.4, most studies on landslide risk focus on specific sites (Agliardi et al., 2009; Ferlisi et al., 2012; Lan et al., 2022) or operate at the catchment scale (Catani et al., 2005; Lu et al., 2014; Shano et al., 2022), with only a limited number of contributions extending to regional (see, Crawford et al., 2022; Nguyen & Kim, 2021) or national scales (see, Dorren et al., 2009; Gaprindashvili & Van Westen, 2016). This work goes beyond such limits and provides a continental overview in which we quantify the possible economic losses induced by landslides across the European landscape. The availability of new databases describing the spatial distribution and relative economic values of exposed elements (Crowley et al., 2020; Scaini et al., 2023; Schiavina et al., 2022) makes achievable the extension to such a geographic extent.

Similar to what we mentioned before in the susceptibility case, the analysis relies on a partition into geomorphological units, which even from the risk perspective improves reliability for both master planning and decision-making purposes. Most risk studies at a small scale are based on regular grids (Erener & Düzgün, 2013), inevitably leading to ambiguous results and associated decisions. For instance, in a coarse grid partition, users cannot determine the direction of the potential landslide path or define whether human settlements might be under threat.

Overall, our risk estimates provide a valuable initial step in identifying sectors at risk by offering a broad overview of possible economic losses across various regions. While this macro-level assessment isn't designed for direct site-specific applications, it may underscore priority sectors that could benefit from further detailed risk analysis. In other words, our landslide risk estimates are not designed for planning mitigation measures or allocating funds, but rather as a guide to prioritize areas for detailed, site-specific investigations. Additionally, expressing risk in €/m^2 offers a straightforward index for evaluating potential losses, which stakeholders can use to identify areas for deeper investigation.

The delineation of risk hotspots we propose in Figure 11 proves to be a powerful tool for facilitating the comprehension of the outcomes as well as the identification of which areas might be more inclined to suffer losses. This representation scheme allows us to bypass the noteworthy role expressed by exposure on this scale of analysis. Consequently, we provide a more reliable product from both a geomorphic and risk user perspective.

In this contribution, we go beyond conventional approaches to evaluating the population at risk. Notably, we offer a cartographic representation at a sub-daily scale (day and night). Therefore, our assessment introduces a dynamic component, treating the population as a mobile element. This choice represents a novelty since the population is generally treated as static in both small (see, Jaedicke et al., 2014) and large-scale studies (see, Garcia et al., 2016).

7.2. Opposing Arguments

The following sections will provide an overview of the limitations related to the two main components presented in this work.

7.2.1. Susceptibility Limitations

Our model output follows the traditional definition of landslide susceptibility. In other words, the probability of landslide occurrence is the outcome of a pure spatial model. In turn, this implies that the obtained probability values for each SU are assumed to be stationary in time. This is a strong and very "old-school" notion, which has been challenged in a number of recent contributions where the susceptibility dynamically varies on a temporal basis (Fang et al., 2023; Samia et al., 2017). Ideally, we would have also implemented a space-time susceptibility model here. However, the temporal information is not included in most of the European inventories. This is a point to be raised as the community is discussing setting up standards for landslide inventory mappings for at least a decade (Guzzetti et al., 2012; Tanyaş et al., 2017). Here, we stress once more the need for a common effort, this time not only for susceptibility or hazard mapping but also to enable dynamic risk assessment practices.

A further limitation regards the target of our landslide susceptibility modeling. To obtain a detailed product, a good practice should be modeling differently all landslide types (Loche et al., 2022; F. Huang et al., 2023; Trigila et al., 2013). The reason behind this is that the triggering and predisposing conditions may have different effects on different failure types. By modeling landslide types separately, one can account for the specific conditions that lead to the respective instabilities. However, as mentioned above, this action is only possible if failure mechanisms and associated evolution are part of the landslide inventory information. The majority of landslide inventories we collected does not divide recorded events into different types. Therefore, our model essentially treats SUs where rockfalls take place in the same way as it treats SUs where debris flows appear. As a result, one should interpret the outcome in terms of generic instability and should assume that in the case of a multi-type inventory, an even better assessment and associated performance could be achieved. Therefore, in analogy to the space-time considerations, we also recommend here the inclusion of landslide types as part of a future inventory standard.

7.2.2. Risk Limitations

Two main limitations affect our analyses. The first one relates to the landslide hazard estimation. Here, we approximated hazard by assuming it to be equal to the susceptibility. However, this is a strong assumption which could be bypassed in the presence of consistent polygonal landslide inventories. In fact, at this scale, the landslide intensity could be expressed as a function of landslide area or landslide area density per SU (Di Napoli, Tanyas, et al., 2023; Fang et al., 2024). This information complements the susceptibility one rather than being its alternative. Specifically, a slope could probabilistically be able to release a large mass while not being susceptible. It is also true the opposite that a SU could be probabilistically very likely to fail but with an expected negligible moving mass. This is something we mention to highlight the need for a systematic hazard assessment that would

touch upon all the three elements of its definition. This includes temporal aspects, as also mentioned above but also the notion of intensity.

The second limitation also relates to the application of Equation 2. In fact, for the equation to be fulfilled, the vulnerability component should be defined for the exposed elements. However, the vulnerability evaluation represents a difficult task even for site-specific studies (Singh et al., 2019), let alone for continental-scale applications. This is due to the difficulty of assessing the response of exposed elements to a phenomenon of a certain intensity. To date, it is impossible to estimate both of these vulnerability components across an area as large as the European territory. This difficulty mainly lies in the availability of homogeneous databases for elements-at-risk as well as the expected landslide intensity. Ideally, such information would support the evaluation of the structural resistance of buildings (Z. Li et al., 2010). Here we bypassed this requirement by assuming vulnerability equal to one, which would inevitably lead to an overestimation of the possible economic consequences in some cases.

The issues we referred to come from a missing landslide inventory standard in Europe and in many other geographic contexts. This is somewhat mitigated in other continental communities such as the USA (e.g., Mirus et al., 2020).

Rather than a limitation, we would also like to raise a point of discussion related to the dominance of the exposure (a function of potential economical and life losses) on the risk estimates, compared to the role of the susceptibility itself. In fact, we observed that the highest risk is typically associated with SUs that are located close to flat areas. These are inevitably less susceptible compared to mountainous SUs, although when converting this risk information into maps, the spatial pattern of the expected landslide losses is skewed towards areas with settlements. This raises the question of whether the current landslide risk equation should feature a weighting system that would express both susceptibility and exposure on the same scale. At the moment, this is not the case, which is also the reason why a SU with a susceptibility equal to 0.1 associated with a potential loss of several billion Euros displays a much higher risk than a SU with a susceptibility equal to 1.0 associated with a potential loss of few million Euros. This is certainly reasonable but it is also something to reflect on as a community when producing continental risk maps, because the control of the exposure appears so strong that it almost saturates the scale to the point of making the susceptibility contribution negligible.

7.3. Interactive Risk Communication: The Rise of WebGIS

In recent years, the sharing and communication of findings resulting from landslide studies has constantly increased thanks to the availability of new digital tools. Among these, the development of WebGIS has revolutionized the way researchers and organizations share the outcome of their works, providing interactive platforms for any user (e.g., stakeholders or scientists) to access, visualize and download data. WebGIS represents a powerful fusion of research data and user-friendly interfaces accessible through web browsers. However, the majority of developed WebGIS systems are primarily designed for the purpose of sharing information about landslide locations rather than susceptibility, hazard or risk. Various landslide inventories can, in fact, be accessed through these WebGIS platforms. One notable example of the early use of such a tool is outlined in the work of Salvati et al. (2009). The authors designed the platform to effectively disseminate information regarding historical landslides and floods in the region of Umbria, central Italy. Similarly, the Italian Landslide Inventory (IFFI) is accessible through the IdroGEO platform (Iadanza et al., 2021). Another illustration of WebGIS platforms as a repository is demonstrated by the NASA's Landslide Viewer. This platform facilitates the visualization of data sourced from the Cooperative Open Online Landslide Repository (COOLR) (Juang et al., 2019). The data set encompasses citizen science landslide reports, data from the Global Landslide Catalog (Kirschbaum et al., 2010), and other pertinent landslide catalog information. Additionally, similar tools have been developed through the years and made their way into the standard systems of several countries and organizations around the globe: for example, the Bhuvan platform in India (Link-BHUVAN), the GeoSure platform in the UK (Link-GeoSure), the U.S. Geological Survey's landslide inventory (Link-USGS), the NVE Atlas in Norway (Link-NVE), or the SIMMA platform in Colombia (Link-SIMMA).

A further use of WebGIS is related to the framework of landslide early warning systems. For instance, B. Ahmed et al. (2018) proposes the development of an early warning system directly accessible in WebGIS. This system is connected to an online weather application programming interface, through which precipitation data is streamlined and used to predict landslide occurrences. In a similar way, WebGIS platforms are also used at the site scale

by combining near-real-time sensors and predefined rainfall threshold for automatic and continuous monitoring purposes (J. Huang et al., 2015).

Beyond this level, WebGIS is still in the process of consolidating its role in the dissemination of landslide scientific results to the public. For instance, WebGIS platforms can be used to convey the results of data-driven models for regional and national scale applications. This can be found in a few cases, for static (Dahal & Lombardo, 2023) and dynamic (M. Ahmed et al., 2023) susceptibility results.

However, no landslide risk information is shared yet through WebGIS, with the only exception being the National Risk Index (NRI) in the USA developed by FEMA (Zuzak et al., 2022). And yet, these platforms could constitute a transparent interface for anyone to be informed about landslide risk, ideally with estimates associated to specific mapping units. In fact, a WebGIS environment could help stakeholders, researchers, and the general public to navigate through spatial data layers representing various components of landslide risk: from the occurrence location to the susceptibility, hazard, exposure, vulnerability and potential triggers.

With respect to the specific point of raising awareness, here we would like to share some more in-depth reflections. In fact, public awareness of landslides in general is very limited despite the fact that portals with reference data sets are multifold. Specific to the European case, EU institutions such as JRC offer various visualization tools on several hazards, yet the public interest is still very limited. The potential use we see of our product, differently from others, is that we plot risk; thus, the public could be potentially drawn into querying whether their property may be under threat or not and the extent of the threat in terms of economic losses. Another potential aspect that we see of value is the frequent occurrence of geohazards witnessed in recent years. This could be an additional reason for the public to access portals as our own to make informed decisions for the future. For instance, buyers could check risk products to guide their investments, whereas insurance companies could reevaluate their premiums. Irrespective of such considerations, it is important to note that the FAIR principles (link-here), dictate that scientists would openly share their outcome. However, there are different ways of sharing and as a result, different ways of receiving such outcomes. For instance, a citizen may not understand if we share our products in vector or raster formats but will probably be able to grasp the meaning of our work if the content is placed in an interactive platform. This is also a fundamental reason why we opted for such a data-sharing option, to raise awareness while also maximizing the reach of our scientific efforts.

8. Concluding Remarks

This contribution starts with an overview of the requirements and limitations associated with landslide risk analysis. The existing literature reveals that the majority of risk studies are focused on specific sites, with few exceptions addressing regional or national scales. This trend is attributed to various methodological and data limitations. In light of these considerations, this work develops on a hybrid basis, mixing elements of literature review with original research. The review component identifies limitations faced at different spatial scales of analysis, highlighting that many of these are associated with the assessment of landslide hazard and the vulnerability of exposed elements in their completeness. These challenges arise from the lack of suitable data, particularly in the context of regional-scale studies.

On the original research front, the study provides a practical case at the European level, in which we quantify the possible economic consequences and present an overview of the population at risk during two sub-daily cycles. To do so, we faced issues regarding cross-national differences in landslide mapping. The analytical protocol, therefore, included a bias-removal landslide susceptibility assessment and associated mapping, which was later combined with economic and population data. Such a procedure is built upon a few assumptions: (a) susceptibility is considered a proxy of hazard, (b) all the exposed elements would be affected and suffer irreparable damages.

By leveraging these aspects, a number of future improvements can already be envisioned. To complete the landslide hazard assessment, it is necessary to model its temporal and intensity components. The first might be achievable by implementing automated mapping protocols that would geo-tag landslides not only in their spatial location but also in their temporal one. As a result, recent space-time models could further produce dynamic occurrence probability and associated intensity maps. The same is valid for the risk, with improvements that could pass by a better assessment of the exposed elements as well as a dynamic risk perception. For instance, information on the typology of different constructions might lead to defining a structural resistance, which combined with the intensity component, would allow an assessment of a reference vulnerability value. However, given the

lack of data and standards across European countries, it is currently impossible to implement these extensions for a comprehensive and consistent risk assessment.

Aside from these aspects, we believe that our findings represent a reasonable initial outlook on the likelihood of landslides and associated losses at the continental level. Our risk estimates offer valuable insights for identifying areas that could face potential economic losses. However, these results are not intended for direct applications, such as fund allocation or mitigation planning. Instead, our approach serves as a preliminary guide, highlighting areas where more detailed risk assessments might be useful. Therefore, we hope that this contribution may represent a starting point for the European community and member states to unify their landslide database, including more notions on the kinematics and frequency of events as well as more detailed and homogeneous databases on exposed elements. Achieving some of these requirements may ultimately lead to a better understanding of the landslide risk and its dynamics, thus improving societal resilience.

Finally, we stress again the importance of facilitating user access to data from these studies. To achieve this, we utilize an innovative tool in the form of a WebApp, where we share our findings in the hope of stimulating analogous interactive environments for stakeholders, governments and the public to access relevant information and raise awareness about the threat of landslides.

This was done taking Europe as a pilot, but analogous considerations and potential improvements could become a standard for global landslide risk assessment studies.

Data Availability Statement

Individual landslide inventories can be accessed or requested using the links provided in Table 1. References and repository of covariates included in the landslide susceptibility modeling are reported in Sections 3.2.1 and 3.2.2. The complete set of codes developed for this contribution can be accessed at Caleca, Dahal, et al. (2024). Notably, the data and codes for reproducing the landslide susceptibility modeling are available at the following GitHub repository: Pan-European_Landslide_Susceptibility_modeling. The results of the landslide risk analysis can be inspected through the WebApp (https://pan-european-landslide-risk.github.io/). The plots are generated using either an *R* or *Python* environment. The maps are created using *Esri ArcGIS Pro 3.1.1* (www.esri.com).

Acknowledgments
We kindly acknowledge GeoSphere Austria, José Luís Zêzere (Centre for Geographical Studies, IGOT, University of Lisbon), and Rosa María Mateos Ruiz (Instituto Geológico y Minero de España—IGME) to share and provide valuable information on landslide inventories from their respective countries. Open access publishing facilitated by Universita degli Studi di Firenze, as part of the Wiley - CRUI-CARE agreement.

References

Abella, E. C., & Van Westen, C. (2007). Generation of a landslide risk index map for Cuba using spatial multi-criteria evaluation. *Landslides*, *4*(4), 311–325. https://doi.org/10.1007/s10346-007-0087-y

Agliardi, F., Crosta, G., & Frattini, P. (2009). Integrating rockfall risk assessment and countermeasure design by 3D modelling techniques. *Natural Hazards and Earth System Sciences*, *9*(4), 1059–1073. https://doi.org/10.5194/nhess-9-1059-2009

Ahmed, B. (2021). The root causes of landslide vulnerability in Bangladesh. *Landslides*, *18*(5), 1707–1720. https://doi.org/10.1007/s10346-020-01606-0

Ahmed, B., Rahman, M. S., Islam, R., Sammonds, P., Zhou, C., Uddin, K., & Al-Hussaini, T. M. (2018). Developing a dynamic Web-GIS based landslide early warning system for the Chittagong Metropolitan Area, Bangladesh. *ISPRS International Journal of Geo-Information*, *7*(12), 485. https://doi.org/10.3390/ijgi7120485

Ahmed, M., Tanyas, H., Huser, R., Dahal, A., Titti, G., Borgatti, L., et al. (2023). Dynamic rainfall-induced landslide susceptibility: A step towards a unified forecasting system. *International Journal of Applied Earth Observation and Geoinformation*, *125*, 103593. https://doi.org/10.1016/j.jag.2023.103593

Alexander, D. (2005). Vulnerability to landslides, *Landslide hazard and risk* (pp. 175–198).

Alonso, E., Pineda, J., & Cardoso, R. (2010). Degradation of marls; two case studies from the Iberian Peninsula. *Geological Society, London, Engineering Geology Special Publications*, *23*(1), 47–75. https://doi.org/10.1144/egsp23.5

Al-Thuwaynee, O. F., Melillo, M., Gariano, S. L., Park, H. J., Kim, S.-W., Lombardo, L., et al. (2023). DEWS: A QGIS tool pack for the automatic selection of reference rain gauges for landslide-triggering rainfall thresholds. *Environmental Modelling & Software*, *162*, 105657. https://doi.org/10.1016/j.envsoft.2023.105657

Alvioli, M., & Baum, R. L. (2016). Parallelization of the TRIGRS model for rainfall-induced landslides using the message passing interface. *Environmental Modelling & Software*, *81*, 122–135. https://doi.org/10.1016/j.envsoft.2016.04.002

Alvioli, M., Marchesini, I., Reichenbach, P., Rossi, M., Ardizzone, F., Fiorucci, F., & Guzzetti, F. (2016). Automatic delineation of geomorphological slope units with r. slopeunits v1. 0 and their optimization for landslide susceptibility modeling. *Geoscientific Model Development*, *9*(11), 3975–3991. https://doi.org/10.5194/gmd-9-3975-2016

Amato, G., Eisank, C., Castro-Camilo, D., & Lombardo, L. (2019). Accounting for covariate distributions in slope-unit-based landslide susceptibility models. A case study in the alpine environment. *Engineering Geology*, *260*, 105237. https://doi.org/10.1016/j.enggeo.2019.105237

Amato, G., Fiorucci, M., Martino, S., Lombardo, L., & Palombi, L. (2023). Earthquake-triggered landslide susceptibility in Italy by means of Artificial Neural Network. *Bulletin of Engineering Geology and the Environment*, *82*(5), 160. https://doi.org/10.1007/s10064-023-03163-x

Antronico, L., De Pascale, F., Coscarelli, R., & Gullà, G. (2020). Landslide risk perception, social vulnerability and community resilience: The case study of Maierato (Calabria, southern Italy). *International Journal of Disaster Risk Reduction*, *46*, 101529. https://doi.org/10.1016/j.ijdrr.2020.101529

Apon, M., Notoka, K., Chang, C. N., Ezung, M., Thong, G. T., & Walling, T. (2024). Analysis of an anthropogenically-induced landslide with emphasis on geological precursors. *Results in Earth Sciences*, *2*, 100020. https://doi.org/10.1016/j.rines.2024.100020

Aristizábal, E., Vélez, J. I., Martínez, H. E., & Jaboyedoff, M. (2016). SHIA_Landslide: A distributed conceptual and physically based model to forecast the temporal and spatial occurrence of shallow landslides triggered by rainfall in tropical and mountainous basins. *Landslides*, *13*(3), 497–517. https://doi.org/10.1007/s10346-015-0580-7

Artese, S., & Perrelli, M. (2018). Monitoring a landslide with high accuracy by total station: A DTM-based model to correct for the atmospheric effects. *Geosciences*, *8*(2), 46. https://doi.org/10.3390/geosciences8020046

Batista e Silva, F., Freire, S., Schiavina, M., Rosina, K., Marín-Herrera, M. A., Ziemba, L., et al. (2020). Uncovering temporal changes in Europe's population density patterns using a data fusion approach. *Nature Communications*, *11*(1), 4631. https://doi.org/10.1038/s41467-020-18344-5

Bednarik, M., Yilmaz, I., & Marschalko, M. (2012). Landslide hazard and risk assessment: A case study from the Hlohovec–Sered'landslide area in South-west Slovakia. *Natural Hazards*, *64*(1), 547–575. https://doi.org/10.1007/s11069-012-0257-7

Bell, R., & Glade, T. (2004). Quantitative risk analysis for landslides–Examples from Bíldudalur, NW-Iceland. *Natural Hazards and Earth System Sciences*, *4*(1), 117–131. https://doi.org/10.5194/nhess-4-117-2004

Bergtold, J. S., Spanos, A., & Onukwugha, E. (2010). Bernoulli regression models: Revisiting the specification of statistical models with binary dependent variables. *Journal of Choice Modelling*, *3*(2), 1–28. https://doi.org/10.1016/s1755-5345(13)70033-2

Bhuyan, K., Meena, S. R., Nava, L., van Westen, C., Floris, M., & Catani, F. (2023). Mapping landslides through a temporal lens: An insight toward multi-temporal landslide mapping using the u-net deep learning model. *GIScience & Remote Sensing*, *60*(1), 2182057. https://doi.org/10.1080/15481603.2023.2182057

Borrelli, L., Ciurleo, M., & Gullà, G. (2018). Shallow landslide susceptibility assessment in granitic rocks using GIS-based statistical methods: The contribution of the weathering grade map. *Landslides*, *15*(6), 1127–1142. https://doi.org/10.1007/s10346-018-0947-7

Bossard, M., Feranec, J., & Otahel, J. (2000). *CORINE land cover technical guide: Addendum 2000* (Technical Report No. 40). European Environment Agency.

Brabb, E. E., Pampeyan, E. H., & Bonilla, M. G. (1972). *Landslide susceptibility in San Mateo County, California* (Technical Report). US Geological Survey.

Brenning, A. (2012). Spatial cross-validation and bootstrap for the assessment of prediction rules in remote sensing: The R package sperrorest. In *2012 IEEE International Geoscience and Remote Sensing Symposium* (pp. 5372–5375).

Brenning, A., Schwinn, M., Ruiz-Páez, A., & Muenchow, J. (2015). Landslide susceptibility near highways is increased by 1 order of magnitude in the Andes of southern Ecuador, Loja province. *Natural Hazards and Earth System Sciences*, *15*(1), 45–57. https://doi.org/10.5194/nhess-15-45-2015

Broeckx, J., Vanmaercke, M., Duchateau, R., & Poesen, J. (2018). A data-based landslide susceptibility map of Africa. *Earth-Science Reviews*, *185*, 102–121. https://doi.org/10.1016/j.earscirev.2018.05.002

Brunetti, M., Guzzetti, F., & Rossi, M. (2009). Probability distributions of landslide volumes. *Nonlinear Processes in Geophysics*, *16*(2), 179–188. https://doi.org/10.5194/npg-16-179-2009

Budetta, P. (2002). Risk assessment from debris flows in pyroclastic deposits along a motorway, Italy. *Bulletin of Engineering Geology and the Environment*, *61*(4), 293–301. https://doi.org/10.1007/s10064-002-0161-6

Budimir, M., Atkinson, P., & Lewis, H. (2015). A systematic review of landslide probability mapping using logistic regression. *Landslides*, *12*(3), 419–436. https://doi.org/10.1007/s10346-014-0550-5

Buggle, B., Hambach, U., Kehl, M., Marković, S. B., Zöller, L., & Glaser, B. (2013). The progressive evolution of a continental climate in southeast-central European lowlands during the Middle Pleistocene recorded in loess paleosol sequences. *Geology*, *41*(7), 771–774. https://doi.org/10.1130/g34198.1

Burns, W., Calhoun, N., Franczyk, J., Koss, E., & Bordal, M. (2017). Estimating losses from landslides in Oregon. *Landslides: Putting Experience, Knowledge and Emerging Technologies Into Practice. Association of Environmental & Engineering Geologists (AEG), Special Publication*, *27*, 473–482.

Caleca, F., Dahal, A., Tanyas, H., Steger, S., Raspini, F., Casagli, N., et al. (2024). Pan-European-landslide-risk/pan-European-landslide-risk. GitHub.io: #RELEASE (#codes) [Software]. *Zenodo*. https://doi.org/10.5281/zenodo.14191121

Caleca, F., Scaini, C., Frodella, W., & Tofani, V. (2024). Regional-scale landslide risk assessment in Central Asia. *Natural Hazards and Earth System Sciences*, *24*(1), 13–27. https://doi.org/10.5194/nhess-24-13-2024

Caleca, F., Tofani, V., Segoni, S., Raspini, F., Rosi, A., Natali, M., et al. (2022). A methodological approach of QRA for slow-moving landslides at a regional scale. *Landslides*, *19*(7), 1539–1561. https://doi.org/10.1007/s10346-022-01875-x

Calvello, M., & Pecoraro, G. (2018). Franeitalia: A catalog of recent Italian landslides. *Geoenvironmental Disasters*, *5*, 1–16. https://doi.org/10.1186/s40677-018-0105-5

Cánovas, J. B., Stoffel, M., Corona, C., Schraml, K., Gobiet, A., Tani, S., et al. (2016). Debris-flow risk analysis in a managed torrent based on a stochastic life-cycle performance. *Science of the Total Environment*, *557*, 142–153.

Cao, Y.-M., Guo, W., Wu, Y.-M., Li, L.-P., Zhang, Y.-X., & Lan, H.-X. (2022). An hourly shallow landslide warning model developed by combining automatic landslide spatial susceptibility and temporal rainfall threshold predictions. *Journal of Mountain Science*, *19*(12), 3370–3387. https://doi.org/10.1007/s11629-022-7370-1

Carrara, A. (1983). Multivariate models for landslide hazard evaluation. *Journal of the International Association for Mathematical Geology*, *15*(3), 403–426. https://doi.org/10.1007/bf01031290

Carrara, A. (1988). Drainage and divide networks derived from high-fidelity digital terrain models. In *Quantitative analysis of mineral and energy resources* (pp. 581–597). Springer.

Carrara, A., Cardinali, M., Detti, R., Guzzetti, F., Pasqui, V., & Reichenbach, P. (1991). GIS techniques and statistical models in evaluating landslide hazard. *Earth Surface Processes and Landforms*, *16*(5), 427–445. https://doi.org/10.1002/esp.3290160505

Catani, F., Casagli, N., Ermini, L., Righini, G., & Menduni, G. (2005). Landslide hazard and risk mapping at catchment scale in the Arno River basin. *Landslides*, *2*(4), 329–342. https://doi.org/10.1007/s10346-005-0021-0

Cendrero, A., Forte, L. M., Remondo, J., & Cuesta-Albertos, J. A. (2020). Anthropocene geomorphic change. Climate or human activities? *Earth's Future*, *8*(5), e2019EF001305. https://doi.org/10.1029/2019ef001305

Chang, M., Dou, X., Su, F., & Yu, B. (2023). Remote sensing and optimized neural networks for landslide risk assessment: Paving the way for mitigating Afghanistan landslide damage. *Ecological Indicators*, *156*, 111179. https://doi.org/10.1016/j.ecolind.2023.111179

Chau, K. T., Sze, Y., Fung, M., Wong, W., Fong, E., & Chan, L. (2004). Landslide hazard analysis for Hong Kong using landslide inventory and GIS. *Computers & Geosciences*, *30*(4), 429–443. https://doi.org/10.1016/j.cageo.2003.08.013

Colombo, A., Lanteri, L., Ramasco, M., & Troisi, C. (2005). Systematic GIS-based landslide inventory as the first step for effective landslide-hazard management. *Landslides*, *2*(4), 291–301. https://doi.org/10.1007/s10346-005-0025-9

Corominas, J., Copons, R., Moya, J., Vilaplana, J. M., Altimir, J., & Amigó, J. (2005). Quantitative assessment of the residual risk in a rockfall protected area. *Landslides*, *2*(4), 343–357. https://doi.org/10.1007/s10346-005-0022-z

Corominas, J., Guzzetti, F., Lan, H., Macciotta, R., Marunteranu, C., McDougall, S., & Strom, A. (2023). Revisiting landslide risk terms: IAEG commission C-37 working group on landslide risk nomenclature. *Bulletin of Engineering Geology and the Environment*, *82*(12), 450. https://doi.org/10.1007/s10064-023-03474-z

Corominas, J., Matas, G., & Ruiz-Carulla, R. (2019). Quantitative analysis of risk from fragmental rockfalls. *Landslides*, *16*(1), 5–21. https://doi.org/10.1007/s10346-018-1087-9

Corominas, J., & Moya, J. (2008). A review of assessing landslide frequency for hazard zoning purposes. *Engineering Geology*, *102*(3–4), 193–213. https://doi.org/10.1016/j.enggeo.2008.03.018

Corominas, J., Moya, J., Lloret, A., Gili, J., Angeli, M., Pasuto, A., & Silvano, S. (2000). Measurement of landslide displacements using a wire extensometer. *Engineering Geology*, *55*(3), 149–166. https://doi.org/10.1016/s0013-7952(99)00086-1

Corominas, J., van Westen, C., Frattini, P., Cascini, L., Malet, J., Fotopoulou, S., et al. (2014). Recommendations for the quantitative analysis of landslide risk. *Bulletin of Engineering Geology and the Environment*, *73*, 209–263.

Crawford, M. M., Dortch, J. M., Koch, H. J., Zhu, Y., Haneberg, W. C., Wang, Z., & Bryson, L. S. (2022). Landslide risk assessment in Eastern Kentucky, USA: Developing a regional scale, limited resource approach. *Remote Sensing*, *14*(24), 6246. https://doi.org/10.3390/rs14246246

Crovelli, R. A. (2000). *Probability models for estimation of number and costs of landslides* (Technical Report). US Geological Survey.

Crowley, H., & Bommer, J. J. (2006). Modelling seismic hazard in earthquake loss models with spatially distributed exposure. *Bulletin of Earthquake Engineering*, *4*(3), 249–273. https://doi.org/10.1007/s10518-006-9009-y

Crowley, H., Despotaki, V., Rodrigues, D., Silva, V., Costa, C., Toma-Danila, D., et al. (2021). European exposure model data repository. *Zenodo*. https://doi.org/10.5281/zenodo.5730071

Crowley, H., Despotaki, V., Rodrigues, D., Silva, V., Toma-Danila, D., Riga, E., et al. (2020). Exposure model for European seismic risk assessment. *Earthquake Spectra*, *36*(1_suppl), 252–273. https://doi.org/10.1177/8755293020919429

Crozier, M. J., & Glade, T. (2005). Landslide hazard and risk: Issues, concepts and approach, *Landslide hazard and risk* (pp. 1–40).

Cuomo, S., Masi, E. B., Tofani, V., Moscariello, M., Rossi, G., & Matano, F. (2021). Multiseasonal probabilistic slope stability analysis of a large area of unsaturated pyroclastic soils. *Landslides*, *18*(4), 1259–1274. https://doi.org/10.1007/s10346-020-01561-w

Cutter, S. L., Emrich, C. T., Morath, D., & Dunning, C. (2013). Integrating social vulnerability into federal flood risk management planning. *Journal of Flood Risk Management*, *6*(4), 332–344. https://doi.org/10.1111/jfr3.12018

Dahal, A., & Lombardo, L. (2023). Explainable artificial intelligence in geoscience: A glimpse into the future of landslide susceptibility modeling. *Computers & Geosciences*, *176*, 105364. https://doi.org/10.1016/j.cageo.2023.105364

Dahal, A., Tanyas, H., van Westen, C. J., van der Meijde, M., Mai, P. M., Huser, R., & Lombardo, L. (2022). Space-time landslide hazard modeling via Ensemble Neural Networks.

Dai, F., Lee, C. F., & Ngai, Y. Y. (2002). Landslide risk assessment and management: An overview. *Engineering Geology*, *64*(1), 65–87. https://doi.org/10.1016/s0013-7952(01)00093-x

D'Ambrosio, D., Di Gregorio, S., Iovine, G., Lupiano, V., Rongo, R., & Spataro, W. (2003). First simulations of the Sarno debris flows through Cellular Automata modelling. *Geomorphology*, *54*(1–2), 91–117. https://doi.org/10.1016/s0169-555x(03)00058-8

Danciu, L., Nandan, S., Reyes, C. G., Basili, R., Weatherill, G., Beauval, C., et al. (2021). *The 2020 update of the European Seismic Hazard Model - ESHM20: Model overview* (Report). European Facilities of Earthquake Hazard and Risk.

de Almeida, L. Q., Welle, T., & Birkmann, J. (2016). Disaster risk indicators in Brazil: A proposal based on the world risk index. *International Journal of Disaster Risk Reduction*, *17*, 251–272. https://doi.org/10.1016/j.ijdrr.2016.04.007

De Bono, A., & Mora, M. G. (2014). A global exposure model for disaster risk assessment. *International Journal of Disaster Risk Reduction*, *10*, 442–451. https://doi.org/10.1016/j.ijdrr.2014.05.008

Deijns, A. A., Michéa, D., Déprez, A., Malet, J.-P., Kervyn, F., Thiery, W., & Dewitte, O. (2024). A semi-supervised multi-temporal landslide and flash flood event detection methodology for unexplored regions using massive satellite image time series. *ISPRS Journal of Photogrammetry and Remote Sensing*, *215*, 400–418. https://doi.org/10.1016/j.isprsjprs.2024.07.010

Dell'Acqua, F., Gamba, P., & Jaiswal, K. (2013). Spatial aspects of building and population exposure data and their implications for global earthquake exposure modeling. *Natural Hazards*, *68*(3), 1291–1309. https://doi.org/10.1007/s11069-012-0241-2

Del Soldato, M., Solari, L., Poggi, F., Raspini, F., Tomás, R., Fanti, R., & Casagli, N. (2019). Landslide-induced damage probability estimation coupling InSAR and field survey data by fragility curves. *Remote Sensing*, *11*(12), 1486. https://doi.org/10.3390/rs11121486

Depicker, A., Jacobs, L., Delvaux, D., Havenith, H.-B., Mateso, J.-C. M., Govers, G., & Dewitte, O. (2020). The added value of a regional landslide susceptibility assessment: The western branch of the East African Rift. *Geomorphology*, *353*, 106886. https://doi.org/10.1016/j.geomorph.2019.106886

Depicker, A., Jacobs, L., Mboga, N., Smets, B., Van Rompaey, A., Lennert, M., et al. (2021). Historical dynamics of landslide risk from population and forest-cover changes in the Kivu Rift. *Nature Sustainability*, *4*(11), 965–974. https://doi.org/10.1038/s41893-021-00757-9

Dille, A., Dewitte, O., Handwerger, A. L., d'Oreye, N., Derauw, D., Ganza Bamulezi, G., et al. (2022). Acceleration of a large deep-seated tropical landslide due to urbanization feedbacks. *Nature Geoscience*, *15*(12), 1048–1055. https://doi.org/10.1038/s41561-022-01073-3

Dille, A., Kervyn, F., Bibentyo, T. M., Delvaux, D., Ganza, G. B., Mawe, G. I., et al. (2019). Causes and triggers of deep-seated hillslope instability in the tropics–Insights from a 60-year record of Ikoma landslide (DR Congo). *Geomorphology*, *345*, 106835. https://doi.org/10.1016/j.geomorph.2019.106835

Di Napoli, M., Miele, P., Guerriero, L., Annibali Corona, M., Calcaterra, D., Ramondini, M., et al. (2023). Multitemporal relative landslide exposure and risk analysis for the sustainable development of rapidly growing cities. *Landslides*, *20*(9), 1–15. https://doi.org/10.1007/s10346-023-02065-z

Di Napoli, M., Tanyas, H., Castro-Camilo, D., Calcaterra, D., Cevasco, A., Di Martire, D., et al. (2023). On the estimation of landslide intensity, hazard and density via data-driven models. *Natural Hazards*, *119*(3), 1513–1530. https://doi.org/10.1007/s11069-023-06153-0

Domènech, G., Alvioli, M., & Corominas, J. (2020). Preparing first-time slope failures hazard maps: From pixel-based to slope unit-based. *Landslides*, *17*(2), 249–265. https://doi.org/10.1007/s10346-019-01279-4

Dorren, L., Sandri, A., Raetzo, H., & Arnold, P. (2009). Landslide risk mapping for the entire Swiss national road network, *Landslide Processes: From geomorphologic mapping to dynamic modeling, Strasbourg, France* (pp. 6–7).

Durgin, P. B. (1977). Landslides and the weathering of granitic rocks. *GSA Reviews in Engineering Geology*, *3*, 125–131. https://doi.org/10.1130/REG3-p125

Emberson, R., Kirschbaum, D., & Stanley, T. (2020). New global characterisation of landslide exposure. *Natural Hazards and Earth System Sciences*, *20*(12), 3413–3424. https://doi.org/10.5194/nhess-20-3413-2020

Erener, A., & Düzgün, H. S. (2013). A regional scale quantitative risk assessment for landslides: Case of Kumluca watershed in Bartin, Turkey. *Landslides*, *10*(1), 55–73. https://doi.org/10.1007/s10346-012-0317-9

Eurostat. (2012). European Commission Data Base.

Fang, Z., Wang, Y., van Westen, C., & Lombardo, L. (2023). Space–time landslide susceptibility modeling based on data-driven methods. *Mathematical Geosciences*, *56*(6), 1–20. https://doi.org/10.1007/s11004-023-10105-6

Fang, Z., Wang, Y., van Westen, C., & Lombardo, L. (2024). Landslide hazard spatiotemporal prediction based on data-driven models: Estimating where, when and how large landslide may be. *International Journal of Applied Earth Observation and Geoinformation*, *126*, 103631. https://doi.org/10.1016/j.jag.2023.103631

Fassnacht, S., Dressler, K., Hultstrand, D., Bales, R., & Patterson, G. (2012). Temporal inconsistencies in coarse-scale snow water equivalent patterns: Colorado River Basin snow telemetry-topography regressions. *Pirineos*, *167*(167), 165–185. https://doi.org/10.3989/pirineos.2012.167008

Fawcett, T. (2006). An introduction to ROC analysis. *Pattern Recognition Letters*, *27*(8), 861–874. https://doi.org/10.1016/j.patrec.2005.10.010

Fell, R. (1994). Landslide risk assessment and acceptable risk. *Canadian Geotechnical Journal*, *31*(2), 261–272. https://doi.org/10.1139/t94-031

Fell, R., Corominas, J., Bonnard, C., Cascini, L., Leroi, E., & Savage, W. Z. (2008). Guidelines for landslide susceptibility, hazard and risk zoning for land use planning. *Engineering Geology*, *102*(3–4), 85–98. https://doi.org/10.1016/j.enggeo.2008.03.022

Fell, R., & Hartford, D. (2018). Landslide risk management. In *Landslide risk assessment* (pp. 51–109). Routledge.

Fell, R., Ho, K. K., Lacasse, S., & Leroi, E. (2005). A framework for landslide risk assessment and management. In *Landslide risk management* (pp. 13–36). CRC Press.

Fell, R., Stapledon, D., & MacGregor, P. (2012). Landslides and geologic environments. In J. J. Clague & D. Stead (Eds.), *Landslides: Types, mechanisms and modeling* (pp. 134–143). Cambridge University Press. https://doi.org/10.1017/CBO9780511740367.013

Ferlisi, S., Cascini, L., Corominas, J., & Matano, F. (2012). Rockfall risk assessment to persons travelling in vehicles along a road: The case study of the Amalfi coastal road (southern Italy). *Natural Hazards*, *62*(2), 691–721. https://doi.org/10.1007/s11069-012-0102-z

Ferrer, J. V., Samprogna Mohor, G., Dewitte, O., Pánek, T., Reyes-Carmona, C., Handwerger, A. L., et al. (2024). Human settlement pressure drives slow-moving landslide exposure. *Earth's Future*, *12*(9), e2024EF004830. https://doi.org/10.1029/2024ef004830

Ferro, V., Carollo, F. G., & Serio, M. A. (2020). Establishing a threshold for rainfall-induced landslides by a kinetic energy–duration relationship. *Hydrological Processes*, *34*(16), 3571–3581. https://doi.org/10.1002/hyp.13821

Finlay, P., Fell, R., & Maguire, P. (1997). The relationship between the probability of landslide occurrence and rainfall. *Canadian Geotechnical Journal*, *34*(6), 811–824. https://doi.org/10.1139/cgj-34-6-811

Formetta, G., Capparelli, G., & Versace, P. (2016). Evaluating performance of simplified physically based models for shallow landslide susceptibility. *Hydrology and Earth System Sciences*, *20*(11), 4585–4603. https://doi.org/10.5194/hess-20-4585-2016

Formetta, G., Rago, V., Capparelli, G., Rigon, R., Muto, F., & Versace, P. (2014). Integrated physically based system for modeling landslide susceptibility. *Procedia Earth and Planetary Science*, *9*, 74–82. https://doi.org/10.1016/j.proeps.2014.06.006

Foster, C., Pennington, C., Culshaw, M., & Lawrie, K. (2012). The national landslide database of Great Britain: Development, evolution and applications. *Environmental Earth Sciences*, *66*(3), 941–953. https://doi.org/10.1007/s12665-011-1304-5

Fotopoulou, S., & Pitilakis, K. (2013). Fragility curves for reinforced concrete buildings to seismically triggered slow-moving slides. *Soil Dynamics and Earthquake Engineering*, *48*, 143–161. https://doi.org/10.1016/j.soildyn.2013.01.004

Frattini, P., Crosta, G., & Sosio, R. (2009). Approaches for defining thresholds and return periods for rainfall-triggered shallow landslides. *Hydrological Processes: International Journal*, *23*(10), 1444–1460. https://doi.org/10.1002/hyp.7269

Froude, M. J., & Petley, D. N. (2018). Global fatal landslide occurrence from 2004 to 2016. *Natural Hazards and Earth System Sciences*, *18*(8), 2161–2181. https://doi.org/10.5194/nhess-18-2161-2018

Fu, S., Chen, L., Woldai, T., Yin, K., Gui, L., Li, D., et al. (2020). Landslide hazard probability and risk assessment at the community level: A case of western Hubei, China. *Natural Hazards and Earth System Sciences*, *20*(2), 581–601. https://doi.org/10.5194/nhess-20-581-2020

Fuchs, S., Keiler, M., Ortlepp, R., Schinke, R., & Papathoma-Köhle, M. (2019). Recent advances in vulnerability assessment for the built environment exposed to torrential hazards: Challenges and the way forward. *Journal of Hydrology*, *575*, 587–595. https://doi.org/10.1016/j.jhydrol.2019.05.067

Galli, M., & Guzzetti, F. (2007). Landslide vulnerability criteria: A case study from Umbria, Central Italy. *Environmental Management*, *40*(4), 649–665. https://doi.org/10.1007/s00267-006-0325-4

Gaprindashvili, G., & Van Westen, C. J. (2016). Generation of a national landslide hazard and risk map for the country of Georgia. *Natural Hazards*, *80*(1), 69–101. https://doi.org/10.1007/s11069-015-1958-5

Garcia, R. A., Oliveira, S. C., & Zêzere, J. L. (2016). Assessing population exposure for landslide risk analysis using dasymetric cartography. *Natural Hazards and Earth System Sciences*, *16*(12), 2769–2782. https://doi.org/10.5194/nhess-16-2769-2016

Gatto, M. P. A., Lentini, V., Montrasio, L., & Castelli, F. (2023). A simplified semi-quantitative procedure based on the SLIP model for landslide risk assessment: The case study of Gioiosa Marea (Sicily, Italy). *Landslides*, *20*(7), 1–23. https://doi.org/10.1007/s10346-023-02040-8

Giles, P. T., & Franklin, S. E. (1998). An automated approach to the classification of the slope units using digital data. *Geomorphology*, *21*(3–4), 251–264. https://doi.org/10.1016/s0169-555x(97)00064-0

Gill, J. C., Taylor, F. E., Duncan, M. J., Mohadjer, S., Budimir, M., Mdala, H., & Bukachi, V. (2021). Invited perspectives: Building sustainable and resilient communities–recommended actions for natural hazard scientists. *Natural Hazards and Earth System Sciences*, *21*(1), 187–202. https://doi.org/10.5194/nhess-21-187-2021

Glade, T. (2003a). Landslide occurrence as a response to land use change: A review of evidence from New Zealand. *Catena*, *51*(3–4), 297–314. https://doi.org/10.1016/s0341-8162(02)00170-4

Glade, T. (2003b). Vulnerability assessment in landslide risk analysis. *Die Erde*, *134*(2), 123–146.

Goetz, J., Brenning, A., Petschko, H., & Leopold, P. (2015). Evaluating machine learning and statistical prediction techniques for landslide susceptibility modeling. *Computers & Geosciences*, *81*, 1–11. https://doi.org/10.1016/j.cageo.2015.04.007

Görüm, T., & Fidan, S. (2021). Spatiotemporal variations of fatal landslides in Turkey. *Landslides*, *18*(5), 1691–1705. https://doi.org/10.1007/s10346-020-01580-7

Grant, A., Wartman, J., & Abou-Jaoude, G. (2016). Multimodal method for coseismic landslide hazard assessment. *Engineering Geology*, *212*, 146–160. https://doi.org/10.1016/j.enggeo.2016.08.005

Guillard-Gonçalves, C., & Zêzere, J. L. (2018). Combining social vulnerability and physical vulnerability to analyse landslide risk at the municipal scale. *Geosciences*, *8*(8), 294. https://doi.org/10.3390/geosciences8080294

Günther, A., Van Den Eeckhaut, M., Malet, J.-P., Reichenbach, P., & Hervás, J. (2014). Climate-physiographically differentiated Pan-European landslide susceptibility assessment using spatial multi-criteria evaluation and transnational landslide information. *Geomorphology*, *224*, 69–85. https://doi.org/10.1016/j.geomorph.2014.07.011

Guo, Z., Chen, L., Yin, K., Shrestha, D. P., & Zhang, L. (2020). Quantitative risk assessment of slow-moving landslides from the viewpoint of decision-making: A case study of the Three Gorges Reservoir in China. *Engineering Geology*, *273*, 105667. https://doi.org/10.1016/j.enggeo.2020.105667

Guzzetti, F. (2005). *Landslide hazard and risk assessment* (Doctoral dissertation). Rheinische Friedrich-Wilhelms-Universität Bonn. Retrieved from https://hdl.handle.net/20.500.11811/2644

Guzzetti, F. (2021). Invited perspectives: Landslide populations–can they be predicted? *Natural Hazards and Earth System Sciences*, *21*(5), 1467–1471. https://doi.org/10.5194/nhess-21-1467-2021

Guzzetti, F., Carrara, A., Cardinali, M., & Reichenbach, P. (1999). Landslide hazard evaluation: A review of current techniques and their application in a multi-scale study, Central Italy. *Geomorphology*, *31*(1–4), 181–216. https://doi.org/10.1016/s0169-555x(99)00078-1

Guzzetti, F., Galli, M., Reichenbach, P., Ardizzone, F., & Cardinali, M. (2006). Landslide hazard assessment in the Collazzone area, Umbria, Central Italy. *Natural Hazards and Earth System Sciences*, *6*(1), 115–131. https://doi.org/10.5194/nhess-6-115-2006

Guzzetti, F., Mondini, A. C., Cardinali, M., Fiorucci, F., Santangelo, M., & Chang, K.-T. (2012). Landslide inventory maps: New tools for an old problem. *Earth-Science Reviews*, *112*(1–2), 42–66. https://doi.org/10.1016/j.earscirev.2012.02.001

Guzzetti, F., Reichenbach, P., Ardizzone, F., Cardinali, M., & Galli, M. (2006). Estimating the quality of landslide susceptibility models. *Geomorphology*, *81*(1–2), 166–184. https://doi.org/10.1016/j.geomorph.2006.04.007

Guzzetti, F., Reichenbach, P., Cardinali, M., Galli, M., & Ardizzone, F. (2005). Probabilistic landslide hazard assessment at the basin scale. *Geomorphology*, *72*(1–4), 272–299. https://doi.org/10.1016/j.geomorph.2005.06.002

Haklay, M., & Weber, P. (2008). Openstreetmap: User-generated street maps. *IEEE Pervasive Computing*, *7*(4), 12–18. https://doi.org/10.1109/mprv.2008.80

Hanley, J. A., & McNeil, B. J. (1982). The meaning and use of the area under a receiver operating characteristic (ROC) curve. *Radiology*, *143*(1), 29–36. https://doi.org/10.1148/radiology.143.1.7063747

Hantz, D., Corominas, J., Crosta, G. B., & Jaboyedoff, M. (2021). Definitions and concepts for quantitative rockfall hazard and risk analysis. *Geosciences*, *11*(4), 158. https://doi.org/10.3390/geosciences11040158

Haque, U., Blum, P., da Silva, P., Andersen, P., Pilz, J., Chalov, S., et al. (2016). Fatal landslides in Europe. *Landslides*, *13*(6), 1545–1554. https://doi.org/10.1007/s10346-016-0689-3

Haque, U., Da Silva, P., Devoli, G., Pilz, J., Zhao, B., Khaloua, A., et al. (2019). The human cost of global warming: Deadly landslides and their triggers (1995–2014). *Science of the Total Environment*, *682*, 673–684. https://doi.org/10.1016/j.scitotenv.2019.03.415

Hastie, T., & Tibshirani, R. (1987). Generalized additive models: Some applications. *Journal of the American Statistical Association*, *82*(398), 371–386. https://doi.org/10.1080/01621459.1987.10478440

Herrera, G., Mateos, R. M., García-Davalillo, J. C., Grandjean, G., Poyiadji, E., Maftei, R., et al. (2018). Landslide databases in the Geological Surveys of Europe. *Landslides*, *15*(2), 359–379. https://doi.org/10.1007/s10346-017-0902-z

Hewitt, K. (2014). *Regions of risk: A geographical introduction to disasters*. Routledge.

Hidalgo, C. A., & Vega, J. A. (2021). Probabilistic landslide risk assessment in water supply basins: La Liboriana River Basin (Salgar-Colombia). *Natural Hazards*, *109*(1), 273–301. https://doi.org/10.1007/s11069-021-04836-0

Hilker, N., Badoux, A., & Hegg, C. (2009). The Swiss flood and landslide damage database 1972–2007. *Natural Hazards and Earth System Sciences*, *9*(3), 913–925. https://doi.org/10.5194/nhess-9-913-2009

Hong, Y., Adler, R., & Huffman, G. (2007). Use of satellite remote sensing data in the mapping of global landslide susceptibility. *Natural Hazards*, *43*(2), 245–256. https://doi.org/10.1007/s11069-006-9104-z

Hosmer, D. W., & Lemeshow, S. (2000). *Applied logistic regression* (Vol. 398). John Wiley & Sons. https://doi.org/10.1002/0471722146

Hosmer, D. W., Jr., Lemeshow, S., & Sturdivant, R. X. (2013). *Applied logistic regression* (Vol. 398). John Wiley & Sons. https://doi.org/10.1002/9781118548387

Huang, F., Tao, S., Chang, Z., Huang, J., Fan, X., Jiang, S.-H., & Li, W. (2021). Efficient and automatic extraction of slope units based on multi-scale segmentation method for landslide assessments. *Landslides*, *18*(11), 3715–3731. https://doi.org/10.1007/s10346-021-01756-9

Huang, F., Xiong, H., Yao, C., Catani, F., Zhou, C., & Huang, J. (2023). Uncertainties of landslide susceptibility prediction considering different landslide types. *Journal of Rock Mechanics and Geotechnical Engineering*, *15*(11), 2954–2972. https://doi.org/10.1016/j.jrmge.2023.03.001

Huang, J., Huang, R., Ju, N., Xu, Q., & He, C. (2015). 3D WebGIS-based platform for debris flow early warning: A case study. *Engineering Geology*, *197*, 57–66. https://doi.org/10.1016/j.enggeo.2015.08.013

Huffman, G. J., Bolvin, D. T., Braithwaite, D., Hsu, K., Joyce, R., Xie, P., & Yoo, S.-H. (2015). NASA global precipitation measurement (GPM) integrated multi-satellite retrievals for GPM (IMERG). *Algorithm Theoretical Basis Document (ATBD) Version*, *4*(26), 30.

Huggel, C., Clague, J. J., & Korup, O. (2012). Is climate change responsible for changing landslide activity in high mountains? *Earth Surface Processes and Landforms*, *37*(1), 77–91. https://doi.org/10.1002/esp.2223

Hungr, O. (1997). Some methods of landslide hazard intensity mapping. In *Landslide risk assessment* (pp. 215–226). Routledge.

Hungr, O., Leroueil, S., & Picarelli, L. (2014). The Varnes classification of landslide types, an update. *Landslides*, *11*(2), 167–194. https://doi.org/10.1007/s10346-013-0436-y

Hunter, G. J., & Williamson, I. P. (1990). The development of a historical digital cadastral database. *International Journal of Geographical Information System*, *4*(2), 169–179. https://doi.org/10.1080/02693799008941538

Iadanza, C., Trigila, A., Starace, P., Dragoni, A., Biondo, T., & Roccisano, M. (2021). IdroGEO: A collaborative web mapping application based on REST API services and open data on landslides and floods in Italy. *ISPRS International Journal of Geo-Information*, *10*(2), 89. https://doi.org/10.3390/ijgi10020089

Ietto, F., Perri, F., & Cella, F. (2016). Geotechnical and landslide aspects in weathered granitoid rock masses (Serre Massif, southern Calabria, Italy). *Catena*, *145*, 301–315. https://doi.org/10.1016/j.catena.2016.06.027

Ihaka, R., & Gentleman, R. (1996). R: A language for data analysis and graphics. *Journal of Computational & Graphical Statistics*, *5*(3), 299–314. https://doi.org/10.1080/10618600.1996.10474713

Jaboyedoff, M., Carrea, D., Derron, M.-H., Oppikofer, T., Penna, I. M., & Rudaz, B. (2020). A review of methods used to estimate initial landslide failure surface depths and volumes. *Engineering Geology*, *267*, 105478. https://doi.org/10.1016/j.enggeo.2020.105478

Jaboyedoff, M., Michoud, C., Derron, M.-H., Voumard, J., Leibundgut, G., Sudmeier-Rieux, K., et al. (2016). Human-induced landslides: Toward the analysis of anthropogenic changes of the slope environment. In *Landslides and engineered slopes. experience, theory and practice: Proceedings of the 12th international symposium on landslides* (pp. 217–232). CRC Press.

Jacobs, L., Dewitte, O., Poesen, J., Maes, J., Mertens, K., Sekajugo, J., & Kervyn, M. (2017). Landslide characteristics and spatial distribution in the Rwenzori Mountains, Uganda. *Journal of African Earth Sciences*, *134*, 917–930. https://doi.org/10.1016/j.jafrearsci.2016.05.013

Jaedicke, C., Lied, K., & Kronholm, K. (2009). Integrated database for rapid mass movements in Norway. *Natural Hazards and Earth System Sciences*, *9*(2), 469–479. https://doi.org/10.5194/nhess-9-469-2009

Jaedicke, C., Van Den Eeckhaut, M., Nadim, F., Hervás, J., Kalsnes, B., Vangelsten, B. V., et al. (2014). Identification of landslide hazard and risk 'hotspots' in Europe. *Bulletin of Engineering Geology and the Environment*, *73*, 325–339.
Jaiswal, P., Van Westen, C., & Jetten, V. (2011). Quantitative estimation of landslide risk from rapid debris slides on natural slopes in the Nilgiri hills, India. *Natural Hazards and Earth System Sciences*, *11*(6), 1723–1743. https://doi.org/10.5194/nhess-11-1723-2011
Jaiswal, P., & van Westen, C. J. (2009). Estimating temporal probability for landslide initiation along transportation routes based on rainfall thresholds. *Geomorphology*, *112*(1–2), 96–105. https://doi.org/10.1016/j.geomorph.2009.05.008
Jakob, M., Hungr, O., & Rickenmann, D. (2005). Runout prediction methods, *Debris-flow hazards and related phenomena* (pp. 305–324).
Jenks, G. F., & Caspall, F. C. (1971). Error on choroplethic maps: Definition, measurement, reduction. *Annals of the Association of American Geographers*, *61*(2), 217–244. https://doi.org/10.1111/j.1467-8306.1971.tb00779.x
Juang, C. S., Stanley, T. A., & Kirschbaum, D. B. (2019). Using citizen science to expand the global map of landslides: Introducing the Cooperative Open Online Landslide Repository (COOLR). *PLoS One*, *14*(7), e0218657. https://doi.org/10.1371/journal.pone.0218657
Justice, C., Townshend, J., Vermote, E., Masuoka, E., Wolfe, R., Saleous, N., et al. (2002). An overview of MODIS Land data processing and product status. *Remote Sensing of Environment*, *83*(1–2), 3–15. https://doi.org/10.1016/s0034-4257(02)00084-6
Kang, H.-S., & Kim, Y.-T. (2016). The physical vulnerability of different types of building structure to debris flow events. *Natural Hazards*, *80*(3), 1475–1493. https://doi.org/10.1007/s11069-015-2032-z
Karantanellis, E., Marinos, V., Vassilakis, E., & Christaras, B. (2020). Object-based analysis using unmanned aerial vehicles (UAVs) for site-specific landslide assessment. *Remote Sensing*, *12*(11), 1711. https://doi.org/10.3390/rs12111711
Kirschbaum, D. B., Adler, R., Hong, Y., Hill, S., & Lerner-Lam, A. (2010). A global landslide catalog for hazard applications: Method, results, and limitations. *Natural Hazards*, *52*(3), 561–575. https://doi.org/10.1007/s11069-009-9401-4
Ko, F. W., & Lo, F. L. (2018). From landslide susceptibility to landslide frequency: A territory-wide study in Hong Kong. *Engineering Geology*, *242*, 12–22. https://doi.org/10.1016/j.enggeo.2018.05.001
Kubwimana, D., Ait Brahim, L., Nkurunziza, P., Dille, A., Depicker, A., Nahimana, L., et al. (2021). Characteristics and distribution of landslides in the populated hillslopes of Bujumbura, Burundi. *Geosciences*, *11*(6), 259. https://doi.org/10.3390/geosciences11060259
Lacroix, P., Dehecq, A., & Taipe, E. (2020). Irrigation-triggered landslides in a Peruvian desert caused by modern intensive farming. *Nature Geoscience*, *13*(1), 56–60. https://doi.org/10.1038/s41561-019-0500-x
Lacroix, P., Handwerger, A. L., & Bièvre, G. (2020). Life and death of slow-moving landslides. *Nature Reviews Earth & Environment*, *1*(8), 404–419. https://doi.org/10.1038/s43017-020-0072-8
Lan, H., Tian, N., Li, L., Wu, Y., Macciotta, R., & Clague, J. J. (2022). Kinematic-based landslide risk management for the Sichuan-Tibet Grid Interconnection Project (STGIP) in China. *Engineering Geology*, *308*, 106823. https://doi.org/10.1016/j.enggeo.2022.106823
Lari, S., Frattini, P., & Crosta, G. (2014). A probabilistic approach for landslide hazard analysis. *Engineering Geology*, *182*, 3–14. https://doi.org/10.1016/j.enggeo.2014.07.015
Lee, E. M., & Jones, D. K. C. (2004). *Landslide risk assessment*. Thomas Telford Publishing. https://doi.org/10.1680/lra.31715
Lei, Y., Huang, J., Cui, Y., Jiang, S.-H., Wu, S., & Ching, J. (2023). Time capsule for landslide risk assessment. *Georisk: Assessment and Management of Risk for Engineered Systems and Geohazards*, *17*(4), 1–22. https://doi.org/10.1080/17499518.2023.2164899
Leoni, G., Barchiesi, F., Catallo, F., Dramis, F., Fubelli, G., Lucifora, S., et al. (2009). GIS methodology to assess landslide susceptibility: Application to a river catchment of Central Italy. *Journal of Maps*, *5*(1), 87–93. https://doi.org/10.4113/jom.2009.1041
Leroi, E. (1996). Landslide hazard-risk maps at different scales: Objectives, tools and developments. In *Landslides* (pp. 35–51).
Li, X., Cheng, J.-L., & Yu, D.-H. (2023). A methodological framework of landslide quantitative risk assessment in areas with incomplete historical landslide information. *Journal of Mountain Science*, *20*(9), 2665–2679. https://doi.org/10.1007/s11629-023-7950-8
Li, Y., Chen, L., Yin, K., Zhang, Y., & Gui, L. (2021). Quantitative risk analysis of the hazard chain triggered by a landslide and the generated tsunami in the Three Gorges Reservoir area. *Landslides*, *18*(2), 667–680. https://doi.org/10.1007/s10346-020-01516-1
Li, Z., Nadim, F., Huang, H., Uzielli, M., & Lacasse, S. (2010). Quantitative vulnerability estimation for scenario-based landslide hazards. *Landslides*, *7*(2), 125–134. https://doi.org/10.1007/s10346-009-0190-3
Liao, X., Xu, W., Zhang, J., Li, Y., & Tian, Y. (2019). Global exposure to rainstorms and the contribution rates of climate change and population change. *Science of the Total Environment*, *663*, 644–653. https://doi.org/10.1016/j.scitotenv.2019.01.290
Lima, P., Steger, S., & Glade, T. (2021). Counteracting flawed landslide data in statistically based landslide susceptibility modelling for very large areas: A national-scale assessment for Austria. *Landslides*, *18*(11), 3531–3546. https://doi.org/10.1007/s10346-021-01693-7
Lin, Q., Lima, P., Steger, S., Glade, T., Jiang, T., Zhang, J., et al. (2021). National-scale data-driven rainfall induced landslide susceptibility mapping for China by accounting for incomplete landslide data. *Geoscience Frontiers*, *12*(6), 101248. https://doi.org/10.1016/j.gsf.2021.101248
Liu, C., Huang, X., Zhu, Z., Chen, H., Tang, X., & Gong, J. (2019). Automatic extraction of built-up area from ZY3 multi-view satellite imagery: Analysis of 45 global cities. *Remote Sensing of Environment*, *226*, 51–73. https://doi.org/10.1016/j.rse.2019.03.033
Liu, X., & Miao, C. (2018). Large-scale assessment of landslide hazard, vulnerability and risk in China. *Geomatics, Natural Hazards and Risk*, *9*(1), 1037–1052. https://doi.org/10.1080/19475705.2018.1502690
Liu, Z., & Rue, H. (2022). Leave-group-out cross-validation for latent Gaussian models. *arXiv preprint arXiv:2210.04482*.
Loche, M., Alvioli, M., Marchesini, I., Bakka, H., & Lombardo, L. (2022). Landslide susceptibility maps of Italy: Lesson learnt from dealing with multiple landslide types and the uneven spatial distribution of the national inventory. *Earth-Science Reviews*, *232*, 104125. https://doi.org/10.1016/j.earscirev.2022.104125
Lombardo, L., & Mai, P. M. (2018). Presenting logistic regression-based landslide susceptibility results. *Engineering Geology*, *244*, 14–24. https://doi.org/10.1016/j.enggeo.2018.07.019
Lombardo, L., Opitz, T., Ardizzone, F., Guzzetti, F., & Huser, R. (2020). Space-time landslide predictive modelling. *Earth-Science Reviews*, *209*, 103318. https://doi.org/10.1016/j.earscirev.2020.103318
Lombardo, L., & Tanyas, H. (2020). Chrono-validation of near-real-time landslide susceptibility models via plug-in statistical simulations. *Engineering Geology*, *278*, 105818. https://doi.org/10.1016/j.enggeo.2020.105818
Lombardo, L., Tanyas, H., Huser, R., Guzzetti, F., & Castro-Camilo, D. (2021). Landslide size matters: A new data-driven, spatial prototype. *Engineering Geology*, *293*, 106288. https://doi.org/10.1016/j.enggeo.2021.106288
Lu, P., Catani, F., Tofani, V., & Casagli, N. (2014). Quantitative hazard and risk assessment for slow-moving landslides from Persistent Scatterer Interferometry. *Landslides*, *11*(4), 685–696. https://doi.org/10.1007/s10346-013-0432-2
Luo, H., Zhang, L., Zhang, L., He, J., & Yin, K. (2023). Vulnerability of buildings to landslides: The state of the art and future needs. *Earth-Science Reviews*, *238*, 104329. https://doi.org/10.1016/j.earscirev.2023.104329
Maes, J., Kervyn, M., de Hontheim, A., Dewitte, O., Jacobs, L., Mertens, K., et al. (2017). Landslide risk reduction measures: A review of practices and challenges for the tropics. *Progress in Physical Geography*, *41*(2), 191–221. https://doi.org/10.1177/0309133316689344

Mahaney, W. C., & Andres, W. (1991). Glacially crushed quartz grains in loess as indicators of long-distance transport from major European ice centers during the Pleistocene. *Boreas*, *20*(3), 231–239. https://doi.org/10.1111/j.1502-3885.1991.tb00153.x

Marjanović, M., Kovačević, M., Bajat, B., & Voženílek, V. (2011). Landslide susceptibility assessment using SVM machine learning algorithm. *Engineering Geology*, *123*(3), 225–234. https://doi.org/10.1016/j.enggeo.2011.09.006

Marra, G., & Wood, S. N. (2011). Practical variable selection for generalized additive models. *Computational Statistics & Data Analysis*, *55*(7), 2372–2387. https://doi.org/10.1016/j.csda.2011.02.004

Martha, T. R., van Westen, C. J., Kerle, N., Jetten, V., & Kumar, K. V. (2013). Landslide hazard and risk assessment using semi-automatically created landslide inventories. *Geomorphology*, *184*, 139–150. https://doi.org/10.1016/j.geomorph.2012.12.001

Martino, S., Battaglia, S., D'alessandro, F., Della Seta, M., Esposito, C., Martini, G., et al. (2020). Earthquake-induced landslide scenarios for seismic microzonation: Application to the Accumoli area (Rieti, Italy). *Bulletin of Earthquake Engineering*, *18*(12), 5655–5673. https://doi.org/10.1007/s10518-019-00589-1

Masek, J. G., Vermote, E. F., Saleous, N. E., Wolfe, R., Hall, F. G., Huemmrich, K. F., et al. (2006). A Landsat surface reflectance dataset for North America, 1990-2000. *IEEE Geoscience and Remote Sensing Letters*, *3*(1), 68–72. https://doi.org/10.1109/lgrs.2005.857030

Masson-Delmotte, V., Zhai, P., Pirani, S., Connors, C., Péan, S., Berger, N., & Scheel Monteiro, P. M. (2021). IPCC, 2021: Summary for Policymakers. In *Climate Change 2021: The Physical Science Basis. Contribution of Working Group I to the Sixth Assessment Report of the Intergovernmental Panel on Climate Change*. Cambridge University Press. Retrieved from http://hdl.handle.net/10204/12710

Mavrouli, O., Fotopoulou, S., Pitilakis, K., Zuccaro, G., Corominas, J., Santo, A., et al. (2014). Vulnerability assessment for reinforced concrete buildings exposed to landslides. *Bulletin of Engineering Geology and the Environment*, *73*, 265–289. https://doi.org/10.1007/s10064-014-0573-0

Medina, V., Hürlimann, M., Guo, Z., Lloret, A., & Vaunat, J. (2021). Fast physically-based model for rainfall-induced landslide susceptibility assessment at regional scale. *Catena*, *201*, 105213. https://doi.org/10.1016/j.catena.2021.105213

Meeus, J. (1995). Pan-European landscapes. *Landscape and Urban Planning*, *31*(1–3), 57–79. https://doi.org/10.1016/0169-2046(94)01036-8

Meinhardt, M., Fink, M., & Tünschel, H. (2015). Landslide susceptibility analysis in central Vietnam based on an incomplete landslide inventory: Comparison of a new method to calculate weighting factors by means of bivariate statistics. *Geomorphology*, *234*, 80–97. https://doi.org/10.1016/j.geomorph.2014.12.042

Mirus, B. B., Belair, G. M., Wood, N. J., Jones, J., & Martinez, S. N. (2024). Parsimonious high-resolution landslide susceptibility modeling at continental scales. *AGU Advances*, *5*(5), e2024AV001214. https://doi.org/10.1029/2024av001214

Mirus, B. B., Jones, E. S., Baum, R. L., Godt, J. W., Slaughter, S., Crawford, M. M., et al. (2020). Landslides across the USA: Occurrence, susceptibility, and data limitations. *Landslides*, *17*(10), 2271–2285. https://doi.org/10.1007/s10346-020-01424-4

Miščević, P., & Vlastelica, G. (2014). Impact of weathering on slope stability in soft rock mass. *Journal of Rock Mechanics and Geotechnical Engineering*, *6*(3), 240–250. https://doi.org/10.1016/j.jrmge.2014.03.006

Molnar, C. (2020). *Interpretable machine learning*. Lulu. com.

Mondini, A. C., Guzzetti, F., & Melillo, M. (2023). Deep learning forecast of rainfall-induced shallow landslides. *Nature Communications*, *14*(1), 2466. https://doi.org/10.1038/s41467-023-38135-y

Monsieurs, E., Jacobs, L., Michellier, C., Basimike Tchangaboba, J., Ganza, G. B., Kervyn, F., et al. (2018). Landslide inventory for hazard assessment in a data-poor context: A regional-scale approach in a tropical African environment. *Landslides*, *15*(11), 2195–2209. https://doi.org/10.1007/s10346-018-1008-y

Moore, I. D., Grayson, R., & Ladson, A. (1991). Digital terrain modelling: A review of hydrological, geomorphological, and biological applications. *Hydrological Processes*, *5*(1), 3–30. https://doi.org/10.1002/hyp.3360050103

Moreno, M., Lombardo, L., Crespi, A., Zellner, P. J., Mair, V., Pittore, M., et al. (2023). Space-time data-driven modeling of precipitation-induced shallow landslides in South Tyrol, Italy. *Science of the Total Environment*, *912*, 169166. https://doi.org/10.1016/j.scitotenv.2023.169166

Moreno, M., Steger, S., Tanyas, H., & Lombardo, L. (2023). Modeling the area of co-seismic landslides via data-driven models: The Kaikōura example. *Engineering Geology*, *320*, 107121. https://doi.org/10.1016/j.enggeo.2023.107121

Morgenstern, N. R. (2018). Toward landslide risk assessment in practice. In *Landslide risk assessment* (pp. 15–23). Routledge.

Moss, J. L. (2000). Using the Global Positioning System to monitor dynamic ground deformation networks on potentially active landslides. *International Journal of Applied Earth Observation and Geoinformation*, *2*(1), 24–32. https://doi.org/10.1016/s0303-2434(00)85023-0

Nadim, F., Kjekstad, O., Peduzzi, P., Herold, C., & Jaedicke, C. (2006). Global landslide and avalanche hotspots. *Landslides*, *3*(2), 159–173. https://doi.org/10.1007/s10346-006-0036-1

Ngadisih, Samodra, G., Bhandary, N. P., & Yatabe, R. (2017). Landslide inventory: Challenge for landslide hazard assessment in Indonesia, *GIS Landslide* (pp. 135–159).

Ngadisih, Yatabe, R., Bhandary, N. P., & Dahal, R. K. (2014). Integration of statistical and heuristic approaches for landslide risk analysis: A case of volcanic mountains in West Java Province, Indonesia. *Georisk: Assessment and Management of Risk for Engineered Systems and Geohazards*, *8*(1), 29–47. https://doi.org/10.1080/17499518.2013.826030

Nguyen, B.-Q.-V., & Kim, Y.-T. (2021). Regional-scale landslide risk assessment on Mt. Umyeon using risk index estimation. *Landslides*, *18*(7), 2547–2564. https://doi.org/10.1007/s10346-021-01622-8

Nielsen, S. B., Gallagher, K., Leighton, C., Balling, N., Svenningsen, L., Jacobsen, B. H., et al. (2009). The evolution of western Scandinavian topography: A review of Neogene uplift versus the ICE (isostasy–climate–erosion) hypothesis. *Journal of Geodynamics*, *47*(2–3), 72–95. https://doi.org/10.1016/j.jog.2008.09.001

Niyokwiringirwa, P., Lombardo, L., Dewitte, O., Deijns, A. A., Wang, N., Van Westen, C. J., & Tanyas, H. (2024). Event-based rainfall-induced landslide inventories and rainfall thresholds for Malawi. *Landslides*, *21*(6), 1–22. https://doi.org/10.1007/s10346-023-02203-7

Nocentini, N., Rosi, A., Segoni, S., & Fanti, R. (2023). Towards landslide space-time forecasting through machine learning: The influence of rainfall parameters and model setting. *Frontiers in Earth Science*, *11*, 1152130. https://doi.org/10.3389/feart.2023.1152130

Nor Diana, M. I., Muhamad, N., Taha, M. R., Osman, A., & Alam, M. M. (2021). Social vulnerability assessment for landslide hazards in Malaysia: A systematic review study. *Land*, *10*(3), 315. https://doi.org/10.3390/land10030315

North, M. A. (2009). A method for implementing a statistically significant number of data classes in the Jenks algorithm. In *2009 6th international Conference on fuzzy Systems and Knowledge Discovery* (Vol. 1, pp. 35–38).

Novellino, A., Cesarano, M., Cappelletti, P., Di Martire, D., Di Napoli, M., Ramondini, M., et al. (2021). Slow-moving landslide risk assessment combining Machine Learning and InSAR techniques. *Catena*, *203*, 105317. https://doi.org/10.1016/j.catena.2021.105317

Ohlmacher, G. C., & Davis, J. C. (2003). Using multiple logistic regression and GIS technology to predict landslide hazard in northeast Kansas, USA. *Engineering Geology*, *69*(3–4), 331–343. https://doi.org/10.1016/s0013-7952(03)00069-3

Ozturk, U., Bozzolan, E., Holcombe, E. A., Shukla, R., Pianosi, F., & Wagener, T. (2022). How climate change and unplanned urban sprawl bring more landslides. *Nature*, *608*(7922), 262–265. https://doi.org/10.1038/d41586-022-02141-9

Papathoma-Köhle, M., Kappes, M., Keiler, M., & Glade, T. (2011). Physical vulnerability assessment for alpine hazards: State of the art and future needs. *Natural Hazards*, *58*(2), 645–680. https://doi.org/10.1007/s11069-010-9632-4

Pardeshi, S. D., Autade, S. E., & Pardeshi, S. S. (2013). Landslide hazard assessment: Recent trends and techniques. *SpringerPlus*, *2*, 1–11. https://doi.org/10.1186/2193-1801-2-523

Parker, R. N., Hales, T. C., Mudd, S. M., Grieve, S. W., & Constantine, J. A. (2016). Colluvium supply in humid regions limits the frequency of storm-triggered landslides. *Scientific Reports*, *6*(1), 34438. https://doi.org/10.1038/srep34438

Peduto, D., Ferlisi, S., Nicodemo, G., Reale, D., Pisciotta, G., & Gullà, G. (2017). Empirical fragility and vulnerability curves for buildings exposed to slow-moving landslides at medium and large scales. *Landslides*, *14*(6), 1993–2007. https://doi.org/10.1007/s10346-017-0826-7

Pellicani, R., Van Westen, C. J., & Spilotro, G. (2014). Assessing landslide exposure in areas with limited landslide information. *Landslides*, *11*(3), 463–480. https://doi.org/10.1007/s10346-013-0386-4

Peng, L., Xu, S., Hou, J., & Peng, J. (2015). Quantitative risk analysis for landslides: The case of the Three Gorges area, China. *Landslides*, *12*(5), 943–960. https://doi.org/10.1007/s10346-014-0518-5

Pereira, S., Garcia, R. A., Zêzere, J. L., Oliveira, S. C., & Silva, M. (2017). Landslide quantitative risk analysis of buildings at the municipal scale based on a rainfall triggering scenario. *Geomatics, Natural Hazards and Risk*, *8*(2), 624–648. https://doi.org/10.1080/19475705.2016.1250116

Pereira, S., Santos, P., Zêzere, J., Tavares, A., Garcia, R., & Oliveira, S. (2020). A landslide risk index for municipal land use planning in Portugal. *Science of the Total Environment*, *735*, 139463. https://doi.org/10.1016/j.scitotenv.2020.139463

Peres, D., & Cancelliere, A. (2018). Modeling impacts of climate change on return period of landslide triggering. *Journal of Hydrology*, *567*, 420–434. https://doi.org/10.1016/j.jhydrol.2018.10.036

Peruccacci, S., Gariano, S. L., Melillo, M., Solimano, M., Guzzetti, F., & Brunetti, M. T. (2023). The ITAlian rainfall-induced LandslIdes CAtalogue, an extensive and accurate spatio-temporal catalogue of rainfall-induced landslides in Italy. *Earth System Science Data*, *15*(7), 2863–2877. https://doi.org/10.5194/essd-15-2863-2023

Pesaresi, M., & Politis, P. (2022). *GHS-BUILT-S R2022A-GHS built-up surface grid, derived from Sentinel-2 composite and Landsat, multi-temporal (1975–2030)*. European Commission, Joint Research Centre (JRC).

Petley, D. (2012). Global patterns of loss of life from landslides. *Geology*, *40*(10), 927–930. https://doi.org/10.1130/g33217.1

Pettorelli, N., Vik, J. O., Mysterud, A., Gaillard, J.-M., Tucker, C. J., & Stenseth, N. C. (2005). Using the satellite-derived NDVI to assess ecological responses to environmental change. *Trends in Ecology & Evolution*, *20*(9), 503–510. https://doi.org/10.1016/j.tree.2005.05.011

Pittore, M., Wieland, M., & Fleming, K. (2017). Perspectives on global dynamic exposure modelling for geo-risk assessment. *Natural Hazards*, *86*(S1), 7–30. https://doi.org/10.1007/s11069-016-2437-3

Pohjankukka, J., Pahikkala, T., Nevalainen, P., & Heikkonen, J. (2017). Estimating the prediction performance of spatial models via spatial k-fold cross validation. *International Journal of Geographical Information Science*, *31*(10), 2001–2019. https://doi.org/10.1080/13658816.2017.1346255

Promper, C., Gassner, C., & Glade, T. (2015). Spatiotemporal patterns of landslide exposure–a step within future landslide risk analysis on a regional scale applied in Waidhofen/Ybbs Austria. *International Journal of Disaster Risk Reduction*, *12*, 25–33. https://doi.org/10.1016/j.ijdrr.2014.11.003

Pudasaini, S. P., & Krautblatter, M. (2022). The landslide velocity. *Earth Surface Dynamics*, *10*(2), 165–189. https://doi.org/10.5194/esurf-10-165-2022

Raspini, F., Bianchini, S., Ciampalini, A., Del Soldato, M., Solari, L., Novali, F., et al. (2018). Continuous, semi-automatic monitoring of ground deformation using Sentinel-1 satellites. *Scientific Reports*, *8*(1), 7253. https://doi.org/10.1038/s41598-018-25369-w

Rautela, P., & Lakhera, R. C. (2000). Landslide risk analysis between Giri and Tons rivers in Himachal Himalaya (India). *International Journal of Applied Earth Observation and Geoinformation*, *2*(3–4), 153–160. https://doi.org/10.1016/s0303-2434(00)85009-6

Reeves, A., Ho, K., & Lo, D. (1999). Interim risk criteria for landslides and boulder falls from natural terrain. In *Proceedings of the Seminar on Geotechnical Risk Management, Geotechnical Division, Hong Kong Institution of Engineers* (pp. 127–136).

Regmi, N. R., Giardino, J. R., & Vitek, J. D. (2014). Characteristics of landslides in western Colorado, USA. *Landslides*, *11*(4), 589–603. https://doi.org/10.1007/s10346-013-0412-6

Reichenbach, P., Rossi, M., Malamud, B. D., Mihir, M., & Guzzetti, F. (2018). A review of statistically-based landslide susceptibility models. *Earth-Science Reviews*, *180*, 60–91. https://doi.org/10.1016/j.earscirev.2018.03.001

Remondo, J., Bonachea, J., & Cendrero, A. (2005). A statistical approach to landslide risk modelling at basin scale: From landslide susceptibility to quantitative risk assessment. *Landslides*, *2*(4), 321–328. https://doi.org/10.1007/s10346-005-0016-x

Remondo, J., Bonachea, J., & Cendrero, A. (2008). Quantitative landslide risk assessment and mapping on the basis of recent occurrences. *Geomorphology*, *94*(3–4), 496–507. https://doi.org/10.1016/j.geomorph.2006.10.041

Rosser, B., Dellow, S., Haubrock, S., & Glassey, P. (2017). New Zealand's national landslide database. *Landslides*, *14*(6), 1949–1959. https://doi.org/10.1007/s10346-017-0843-6

Rossi, G., Catani, F., Leoni, L., Segoni, S., & Tofani, V. (2013). HIRESSS: A physically based slope stability simulator for HPC applications. *Natural Hazards and Earth System Sciences*, *13*(1), 151–166. https://doi.org/10.5194/nhess-13-151-2013

Rossi, M., Guzzetti, F., Salvati, P., Donnini, M., Napolitano, E., & Bianchi, C. (2019). A predictive model of societal landslide risk in Italy. *Earth-Science Reviews*, *196*, 102849. https://doi.org/10.1016/j.earscirev.2019.04.021

Saleem, N., Huq, M. E., Twumasi, N. Y. D., Javed, A., & Sajjad, A. (2019). Parameters derived from and/or used with digital elevation models (DEMs) for landslide susceptibility mapping and landslide risk assessment: A review. *ISPRS International Journal of Geo-Information*, *8*(12), 545. https://doi.org/10.3390/ijgi8120545

Salvati, P., Balducci, V., Bianchi, C., Guzzetti, F., & Tonelli, G. (2009). A WebGIS for the dissemination of information on historical landslides and floods in Umbria, Italy. *GeoInformatica*, *13*(3), 305–322. https://doi.org/10.1007/s10707-008-0072-1

Salvatici, T., Tofani, V., Rossi, G., D'Ambrosio, M., Tacconi Stefanelli, C., Masi, E. B., et al. (2018). Application of a physically based model to forecast shallow landslides at a regional scale. *Natural Hazards and Earth System Sciences*, *18*(7), 1919–1935. https://doi.org/10.5194/nhess-18-1919-2018

Samia, J., Temme, A., Bregt, A., Wallinga, J., Guzzetti, F., Ardizzone, F., & Rossi, M. (2017). Do landslides follow landslides? Insights in path dependency from a multi-temporal landslide inventory. *Landslides*, *14*(2), 547–558. https://doi.org/10.1007/s10346-016-0739-x

Samodra, G., Chen, G., Sartohadi, J., & Kasama, K. (2018). Generating landslide inventory by participatory mapping: An example in Purwosari Area, Yogyakarta, Java. *Geomorphology*, *306*, 306–313. https://doi.org/10.1016/j.geomorph.2015.07.035

Scaini, C., Tamaro, A., Adilkhan, B., Sarzhanov, S., Ismailov, V., Umaraliev, R., et al. (2023). A new regionally consistent exposure database for Central Asia: Population and residential buildings. *Natural Hazards and Earth System Sciences Discussions*, *2023*, 1–17.

Schiavina, M., Melchiorri, M., Pesaresi, M., Politis, P., Freire, S., Maffenini, L., et al. (2022). *GHSL data package 2022*. Publications Office of the European Union.

Schilirò, L., Montrasio, L., & Mugnozza, G. S. (2016). Prediction of shallow landslide occurrence: Validation of a physically-based approach through a real case study. *Science of the Total Environment*, *569*, 134–144.
Schlögel, R., Marchesini, I., Alvioli, M., Reichenbach, P., Rossi, M., & Malet, J.-P. (2018). Optimizing landslide susceptibility zonation: Effects of DEM spatial resolution and slope unit delineation on logistic regression models. *Geomorphology*, *301*, 10–20. https://doi.org/10.1016/j.geomorph.2017.10.018
Segoni, S., & Caleca, F. (2021). Definition of environmental indicators for a fast estimation of landslide risk at national scale. *Land*, *10*(6), 621. https://doi.org/10.3390/land10060621
Segoni, S., Piciullo, L., & Gariano, S. L. (2018). A review of the recent literature on rainfall thresholds for landslide occurrence. *Landslides*, *15*(8), 1483–1501. https://doi.org/10.1007/s10346-018-0966-4
Seyed-Kolbadi, S., Sadoghi-Yazdi, J., & Hariri-Ardebili, M. (2019). An improved strength reduction-based slope stability analysis. *Geosciences*, *9*(1), 55. https://doi.org/10.3390/geosciences9010055
Shano, L., Raghuvanshi, T. K., & Meten, M. (2022). Fuzzy set theory and pixel-based landslide risk assessment: The case of Shafe and Baso catchments, Gamo highland, Ethiopia. *Earth Science Informatics*, *15*(2), 993–1006. https://doi.org/10.1007/s12145-022-00774-y
Sim, K. B., Lee, M. L., & Wong, S. Y. (2022). A review of landslide acceptable risk and tolerable risk. *Geoenvironmental Disasters*, *9*(1), 3. https://doi.org/10.1186/s40677-022-00205-6
Singh, A., Kanungo, D., & Pal, S. (2019). Physical vulnerability assessment of buildings exposed to landslides in India. *Natural Hazards*, *96*(2), 753–790. https://doi.org/10.1007/s11069-018-03568-y
Singh, A., Pal, S., Kanungo, D. P., & Pareek, N. (2017). An overview of recent developments in landslide vulnerability assessment-presentation of a new conceptual framework. *Advancing Culture of Living with Landslides: Volume 2 Advances in Landslide Science* (pp. 795–802).
Solari, L., Bianchini, S., Franceschini, R., Barra, A., Monserrat, O., Thuegaz, P., et al. (2020). Satellite interferometric data for landslide intensity evaluation in mountainous regions. *International Journal of Applied Earth Observation and Geoinformation*, *87*, 102028. https://doi.org/10.1016/j.jag.2019.102028
Stanley, T., & Kirschbaum, D. B. (2017a). Effects of inventory bias on landslide susceptibility calculations. In *Proceedings of the 3rd North American Symposium on Landslides*.
Stanley, T., & Kirschbaum, D. B. (2017b). A heuristic approach to global landslide susceptibility mapping. *Natural Hazards*, *87*(1), 145–164. https://doi.org/10.1007/s11069-017-2757-y
Steger, S., Brenning, A., Bell, R., & Glade, T. (2016). The propagation of inventory-based positional errors into statistical landslide susceptibility models. *Natural Hazards and Earth System Sciences*, *16*(12), 2729–2745. https://doi.org/10.5194/nhess-16-2729-2016
Steger, S., Brenning, A., Bell, R., & Glade, T. (2017). The influence of systematically incomplete shallow landslide inventories on statistical susceptibility models and suggestions for improvements. *Landslides*, *14*(5), 1767–1781. https://doi.org/10.1007/s10346-017-0820-0
Steger, S., Brenning, A., Bell, R., Petschko, H., & Glade, T. (2016). Exploring discrepancies between quantitative validation results and the geomorphic plausibility of statistical landslide susceptibility maps. *Geomorphology*, *262*, 8–23. https://doi.org/10.1016/j.geomorph.2016.03.015
Steger, S., Mair, V., Kofler, C., Pittore, M., Zebisch, M., & Schneiderbauer, S. (2021). Correlation does not imply geomorphic causation in data-driven landslide susceptibility modelling–Benefits of exploring landslide data collection effects. *Science of the Total Environment*, *776*, 145935. https://doi.org/10.1016/j.scitotenv.2021.145935
Steger, S., Moreno, M., Crespi, A., Gariano, S. L., Brunetti, M. T., Melillo, M., et al. (2024). Adopting the margin of stability for space–time landslide prediction–a data-driven approach for generating spatial dynamic thresholds. *Geoscience Frontiers*, *15*(5), 101822. https://doi.org/10.1016/j.gsf.2024.101822
Steger, S., Moreno, M., Crespi, A., Zellner, P. J., Gariano, S. L., Brunetti, M. T., et al. (2023). Deciphering seasonal effects of triggering and preparatory precipitation for improved shallow landslide prediction using generalized additive mixed models. *Natural Hazards and Earth System Sciences*, *23*(4), 1483–1506. https://doi.org/10.5194/nhess-23-1483-2023
Stoffel, M., Tiranti, D., & Huggel, C. (2014). Climate change impacts on mass movements—Case studies from the European Alps. *Science of the Total Environment*, *493*, 1255–1266. https://doi.org/10.1016/j.scitotenv.2014.02.102
Tanyaş, H., van Westen, C. J., Allstadt, K. E., Anna Nowicki Jessee, M., Görüm, T., Jibson, R. W., et al. (2017). Presentation and analysis of a worldwide database of earthquake-induced landslide inventories. *Journal of Geophysical Research: Earth Surface*, *122*(10), 1991–2015. https://doi.org/10.1002/2017jf004236
Tapsell, S., McCarthy, S., Faulkner, H., Alexander, M., Steinführer, A., Kuhlicke, C., et al. (2010). *Social vulnerability to natural hazards (Report for the EC FP7 Caphaz-Net Project)*. European Commission.
Titti, G., Borgatti, L., Zou, Q., Cui, P., & Pasuto, A. (2021). Landslide susceptibility in the Belt and Road Countries: Continental step of a multi-scale approach. *Environmental Earth Sciences*, *80*, 1–18. https://doi.org/10.1007/s12665-021-09910-1
Tofani, V., Bicocchi, G., Rossi, G., Segoni, S., D'Ambrosio, M., Casagli, N., & Catani, F. (2017). Soil characterization for shallow landslides modeling: A case study in the Northern Apennines (Central Italy). *Landslides*, *14*(2), 755–770. https://doi.org/10.1007/s10346-017-0809-8
Tofani, V., Del Ventisette, C., Moretti, S., & Casagli, N. (2014). Integration of remote sensing techniques for intensity zonation within a landslide area: A case study in the northern Apennines, Italy. *Remote Sensing*, *6*(2), 907–924. https://doi.org/10.3390/rs6020907
Trigila, A., Frattini, P., Casagli, N., Catani, F., Crosta, G., Esposito, C., et al. (2013). Landslide susceptibility mapping at national scale: The Italian case study, *Landslide Science and Practice: Volume 1: Landslide Inventory and Susceptibility and Hazard Zoning* (pp. 287–295).
Trigila, A., Iadanza, C., Guerrieri, L., & Hervás, J. (2007). The IFFI project (Italian landslide inventory): Methodology and results, *Guidelines for mapping areas at risk of landslides in Europe* (Vol. *23*, p. 15).
Tsunetaka, H. (2021). Comparison of the return period for landslide-triggering rainfall events in Japan based on standardization of the rainfall period. *Earth Surface Processes and Landforms*, *46*(14), 2984–2998. https://doi.org/10.1002/esp.5228
Uzielli, M., Catani, F., Tofani, V., & Casagli, N. (2015). Risk analysis for the Ancona landslide—II: Estimation of risk to buildings. *Landslides*, *12*(1), 83–100. https://doi.org/10.1007/s10346-014-0477-x
Van den Bout, B., Lombardo, L., Chiyang, M., van Westen, C., & Jetten, V. (2021). Physically-based catchment-scale prediction of slope failure volume and geometry. *Engineering Geology*, *284*, 105942. https://doi.org/10.1016/j.enggeo.2020.105942
Van Den Eeckhaut, M., & Hervás, J. (2012). State of the art of national landslide databases in Europe and their potential for assessing landslide susceptibility, hazard and risk. *Geomorphology*, *139*, 545–558. https://doi.org/10.1016/j.geomorph.2011.12.006
Van Der Linde, A. (2005). DIC in variable selection. *Statistica Neerlandica*, *59*(1), 45–56. https://doi.org/10.1111/j.1467-9574.2005.00278.x
Van Westen, C. (2004). Geo-information tools for landslide risk assessment: An overview of recent developments, *Landslides: Evaluation and stabilization* (Vol. *1*, pp. 39–56). https://doi.org/10.1201/b16816-6
Van Westen, C., Seijmonsbergen, A., & Mantovani, F. (1999). Comparing landslide hazard maps. *Natural Hazards*, *20*(2/3), 137–158. https://doi.org/10.1023/a:1008036810401

Van Westen, C., Van Asch, T. W., & Soeters, R. (2006). Landslide hazard and risk zonation—Why is it still so difficult? *Bulletin of Engineering Geology and the Environment*, *65*(2), 167–184. https://doi.org/10.1007/s10064-005-0023-0

Van Westen, C. J., Castellanos, E., & Kuriakose, S. L. (2008). Spatial data for landslide susceptibility, hazard, and vulnerability assessment: An overview. *Engineering Geology*, *102*(3–4), 112–131. https://doi.org/10.1016/j.enggeo.2008.03.010

Varnes, D. J. (1984). *Landslide hazard zonation: A review of principles and practice* (Vol. 3). UNESCO.

Vranken, L., Vantilt, G., Van Den Eeckhaut, M., Vandekerckhove, L., & Poesen, J. (2015). Landslide risk assessment in a densely populated hilly area. *Landslides*, *12*(4), 787–798. https://doi.org/10.1007/s10346-014-0506-9

Wang, D., Hao, M., Chen, S., Meng, Z., Jiang, D., & Ding, F. (2021). Assessment of landslide susceptibility and risk factors in China. *Natural Hazards*, *108*(3), 3045–3059. https://doi.org/10.1007/s11069-021-04812-8

Wang, K., Zhang, S., DelgadoTéllez, R., & Wei, F. (2019). A new slope unit extraction method for regional landslide analysis based on morphological image analysis. *Bulletin of Engineering Geology and the Environment*, *78*(6), 4139–4151. https://doi.org/10.1007/s10064-018-1389-0

Wang, N., Cheng, W., Marconcini, M., Bachofer, F., Liu, C., Xiong, J., & Lombardo, L. (2022). Space-time susceptibility modeling of hydro-morphological processes at the Chinese national scale. *Engineering Geology*, *301*, 106586. https://doi.org/10.1016/j.enggeo.2022.106586

Wang, X., Frattini, P., Crosta, G., Zhang, L., Agliardi, F., Lari, S., & Yang, Z. (2014). Uncertainty assessment in quantitative rockfall risk assessment. *Landslides*, *11*(4), 711–722. https://doi.org/10.1007/s10346-013-0447-8

Wijaya, A. P., & Hong, J.-H. (2018). Quantitative assessment of social vulnerability for landslide disaster risk reduction using gis approach (case study: Cilacap regency, province of central Java, Indonesia). *The International Archives of the Photogrammetry, Remote Sensing and Spatial Information Sciences*, *42*, 703–709. https://doi.org/10.5194/isprs-archives-xlii-4-703-2018

Wilde, M., Günther, A., Reichenbach, P., Malet, J.-P., & Hervás, J. (2018). Pan-European landslide susceptibility mapping: ELSUS Version 2. *Journal of Maps*, *14*(2), 97–104. https://doi.org/10.1080/17445647.2018.1432511

Wong, H. (2005). Landslide risk assessment for individual facilities. In *Landslide risk management* (pp. 247–306). CRC Press.

Wood, S. N. (2013). A simple test for random effects in regression models. *Biometrika*, *100*(4), 1005–1010. https://doi.org/10.1093/biomet/ast038

Wood, S. N. (2017). *Generalized additive models: An introduction with R*. CRC Press.

Xiao, L., Wang, J., Zhu, Y., & Zhang, J. (2020). Quantitative risk analysis of a rainfall-induced complex landslide in Wanzhou County, Three Gorges Reservoir, China. *International Journal of Disaster Risk Science*, *11*(3), 347–363. https://doi.org/10.1007/s13753-020-00257-y

Xiao, Y., Tang, X., Li, Y., Huang, H., & An, B.-W. (2022). Social vulnerability assessment of landslide disaster based on improved TOPSIS method: Case study of eleven small towns in China. *Ecological Indicators*, *143*, 109316. https://doi.org/10.1016/j.ecolind.2022.109316

Yadav, R., Huser, R., Opitz, T., & Lombardo, L. (2023). Joint modelling of landslide counts and sizes using spatial marked point processes with sub-asymptotic mark distributions. *Journal of the Royal Statistical Society Series C: Applied Statistics*, *72*(5), 1139–1161. https://doi.org/10.1093/jrsssc/qlad077

Yalcin, A. (2007). The effects of clay on landslides: A case study. *Applied Clay Science*, *38*(1–2), 77–85. https://doi.org/10.1016/j.clay.2007.01.007

Zevenbergen, L. W., & Thorne, C. R. (1987). Quantitative analysis of land surface topography. *Earth Surface Processes and Landforms*, *12*(1), 47–56. https://doi.org/10.1002/esp.3290120107

Zêzere, J., Garcia, R., Oliveira, S., & Reis, E. (2008). Probabilistic landslide risk analysis considering direct costs in the area north of Lisbon (Portugal). *Geomorphology*, *94*(3–4), 467–495. https://doi.org/10.1016/j.geomorph.2006.10.040

Zuzak, C., Mowrer, M., Goodenough, E., Burns, J., Ranalli, N., & Rozelle, J. (2022). The national risk index: Establishing a nationwide baseline for natural hazard risk in the US. *Natural Hazards*, *114*(2), 2331–2355. https://doi.org/10.1007/s11069-022-05474-w